LNG Railcar Spill Modeling

Rev	Issue Purpose:	Date:	BY	CHK	APP
A	Issued for Client Review	March 16, 2020	FG	JW	PS

Table of Contents

Section **Page**

List of Tables and Figures

Table/Figure **Page**

1 Background

The Federal Railroad Administration (FRA) of the U.S. Department of Transportation (DOT) has been evaluating several safety related aspects associated with the transport of liquefied natural gas (LNG) by rail. As part of this evaluation, Blue Engineering and Consulting (BLUE) was requested to perform vapor dispersion calculations for a set of specified LNG spill scenarios. BLUE utilized the modeling software Phast version 6.7, which is approved by the DOT's Pipeline and Hazardous Material Safety Administration (PHMSA) for LNG vapor dispersion modeling, to perform the requested calculations.

The following sections describe the specified spill scenarios, the modeling software and assumptions, and present the modeling results.

2 LNG Spill Scenarios

The FRA has been performing a risk assessment on the transportation of LNG by rail. As part of this risk assessment, they have postulated a set of scenarios in which one or more tank cars carrying LNG would derail and be punctured, resulting in the release of their contents.

Given the large number of parameters that could affect the results in any specific derailment scenario, the FRA developed a set of assumptions in order to obtain estimates of the possible consequences of an LNG release, as follows:

- Three (3) distinct scenarios were considered:
  - the puncturing of one (1) tank car;
  - the puncturing of two (2) tank cars; and
  - the puncturing of five (5) tank cars;
- Each punctured tank car was assumed to fully deinventory from the maximum fill level;
- For each scenario, the release flow rate was calculated based on the pressure at the bottom of the tank and the assumed breach area. The release rate was assumed to remain constant until each tank was emptied;
- The LNG outflow was separated into a portion that immediately flashed to vapor, and a portion that formed a liquid pool on the ground;
- When two or more tank cars were punctured, the spill locations were assumed to be close enough such that a single LNG pool would be formed;
- The LNG pool was free to expand unconstrained, and the maximum pool dimensions were calculated based on the equilibrium between spill and predation rates;
- The vapor source term for the LNG vapor dispersion modeling was calculated based on the maximum pool dimensions.

Table 2-1 summarizes the data provided by the FRA for the LNG vapor dispersion modeling of the three scenarios.

Table 2-1. Parameters and values for use in the dispersion calculations.

Tank cars breached	1	2	5
Spill duration at max release rate [s]	41	41	41
Maximum liquid spill rate onto the ground [kg/s]	883	1,766	4,414
Maximum rate of release of flashed vapor [kg/s]	152	304	761
Maximum diameter of LNG pool [m]	102	136	191
Mass flux of vapor from the LNG pool [kg/s/m^2][1]	0.125	0.143	0.181

Each scenario was to be modeled under the same ambient conditions, specified by the FRA as follows:

- Ambient temperature = 20°C
- Wind speed = 2.5 m/s
- Atmospheric stability class = F
- Flat terrain with terrain roughness factor = 0.05 m

The Phast model, which was used for the vapor dispersion calculations, requires additional ambient parameters to be defined. Therefore, BLUE specified the following values:

- Relative humidity = 50% (consistent with the requirements in 49 CFR Part 193.2059)
- Solar radiation = 0 W/m^2 (the most conservative option, consistent with nighttime events)

It should be noted that BLUE's scope was solely limited to modeling – therefore, BLUE is not able to comment on the applicability of the assumptions related to the LNG spill scenarios as specified by FRA.

3 The Phast Model

The Phast model is one of three models currently approved by PHMSA for LNG vapor dispersion modeling:

[1] This includes both vapor from LNG evaporation and flashed vapor (distributed uniformly across the pool area).

- DEGADIS (Dense Gas Dispersion Model);
- Phast (Process Hazard Analysis Software Tool); and
- FLACS (FLame ACceleration Simulator)

Phast was selected for this study because it strikes the best balance between being widely used and not overly complicated for the scenarios in question. While other models, such a FLACS, would be able to demonstrate land and terrain impacts on a release, to be conservative this 2-dimensional, unmitigated model has been utilized. Phast version 6.7 was used, instead of the current version (8.22), because it is the most recent version to have been formally reviewed and approved by PHMSA[2].

The Phast software package includes capabilities to calculate several different hazard scenarios, including: flammable and vapor dispersion from liquid spills or pressurized releases, pool and jet fires, vapor cloud explosions, etc. For the current study, the calculations were performed by providing a user-defined vapor source term (based on the input data provided by the FRA) to the Unified Dispersion Model (UDM), which then calculated the dispersion of the vapor cloud.

The UDM is an integral model intended to simulate the advection and dispersion of gas releases (continuous, instantaneous, and time-varying); it incorporates parameterized turbulent diffusion coefficients as well as air entrainment at the top and edges of the cloud. The UDM calculates time-dependent gas concentration and temperature along the cloud centerline, and then applies similarity solutions to calculate vertical and crosswind profiles. The model incorporates thermodynamic properties (based on the DIPPR database), heat transfer to/from the air and the ground, and can take into account the effects of relative humidity as well as chemical reactions where applicable. The UDM model utilizes the input ambient conditions to define a steady-state wind profile. The UDM solves is set of ordinary differential equations using well-established numerical solvers and has been subjected to both verification against a number of analytical solutions and validation against experimental data from the "Validation database for evaluating vapor dispersion models for safety analysis of LNG facilities"[3].

3.1 Modeling Methodology

The vapor source term was calculated in Phast using the "Pool Vaporization" module. This model requires the user to first enter the material being spilled: in this case, methane

[2] Final Decision on petition for approval of PHAST-UDM version 6.6 and 6.7, PHMSA Docket No. 2011-0075 (October 7, 2011).

[3] Coldrick, S., Lea, C. J., & Ivings, M. J. (2009). Validation database for evaluating vapor dispersion models for safety analysis of LNG facilities. The Fire Protection Research Foundation.

was used to represent LNG. Then, the Pool Vaporization module allows the user to specify either a "User-Defined" or "Modeled" type of pool. In this case, the User-Defined option was selected, which required the following inputs:

- Pool Radius;
- Vapor Release Rate;
- Release Duration;
- Vapor Release Temperature.

Most of the numerical values for the required inputs were obtained from Table 2-1, as provided by FRA; the vapor release temperature was set to the normal boiling point for methane (-161.5°C).

The output from the pool vaporization module in Phast consists of a vapor source term, which was supplied to the UDM, together with the ambient conditions provided above, to calculate the vapor cloud dispersion. The vapor dispersion module applied the vapor source term as a ground-level vertical release with only the momentum resulting from the rate of vapor generation, approximately 0.07-0.10 m/s.

No user-selectable parameters in the Phast model (besides the scenario-specific inputs listed above) were modified from the default values for the calculations performed in the study.

The output from the UDM calculations consists of tabulated values listing the cloud's position and dimensions, the centerline height, temperature and gas concentration, at discrete time intervals. The Phast model also allows several types of graphical outputs that depict, for example, the cloud's footprint or cross-section at different times and locations. The cloud's footprint at the time it reaches its maximum area will be shown in the Modeling Results section.

4 Modeling Results

The modeling results for the three LNG spill scenarios described in Table 2-1 are summarized in Table 4-1, which includes the output parameters requested by the FRA. Note that, as requested, the reported values used as the concentration threshold the lower flammable limit (LFL), which is equal to 5% for LNG, without safety factors being applied.

Table 4-1. Phast modeling results.[4]

Tank cars breached	1	2	5
Max. cloud distance to LFL [m]	1,310	1,760	2,380
Max. cloud width to LFL [m]	350	450	530
Max. cloud depth to LFL [m]	20	23	27
Max. ground level cloud area to LFL [m^2]	56,300	103,500	221,300

It is important to note that the above listed values occur each at a different time during the evolution of the vapor cloud. Therefore, the flammable vapor cloud for the 1 tank car scenario, for example, will never be 1310 m long, 350 m wide, and 20 m tall. In order to illustrate that, Figure 4-1, Figure 4-2 and Figure 4-3 show the flammable vapor cloud footprint at the time it reaches its maximum area for each of the three scenarios; the figures show that the maximum area is reached relatively early in the dispersion process, when the cloud has just become detached from the pool and is well short of its maximum downwind dispersion distance.

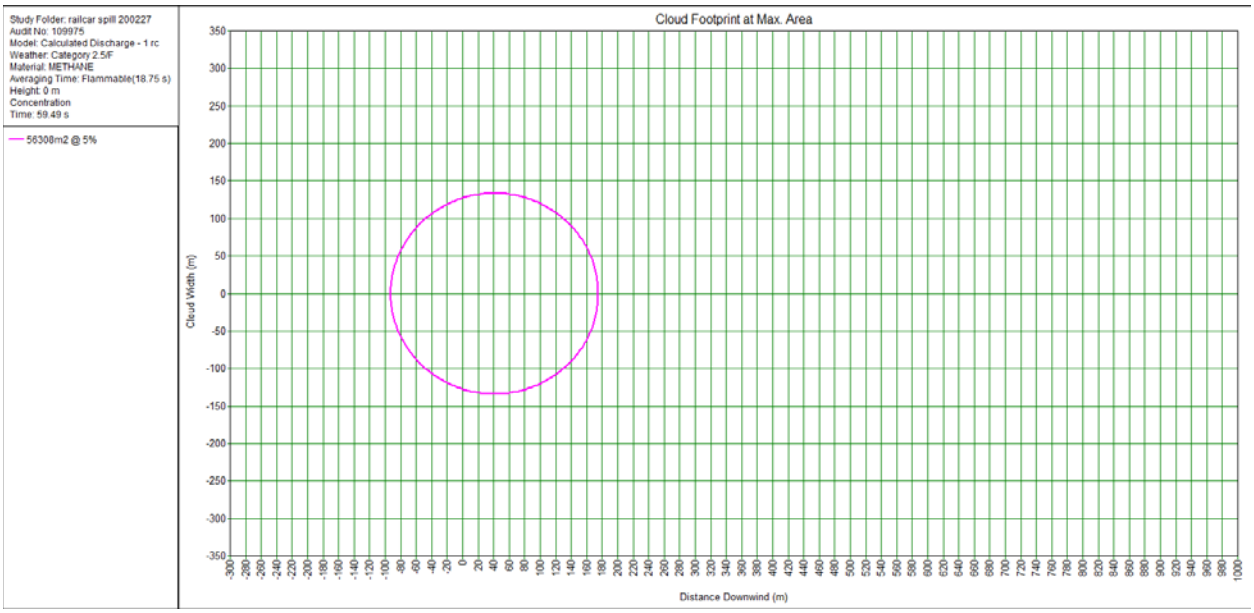

Figure 4-1: Flammable vapor cloud at time of maximum area, for 1 tank car scenario.

[4] the values listed in the table were rounded to the nearest:

- 10 m for cloud distance and width
- 1 m for cloud depth
- 100 m^2 for cloud area

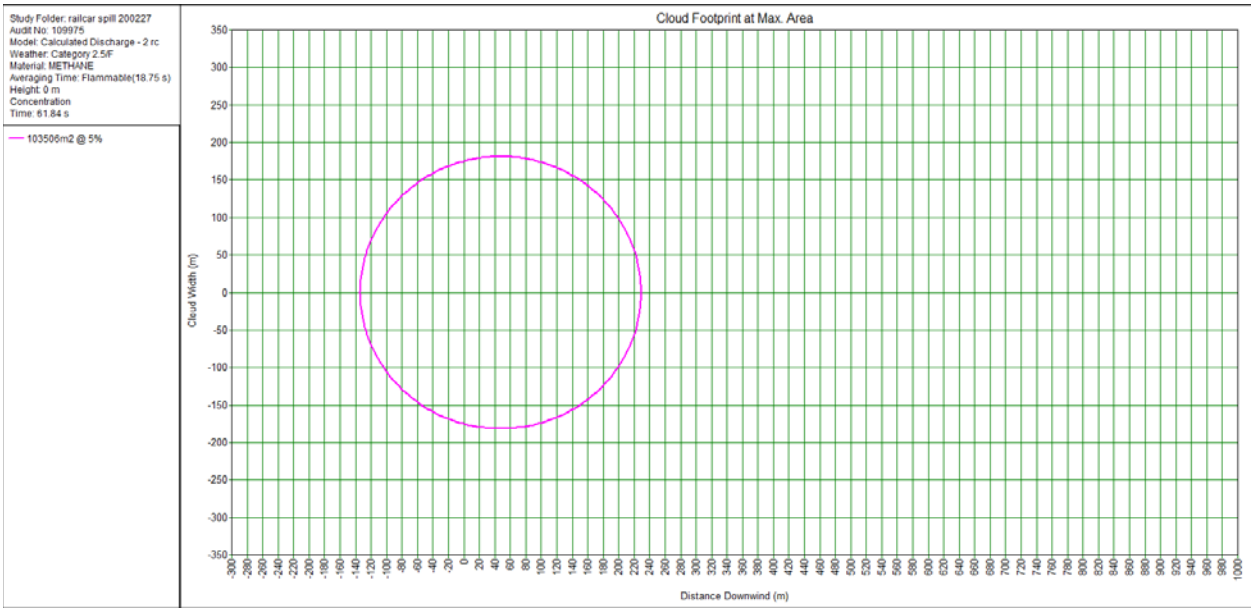

Figure 4-2: Flammable vapor cloud at time of maximum area, for 2 tank cars scenario.

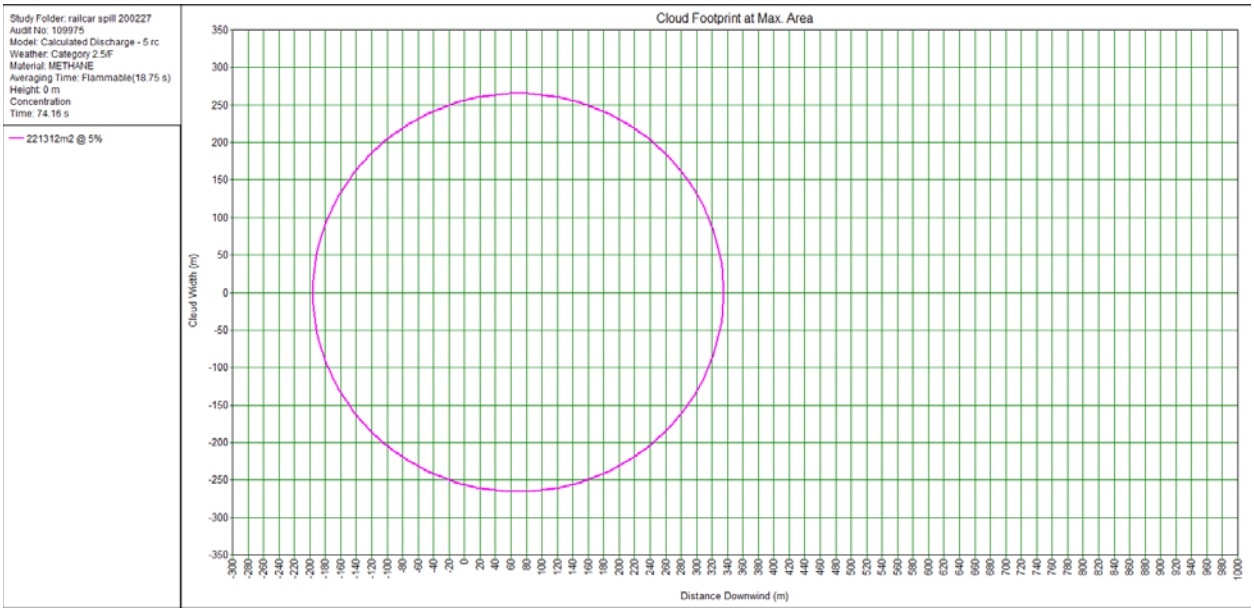

Figure 4-3: Flammable vapor cloud at time of maximum area, for 5 tank cars scenario.

5 Summary

BLUE was requested to perform vapor dispersion modeling for a defined set of LNG spill scenarios by the FRA associated with railcar accidents. The scenarios consisted of liquid spills of LNG onto the ground, evaporating and being dispersed by the wind; different spill volumes and flow rates were evaluated, corresponding to the puncturing of 1, 2, and 5 tank cars.

The modeling utilized Phast version 6.7. More specifically, it applied the "user-defined" pool type in the pool vaporization module, to generate a source term suitable for use with the Unified Dispersion Model.

This report lists the input data provided by the FRA, a brief description of the Phast model and modeling assumptions, and the output parameters requested by the FRA. BLUE's scope was solely limited to modeling – therefore, BLUE is not able to comment on the applicability of the assumptions related to the LNG Spill Scenarios as specified by FRA.

Preliminary Puncture Estimates

LNG Unit Trains

Draft

Overview

- Simulations of:
  - 100 LNG Tanks (DOT113s)
    - 7/16” Shell, 0.5” Head, 0.25” Inner Tank
    - Rear DP Configuration
  - Derailments are initiated at the head end of the train.

Preliminary Results

Speed	30 mph	40 mph	50 mph
No. of derailed cars	16	23	32
No. of Punctures	3	6	8

Draft

Liquefied Natural Gas (LNG)

(Properties, Hazards and Field Test Results)

Presentation to

Pipeline & Hazardous Materials Safety Administration

[Presentation based on training provided to

The US Coast Guard Personnel

First Coast Guard District, Boston]

by

Dr. Phani Raj

Hazmat Division, Office of Safety

Federal Railroad Administration, US DOT

Washington, DC 20590

19th February, 2020

Organization of the Presentation

1. Natural gas and LNG Properties
2. LNG vapor dispersion in the atmosphere
3. Fire scenarios
4. Assessment of fire effects
5. LNG release underwater
6. Conclusions & Discussions

PART 1

Natural Gas & LNG Properties

Natural Gas vs. LNG

- **Natural Gas ("NG")**: is a by-product of oil pumping ("associated gas") or is extracted from gas deposits ("non associated gas"). Gas is mainly methane.

- **Natural Gas** is first stripped of heavier hydrocarbons, water, H_2S, CO_2 and other condensates before cooling to produce LNG.

Natural Gas (NG)

Natural Gas at atmospheric pressure and temperature is lighter than air

Gas	Gas density in units of	
	kg/m^3	lb/ft^3
Natural Gas	0.666	0.042
Air	1.2	0.075
NG sp. gr.	*0.55*	

Methane at atmospheric pressure is Neutrally buoyant in air at

163 K [- 110 ^{O}C or -167 ^{O}F]

Liquefied Natural Gas (LNG)

LNG is produced by cooling **NG** to -162 °C (-260 °F)

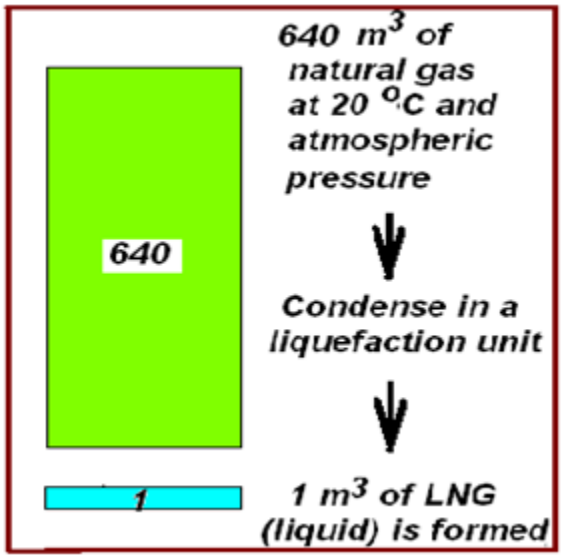

Liquid	Liquid density in units of	
	kg/m^3	lb/ft^3
LNG	425	3.55
Water	1000	8.35
LNG sp. gr.	*0.425*	

Composition of LNG

LNG is a mixture of hydrocarbons. Methane is the principal constituent. Composition depends on the source of NG.

Volume % of components in the liquid

Source of LNG	Methane	Ethane	Propane	Iso-Butane	n-Pentane	Nitrogen
Trinidad	96.70	2.80	0.34	0.03	0.03	0.02
Yemen	92.80	5.90	1.10	0.08	0.09	0.03
Das Island (UAE)	84.82	13.39	1.34	0.28	0.00	0.17
Typical	90.33	8.95	0.34	0.02	0.02	0.34

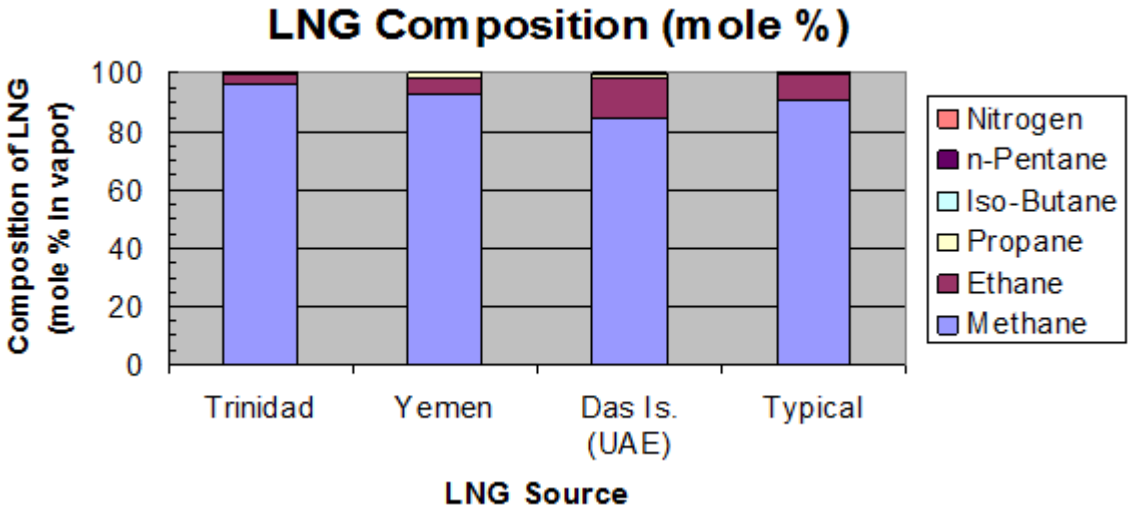

LNG boiling in a beaker

LNG boiling & distilling on ground or on water

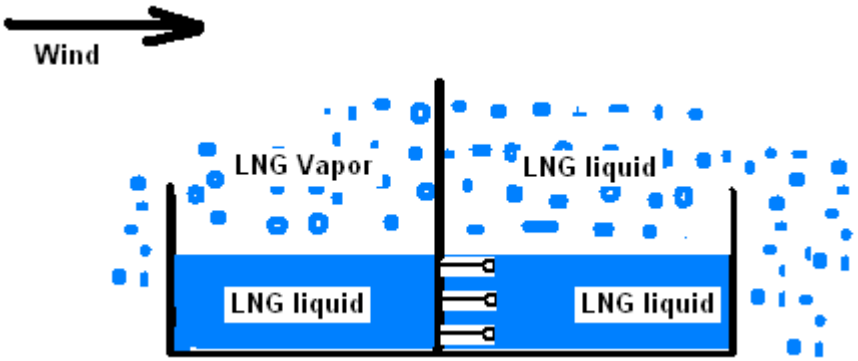

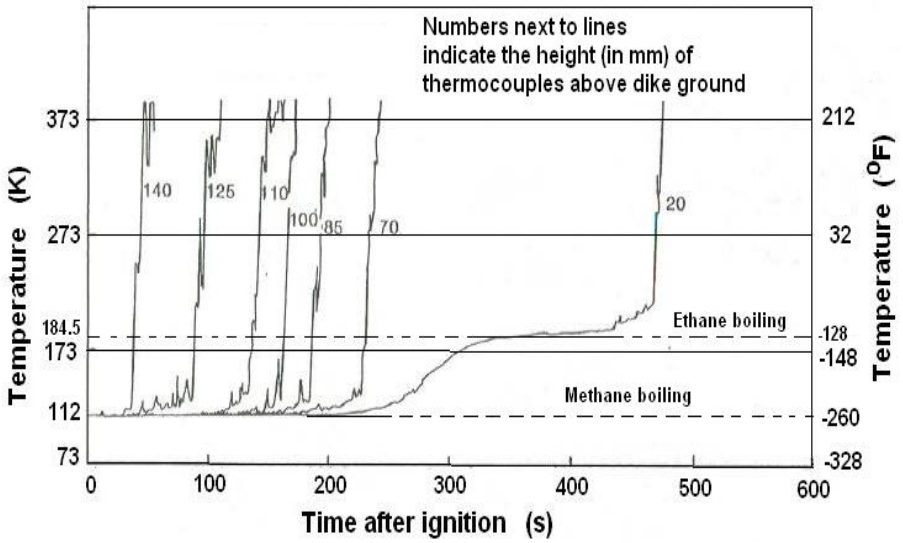

LNG (liquid) properties

- LNG spilled on ground or on water will boil and vaporize, rapidly.
- The boiling is due to significant temperature difference between ground or water and LNG.
- LNG is lighter than water. LNG spilled on water will form a floating, spreading and boiling pool.
- LNG being a mixture releases methane first when boiling on a substrate.

PART 2

LNG Vapor Dispersion In the Atmosphere

LNG Vapor Cloud Characteristics

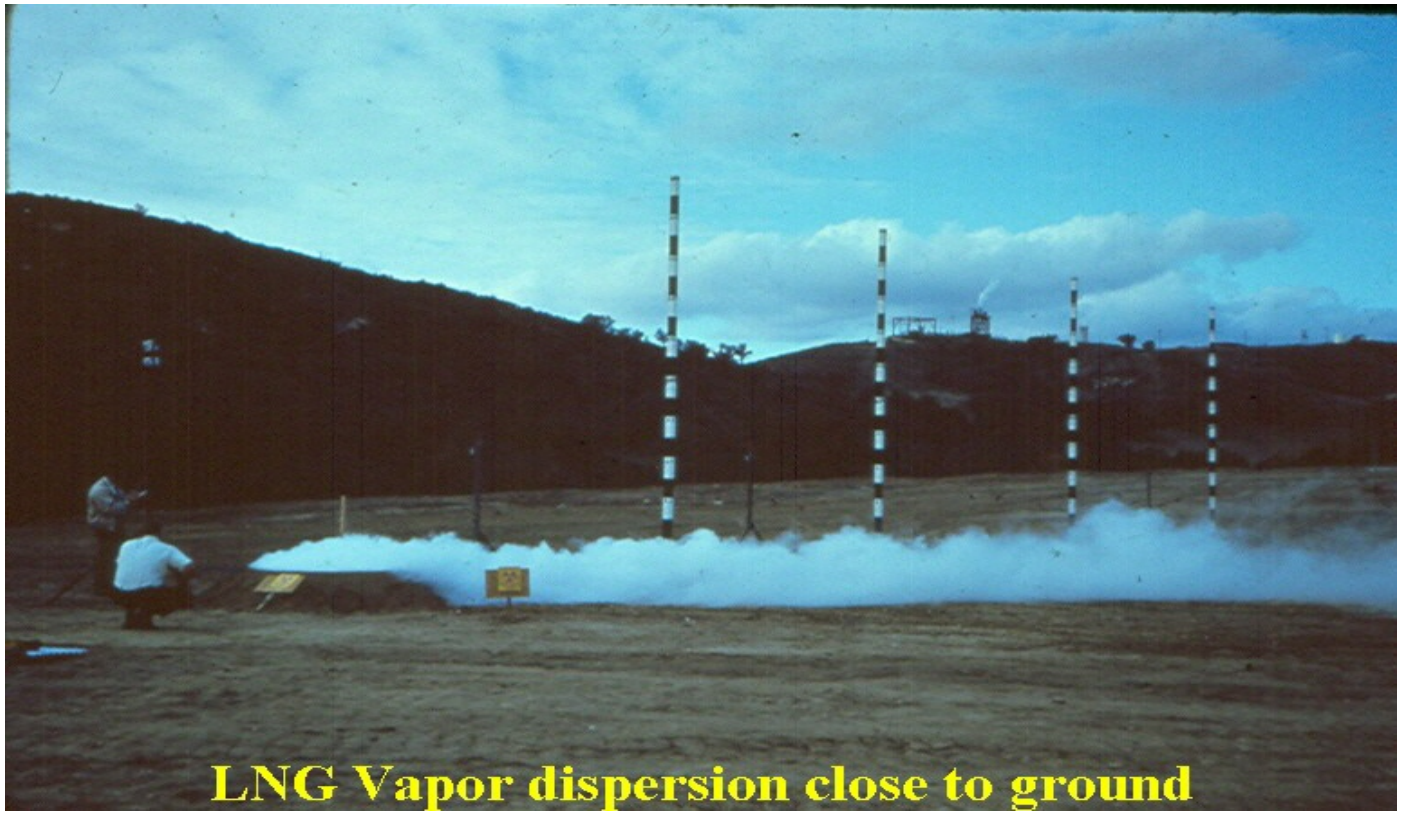

LNG vapor @ 110 K (-260 ^{O}F) is heavier than air

(Density= 1.84 kg/m^3; i.e., 1.5 times that of air)

Density of LNG vapor-air mixture

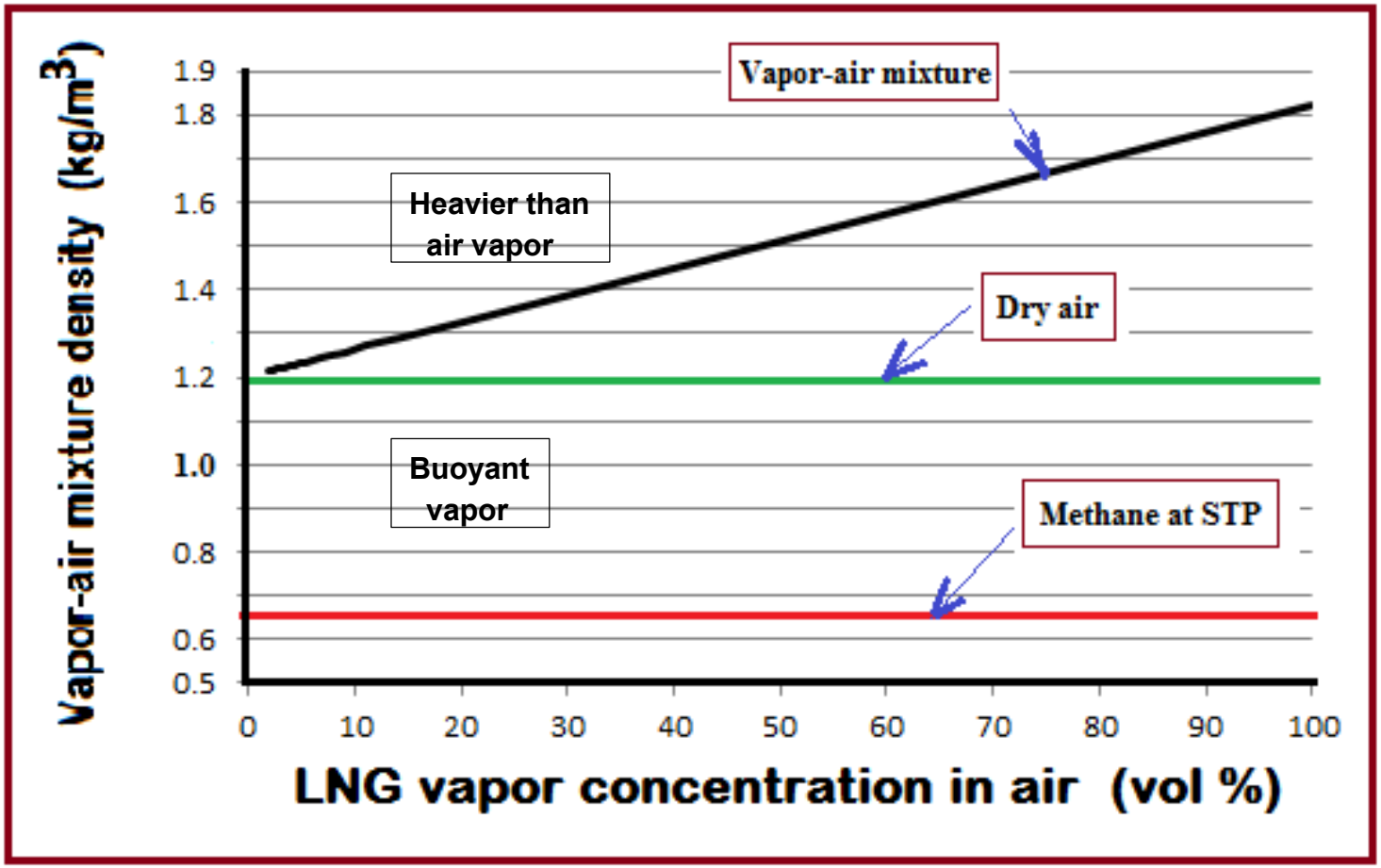

Vapor Dispersion Clip

Concentration variation within the LNG vapor cloud

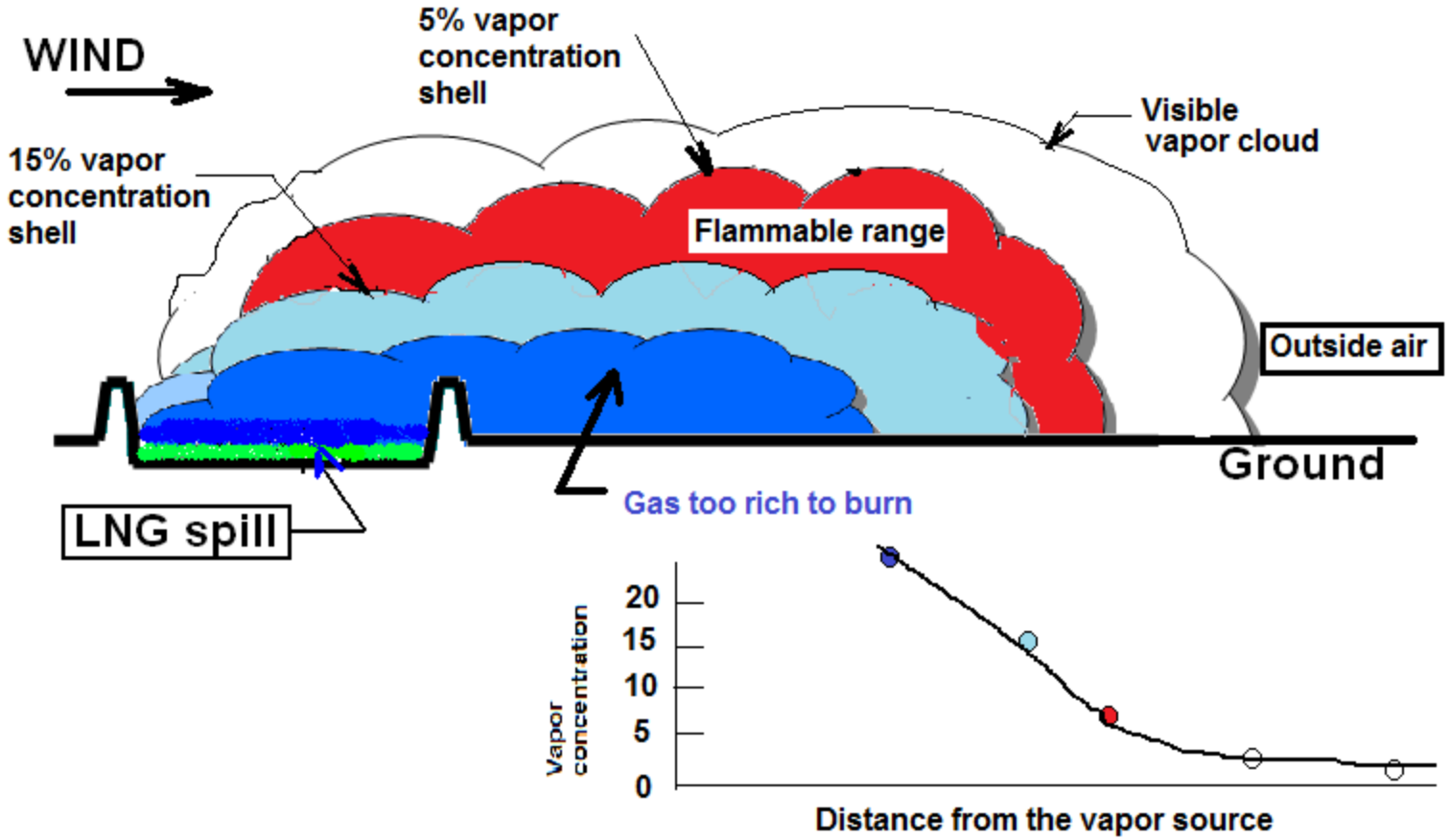

Flammability Characteristics

- NG vapor is flammable in air in the volumetric concentration range 5% (LFL) to 15% (UFL).

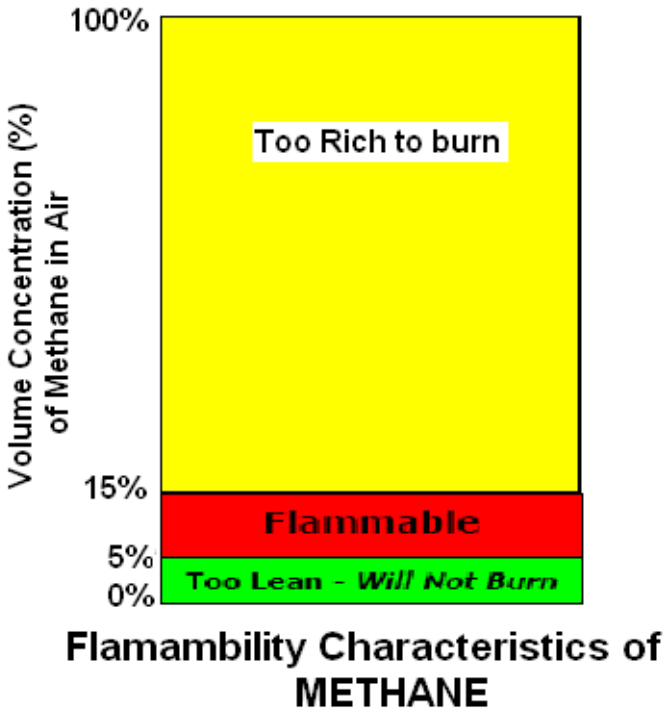

Flammable concentration is within the cloud only when atmospheric relative humidity > 55%

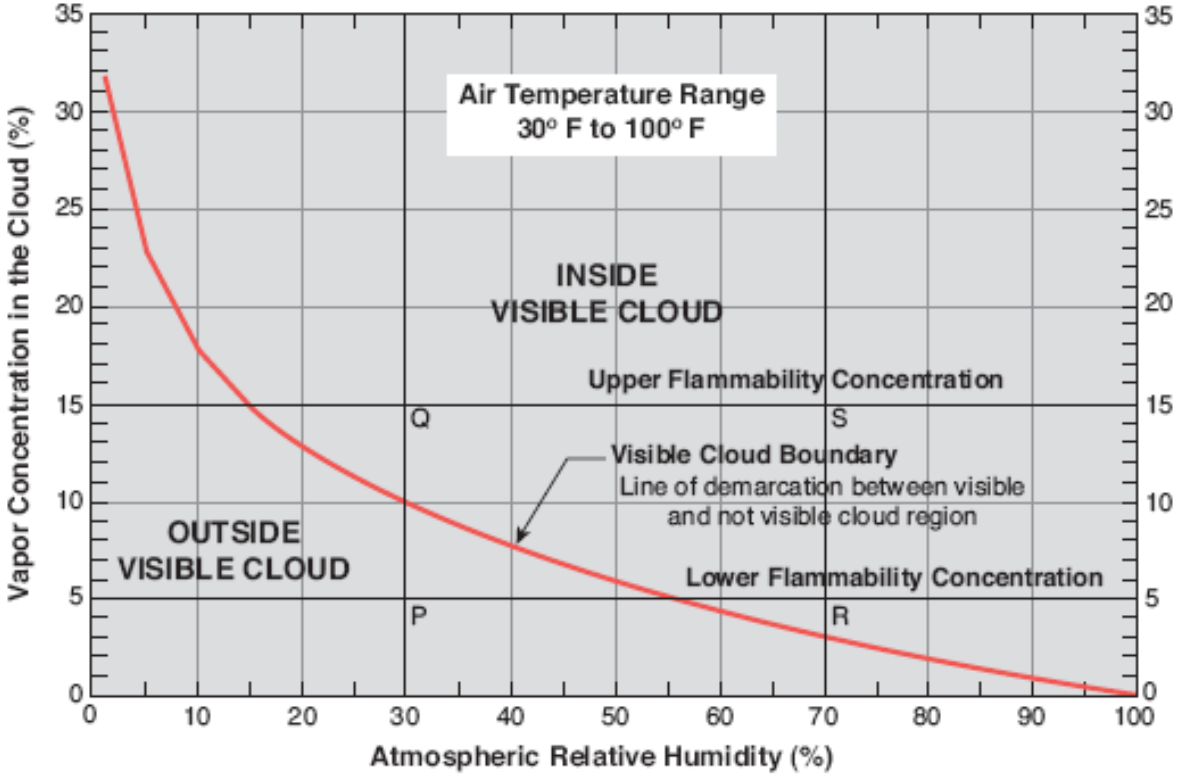

Recap of basic LNG Properties

- LNG spill on land or water results in rapid liquid evaporation and formation of a visible vapor cloud.
- The vapor cloud is denser than air and, hence, disperses at ground level (or over water)
- Vapor is flammable in air in the range 5% (LFL) to 15% (UFL) concentration.
- The LFL concentration is always within the visible vapor cloud for atmospheric relative humidity greater than 55%.

PART 3

Fire Scenarios

Comparison of fuel heating values and theoretical fire temperatures

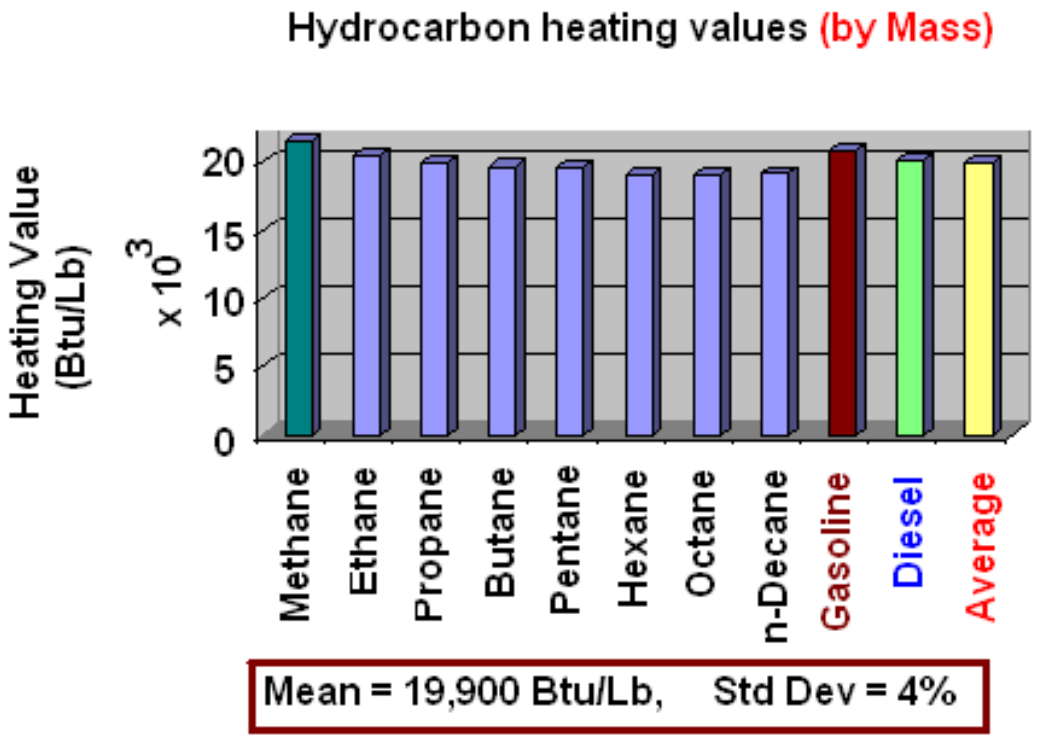

Stoichiometric air to fuel mass ratio for all hydrocarbons 15.6 ± 0.8
Average temperature of fires of most hydrocarbons = (3050 ± 50) °F

China Lake LNG Pool Fire Tests

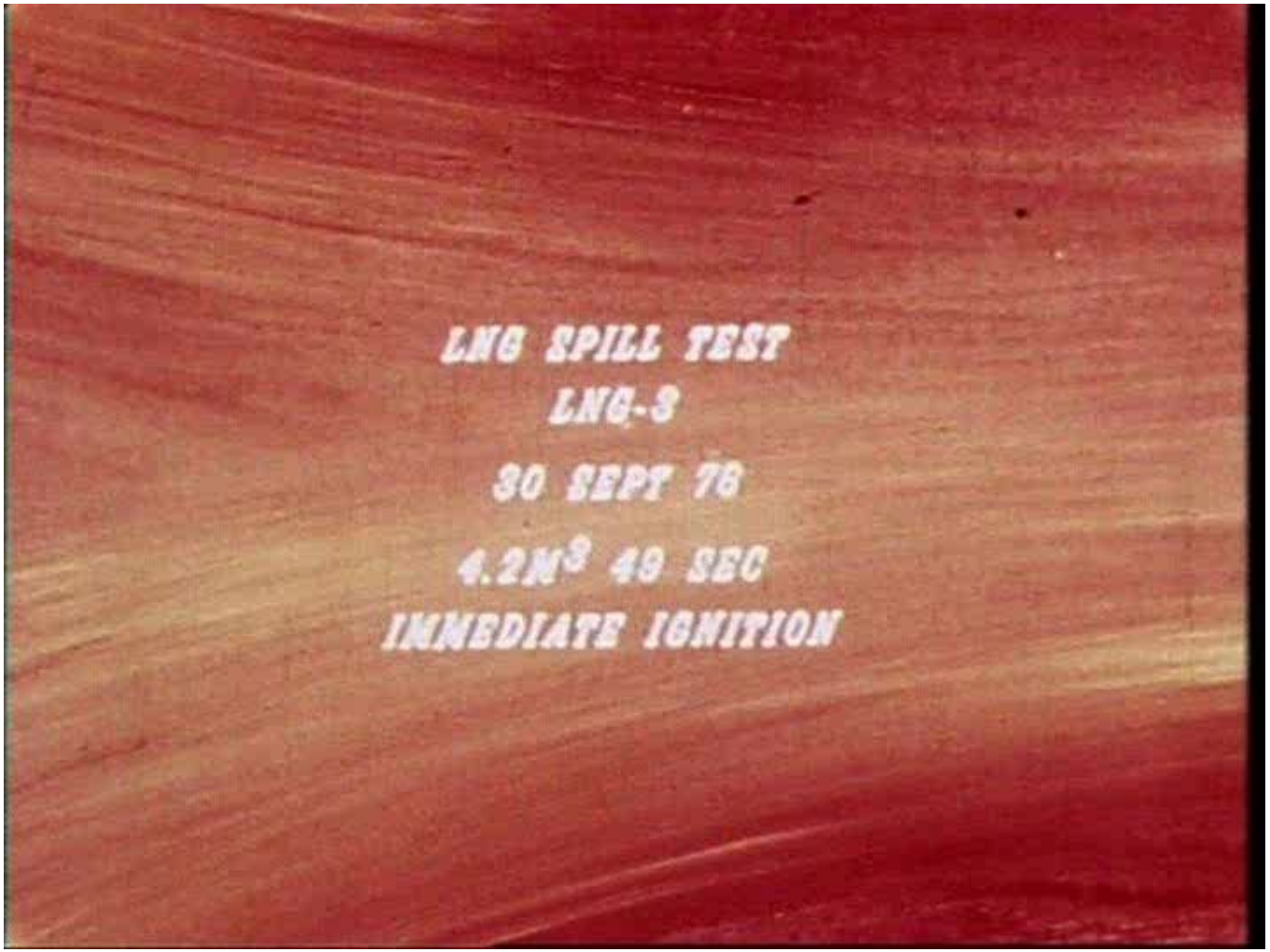

LNG Fire Characteristics at Different Burn Stages

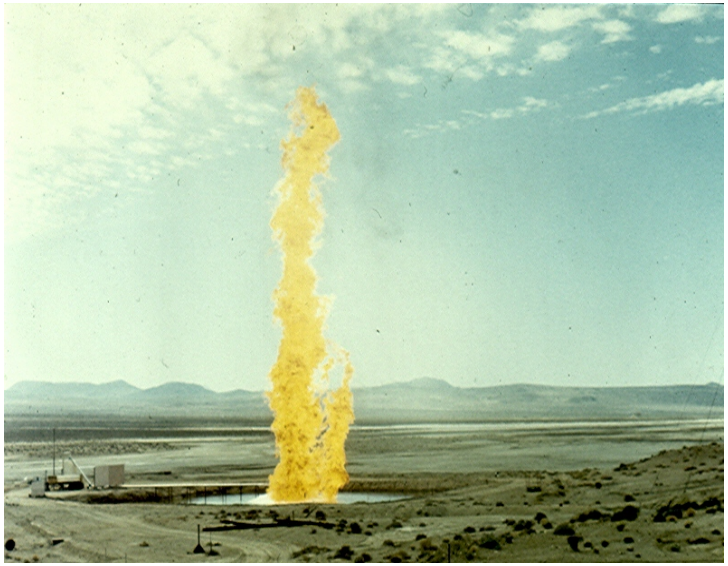

LNG Pool Fire on Water - mid Stage

LNG Pool Fire - Near End Stage

LNG Pool Fire - End of Burning

35 m diameter LNGPool Fire Tests (Montoir, France)

Burning characteristic similarities in large LNG pool fire & Oil pool fire

35 m diameter LNG fire test – Montoir 1987

Fire from an oil pipeline spill – Iraq 2004

Recent Pool Fire Tests by Sandia National Lab

LNG - 21 m SNL 2009

LNG - 83 m SNL 2009

China Lake Vapor Fire Test

GdF Vapor Fire Test

TEEX Vapor & Fire Test

China Lake VCE Tests

Rapid phase transition (RPT) behavior

LNG Pool Fire Behavior with Water Spray into the Pool

Fire and other combustion related hazards

- **Pool Fire**: Radiant heat effect hazards at locations outside the fire.
- **Vapor Fire:** Dispersion of vapor and its ignition at some downwind location.
- **Vapor Cloud Explosion**: Ignition of a dispersed LNG vapor cloud and explosion.
- **Rapid Phase Transition**: LNG contacting water resulting in a superheat explosion

PART 4

Assessment of Fire Effects

Important parameters in radiant heat effect calculation

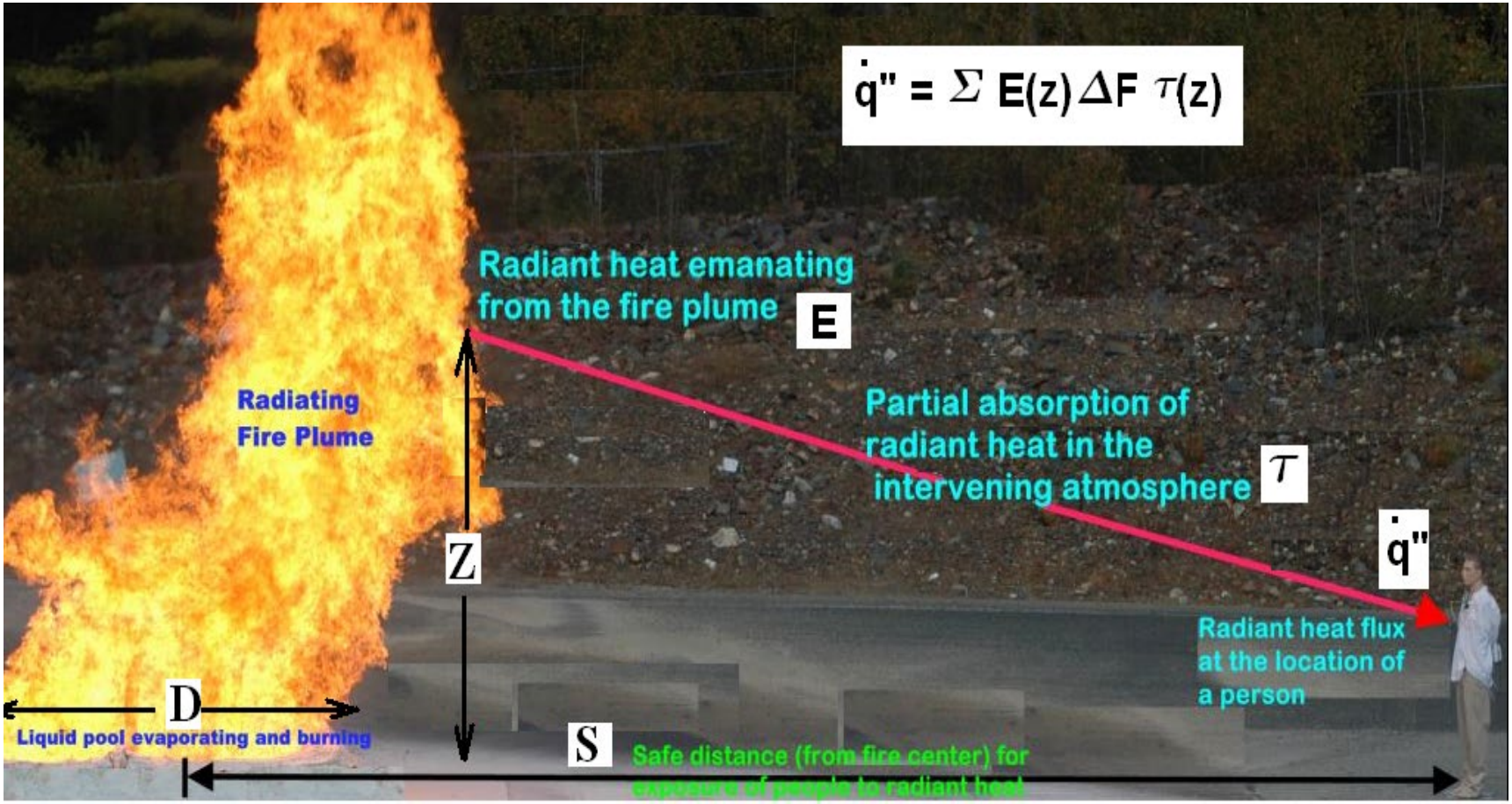

Human Exposure to LNG Pool Fire Radiant Heat

Exposure of mannequins and a human to LNG Fire – Temperature data

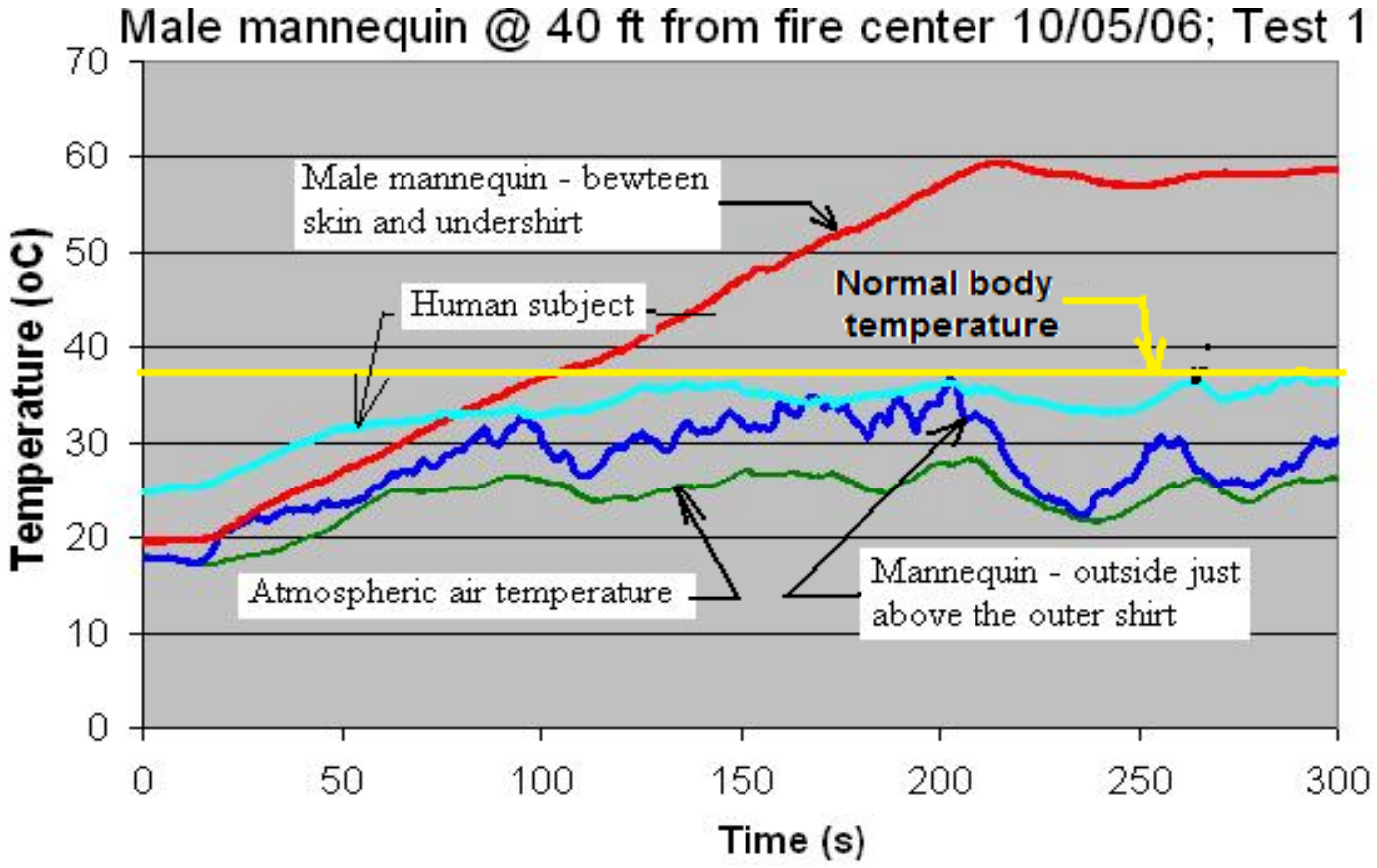

Tests of 10/05/2006

Effect of newspaper shade

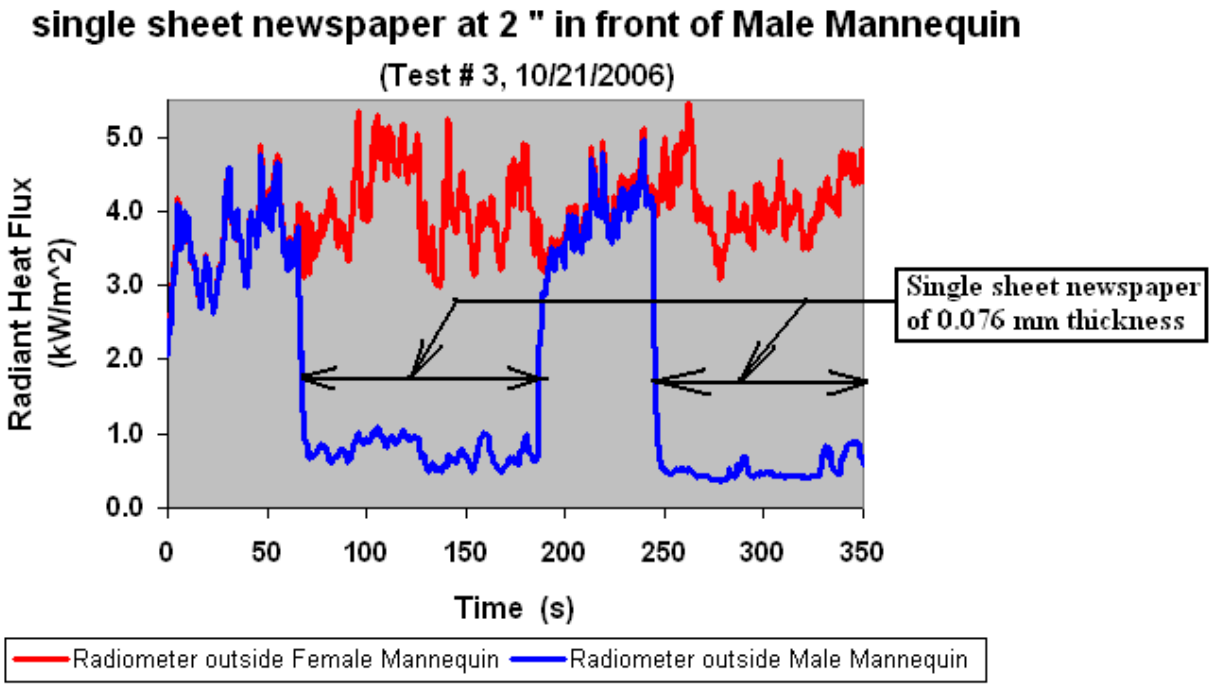

PART 5

LNG Release Underwater

Dispersion of vapor released from water surface – LNG released underwater

Recap of LNG fire behaviors

- Un-ignited, LNG vapor disperses at ground level
- Small pool fires of LNG are highly radiative; however large fires are similar to oil fires
- Conventional ignition of vapor, in the absence of obstructions, results in a flash fire with no explosive burning.

Recap of LNG fire behaviors (cont'd)

- LNG vapor with higher % of propane, butane, etc., ignited energetically, may result in a vapor cloud explosion.
- LNG released underwater results in very high evaporation rate.
- The vapor released from underwater LNG release is buoyant.
- Occasionally, LNG spilled on water can create a localized, flameless explosion, termed the RPT.

PART 6

Vulnerability of LNG Ship

LNG ship tank and double hull

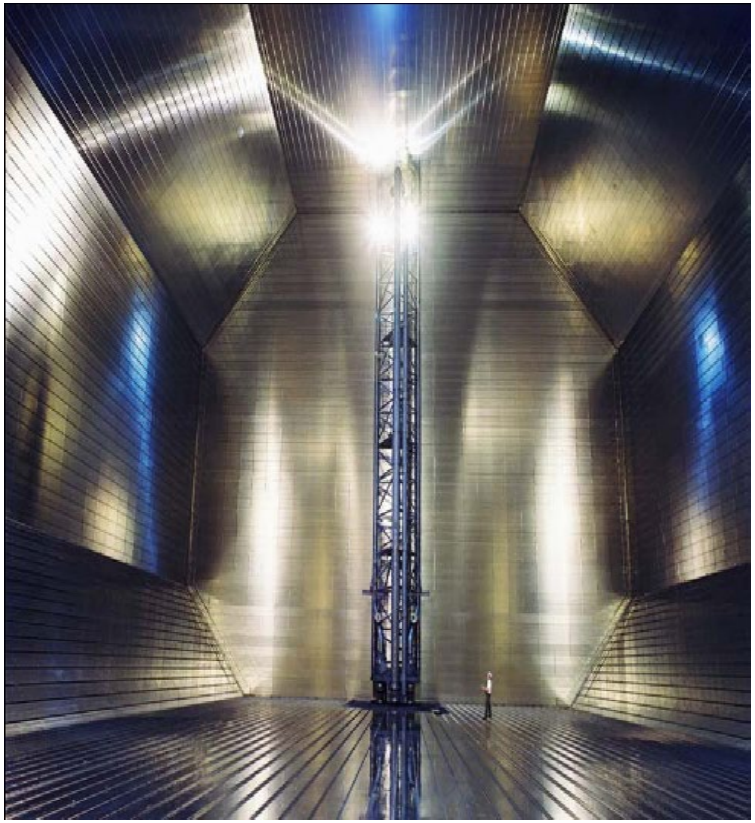

El Paso Paul Kayser – In Dry Dock after grounding in Straits of Gibraltar

SANDIA Study (2012) on Cryogenic & Fire Effects on LNG Vessel

- Cryogenic cracking will occur only in those areas where the LNG actually impacts the vessel wall.
- Cryogenic damage causes approximately 30% to 70 % reduction in steel strength, within 3 to 10 minutes.
- Vessel structure near the pool fire, on both side and top of the vessel, will reach temperatures between 775°C (inner hull) and 1000°C (outer hull).
- At these temperatures, the vessel's structural steels are severely weakened (to less than 25 percent of their original strength), and will deform significantly.
- Pool fire on water will cause an additional 10 to 20 percent reduction in strength of steel in about 20 and 30 minutes.

PART 7

Conclusions

Conclusions

Field Scale Tests indicate that

- Large LNG fires are similar in physical and radiative characteristics to other oil fires.
- Recent SNL tests indicate that LNG pool fires on water are about half the diameter of the LNG pools that form on water.
- Unconfined vapor clouds when ignited form only a slow deflagration vapor fire. No detonations have been observed.
- Significant concentration of propane (and other higher hydrocarbons) in methane air mixture, together with a strong ignition source & semi confinement is needed to initiate vapor cloud explosion.
- Turbulence enhancing obstructions (trees, pipe racks, buildings) may initiate transition to detonation

Conclusions (cont'd)

- A person clothed in normal civilian clothing can withstand a radiant heat intensity of 5 kW/m2 for 30 seconds without incurring any burns or severe pain.
- When LNG is released underwater, it rapidly evaporates in the water body leading to the formation of vapor which is heated by water.
- The vapor emerging from water surface for release depths of more than about 2 m is buoyant and disperses in the atmosphere as natural gas release. No pool is formed on the water surface.
- It is possible that for LNG releases plunging into water (due to releases from large heights) would behave in a manner similar to the underwater release.

Conclusions (cont'd)

- LNG is a hazardous/flammable material. However, LNG hazards are not much different than those from other hydrocarbon fuels that society uses in very large quantities.
- LNG released from LNG-ship tanks will impact carbon steel structures within the ship very likely resulting in brittle fracture and significant structural damage.
- Extended duration LNG pool fire outside the ship may cause structural damage to the hull by overheating.
- Vapor formed by LNG ship tank leak into the hold space will very likely NOT cause any explosions since the vapor-air mixture will be very rich.
- LNG released underwater will very rapidly evaporate. The vapor released into the atmosphere will most likely be buoyant (depending upon the depth of LNG release).

TMS Inc.

Emergency responder actions on LNG fires

- If one is properly trained to respond to large gasoline or other hydrocarbon fires, LNG fire response will not be much different.
- Very large fires of LNG are as difficult to deal with as are very large hydrocarbon (gasoline) fires. Large LNG spill fires cannot be quenched.
- Water should not be directed into LNG pool fires.
- Resources must be used to prevent leaks. In case of a large fire, priority should be to protect people, property and to minimize possibilities of secondary fires.

Thank you for your attention and interest

Questions?

U.S. Department of Transportation

Federal Railroad Administration

Objective Evaluation of Risk Reduction from Tank Car Design and Operations Improvements – Extended Study

Office of Research,
Development
and Technology
Washington, DC 20590

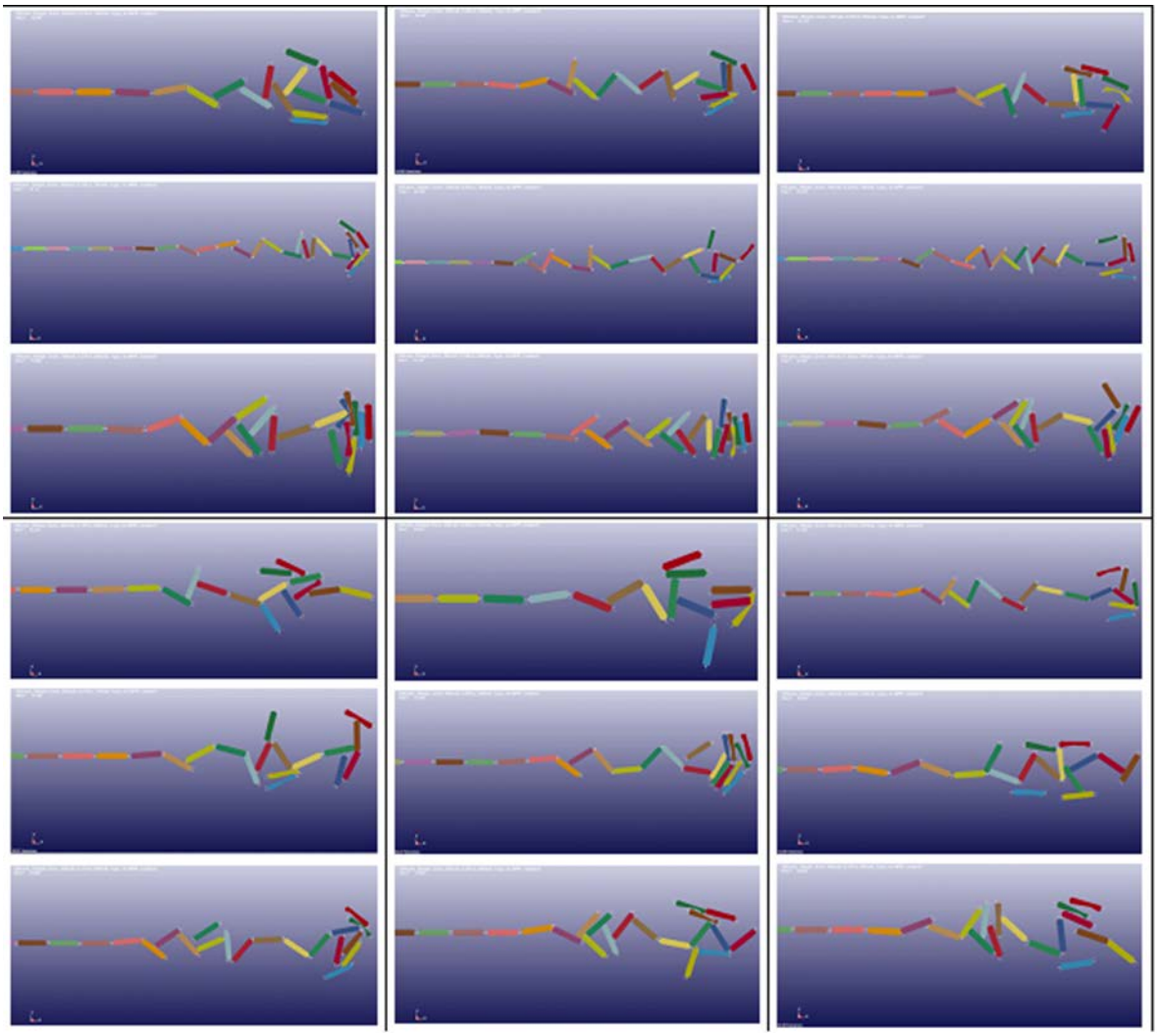

DOT/FRA/ORD-18/36

Final Report
October 2018

NOTICE

This document is disseminated under the sponsorship of the Department of Transportation in the interest of information exchange. The United States Government assumes no liability for its contents or use thereof. Any opinions, findings and conclusions, or recommendations expressed in this material do not necessarily reflect the views or policies of the United States Government, nor does mention of trade names, commercial products, or organizations imply endorsement by the United States Government. The United States Government assumes no liability for the content or use of the material contained in this document.

NOTICE

The United States Government does not endorse products or manufacturers. Trade or manufacturers' names appear herein solely because they are considered essential to the objective of this report.

REPORT DOCUMENTATION PAGE

Form Approved
OMB No. 0704-0188

1. AGENCY USE ONLY (Leave blank)	2. REPORT DATE	3. REPORT TYPE AND DATES COVERED
	October 2018	Technical Report – May 2015

4. TITLE AND SUBTITLE
Objective Evaluation of Risk Reduction from Tank Car Design and Operations Improvements – Extended Study

5. FUNDING NUMBERS
DTFR53-15-P-00011

6. AUTHOR(S)
Anand Prabhakaran, Gray Booth.

7. PERFORMING ORGANIZATION NAME(S) AND ADDRESS(ES)
Sharma & Associates, Inc.
5810 S Grant Street
Hinsdale, IL 60521

8. PERFORMING ORGANIZATION REPORT NUMBER

9. SPONSORING/MONITORING AGENCY NAME(S) AND ADDRESS(ES)
U.S. Department of Transportation
Federal Railroad Administration
Office of Railroad Policy and Development
Office of Research, Development and Technology
Washington, DC 20590

10. SPONSORING/MONITORING AGENCY REPORT NUMBER
DOT/FRA/ORD-18/36

11. SUPPLEMENTARY NOTES
COR: Francisco González, III

12a. DISTRIBUTION/AVAILABILITY STATEMENT
This document is available to the public through the FRA Web site at http://www.fra.dot.gov.

12b. DISTRIBUTION CODE

13. ABSTRACT (Maximum 200 words)

This report describes a novel and objective methodology for quantifying and characterizing how changes to tank car designs or the tank car operating environment lead to reductions in risk (or reductions in puncture probabilities). The methodology captures several parameters that are relevant to tank car performance under derailment conditions—including multiple derailment scenarios, derailment dynamics, impact load distributions, impactor sizes, operating conditions, tank car designs, etc.—and combines them into a consistent probabilistic framework that estimates the relative merit of proposed mitigation strategies.

Comparison of the estimates from this methodology to actual derailment data suggests that the gross dynamics of a tank car train derailment and the resulting puncture performance of the tank cars are captured well by this methodology. The model's estimates of the number of cars derailed and number of punctures, as a function of train speed, also compare favorably with actual derailment data. These validation efforts add further credibility to the efficacy of the methodology and the results derived from it.

14. SUBJECT TERMS
Hazardous materials, probability of puncture, risk evaluation, tank car puncture resistance

15. NUMBER OF PAGES
36

16. PRICE CODE

17. SECURITY CLASSIFICATION OF REPORT	18. SECURITY CLASSIFICATION OF THIS PAGE	19. SECURITY CLASSIFICATION OF ABSTRACT	20. LIMITATION OF ABSTRACT
Unclassified	Unclassified	Unclassified	

NSN 7540-01-280-5500
Standard Form 298 (Rev. 2-89)
Prescribed by ANSI Std. 239-18
298-102

METRIC/ENGLISH CONVERSION FACTORS

ENGLISH TO METRIC	METRIC TO ENGLISH
LENGTH (APPROXIMATE)	**LENGTH (APPROXIMATE)**
1 inch (in) = 2.5 centimeters (cm)	1 millimeter (mm) = 0.04 inch (in)
1 foot (ft) = 30 centimeters (cm)	1 centimeter (cm) = 0.4 inch (in)
1 yard (yd) = 0.9 meter (m)	1 meter (m) = 3.3 feet (ft)
1 mile (mi) = 1.6 kilometers (km)	1 meter (m) = 1.1 yards (yd)
	1 kilometer (km) = 0.6 mile (mi)
AREA (APPROXIMATE)	**AREA (APPROXIMATE)**
1 square inch (sq in, in^2) = 6.5 square centimeters (cm^2)	1 square centimeter (cm^2) = 0.16 square inch (sq in, in^2)
1 square foot (sq ft, ft^2) = 0.09 square meter (m^2)	1 square meter (m^2) = 1.2 square yards (sq yd, yd^2)
1 square yard (sq yd, yd^2) = 0.8 square meter (m^2)	1 square kilometer (km^2) = 0.4 square mile (sq mi, mi^2)
1 square mile (sq mi, mi^2) = 2.6 square kilometers (km^2)	10,000 square meters (m^2) = 1 hectare (ha) = 2.5 acres
1 acre = 0.4 hectare (he) = 4,000 square meters (m^2)	
MASS - WEIGHT (APPROXIMATE)	**MASS - WEIGHT (APPROXIMATE)**
1 ounce (oz) = 28 grams (gm)	1 gram (gm) = 0.036 ounce (oz)
1 pound (lb) = 0.45 kilogram (kg)	1 kilogram (kg) = 2.2 pounds (lb)
1 short ton = 2,000 pounds (lb) = 0.9 tonne (t)	1 tonne (t) = 1,000 kilograms (kg)
	= 1.1 short tons
VOLUME (APPROXIMATE)	**VOLUME (APPROXIMATE)**
1 teaspoon (tsp) = 5 milliliters (ml)	1 milliliter (ml) = 0.03 fluid ounce (fl oz)
1 tablespoon (tbsp) = 15 milliliters (ml)	1 liter (l) = 2.1 pints (pt)
1 fluid ounce (fl oz) = 30 milliliters (ml)	1 liter (l) = 1.06 quarts (qt)
1 cup (c) = 0.24 liter (l)	1 liter (l) = 0.26 gallon (gal)
1 pint (pt) = 0.47 liter (l)	
1 quart (qt) = 0.96 liter (l)	
1 gallon (gal) = 3.8 liters (l)	
1 cubic foot (cu ft, ft^3) = 0.03 cubic meter (m^3)	1 cubic meter (m^3) = 36 cubic feet (cu ft, ft^3)
1 cubic yard (cu yd, yd^3) = 0.76 cubic meter (m^3)	1 cubic meter (m^3) = 1.3 cubic yards (cu yd, yd^3)
TEMPERATURE (EXACT)	**TEMPERATURE (EXACT)**
[(x-32)(5/9)] °F = y °C	[(9/5) y + 32] °C = x °F

QUICK INCH - CENTIMETER LENGTH CONVERSION

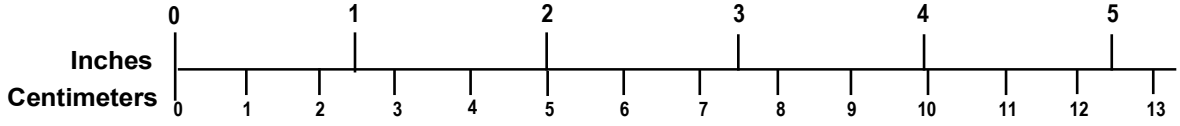

QUICK FAHRENHEIT - CELSIUS TEMPERATURE CONVERSIO

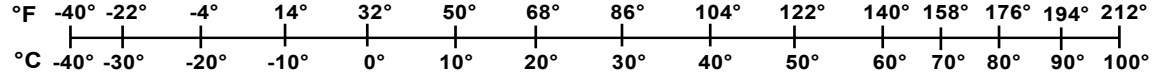

For more exact and or other conversion factors, see NIST Miscellaneous Publication 286, Units of Weights and Measures. Price $2.50 SD Catalog No. C13 10286

Updated 6/17/98

Acknowledgements

The authors would like to convey our thanks to Francisco González, III, Program Manager, Hazardous Materials & Tank Car; Kevin Kesler, Chief (Former), Federal Railroad Administration (FRA) Rolling Stock Research Division; and Dr. John Tunna, Director (Former) of the FRA Office of Research, Development and Technology for their support.

Our sincere gratitude is also due to Mr. Karl Alexy, Director, Hazardous Materials Safety, Office of Safety for his technical guidance and encouragement.

Contents

Illustrations

Tables

Executive Summary

Given the known accident history associated with hazardous material transport, the tank car community has been focused on improving the performance of tank cars against the potential for puncture under derailment conditions. Proposed strategies for improving puncture performance have included design changes to tank cars, as well as operational considerations such as reduced speeds and improved braking performance. Since puncture hazards have a wide variety of impactor sizes, shapes, speeds, etc., it has been difficult to quantify objectively and globally, the overall 'real-world' safety improvement resulting from any given proposed change.

An earlier letter report on the subject described the prior work [1]. The research was conducted through May 2015 by Sharma Associates, Inc. at their facility with funding from the Federal Railroad Administration. This report describes how this effort was extended to include additional cases, additional speeds, and additional considerations for alternate brake systems. Much of the original descriptive language from this earlier report has been retained to make this document more complete [1].

This report describes an innovative and objective methodology for quantifying and characterizing the reductions in risk (or reductions in puncture probabilities) that may result from changes to tank car designs or the tank car operating environment. The methodology captured several parameters that are relevant to tank car derailment performance—including multiple derailment scenarios, derailment dynamics, impact load distributions, impactor sizes, operating conditions, tank car designs, etc.—and combined them into a consistent probabilistic framework that can estimate the relative merit of proposed mitigation strategies.

For example, the methodology estimated that the impact performance of a proposed tank car design with a 9/16" thick shell, 11-gage jacket and ½" full-height head shield would be over 50 percent better than the performance of a base case Department of Transportation (DOT)-111 tank car. Similarly, the analysis also estimated that reducing the operating speed from 40 mph to 30 mph offered a 42 percent reduction in puncture likelihood for the proposed design. The methodology also estimated that the use of Electronically Controlled Pneumatic (ECP) braking results in about 30 percent fewer punctures during a derailment.

A comparison of the estimates from this methodology to actual derailment data suggested that the gross dynamics of a tank car train derailment and the resulting puncture performance of the tank cars were captured well by this methodology. In addition, the model's estimates regarding the number of cars derailed and number of punctures, as a function of train speed, compare favorably with actual derailment data. Also, puncture risk reduction correlates well with the engineering estimates that correspond to increased tank shell thickness and material strength. These validation efforts improved the credibility of the methodology's efficacy and the results derived from it.

1. Introduction

Given the known accident history associated with hazardous material transport, the tank car community has focused on improving the puncture performance of tank cars under derailment conditions. As the number of shipments by rail of hazardous material (particularly crude oil) has increased, the focus on improving safety, either through changes in tank car design or train operations, has further intensified.

This safety effort focused on enhancing safety by improving the design of tank cars and limiting operating speeds. As the tank car community reviews potential mitigating solutions for implementation, it becomes critical to have an objective measure of the expected improvements (i.e., reductions in risk or probability of puncture) that these solutions afford. While the industry has made progress towards developing analytical techniques that quantify puncture resistance for specific designs and specific impactor sizes, objective mechanisms to translate these analyses into overall safety improvement do not currently exist.

Tank cars are exposed to a wide range of hazards during derailments, including different impactor sizes, impactor shapes, impact speeds, etc., which makes it difficult to quantify the overall 'real-world' safety improvement from any given change. To objectively compare the overall effectiveness of a proposed mitigating solution, whether it is a thickness increase or an operational change, one needs to measure how the solution is expected to perform in real life against a variety of potential hazards. From a regulatory or a standards perspective, one needs to be able to answer questions such as:

- *What is the overall reduction in risk (or reduction in the probability of puncture) afforded by increasing the minimum required shell thickness to "X" inches?*
- *What is the overall reduction in risk (or reduction in the probability of puncture) afforded by making a given operational change/speed restriction?*

This research effort addressed this with a methodology which calculated resultant puncture probabilities and risk reduction in an objective manner. It connected the load environment under impact conditions to analytical and test-based measures of tank car puncture resistance capacity (which have been further adapted for expected operating conditions). While the methodology is not supposed to predict the precise results of a given accident, it provided a basis for comparing the relative benefits or risk reduction resulting from various mitigation strategies.

An earlier letter report describes prior work on this subject [1]. This report documents additional work done, including the consideration of additional designs, additional operating speeds, and alternate braking systems.

2. Overview of Technical Approach

The probability that a given tank car be punctured during a derailment is affected by multiple variables and circumstances, including:

- The derailment scenario, including the speed of derailment initiation, the surrounding terrain, etc. For example, higher derailment initiation speeds tend to lead to more cars derailing as well as higher magnitudes of forces, and thereby, a higher probability of puncture. The surrounding terrain can also have a significant effect on how the derailment unfolds and thus affect puncture probabilities
- The derailment (impact) load spectrum experienced by the tank during the event: the higher the load, the higher the probability of puncture
- The distribution of impactor sizes: the smaller the impactor, the higher the probability of puncture
- The puncture resistance of the tank shell: the thinner the tank shell, the higher the probability of puncture

The approach taken in this report combines the above parameters and circumstances to evaluate the probability that a certain number of tanks of a given design might experience puncture during a derailment event. Rather than focusing on specific values of the above parameters, this approach allows one to consider a nominal distribution of values for each given parameter to ensure that the method is not specific to or biased towards any particular event or circumstance. An overview of this approach is presented in Figure 1. Validation of the model against known historical derailment data is a critical element of the overall methodology.

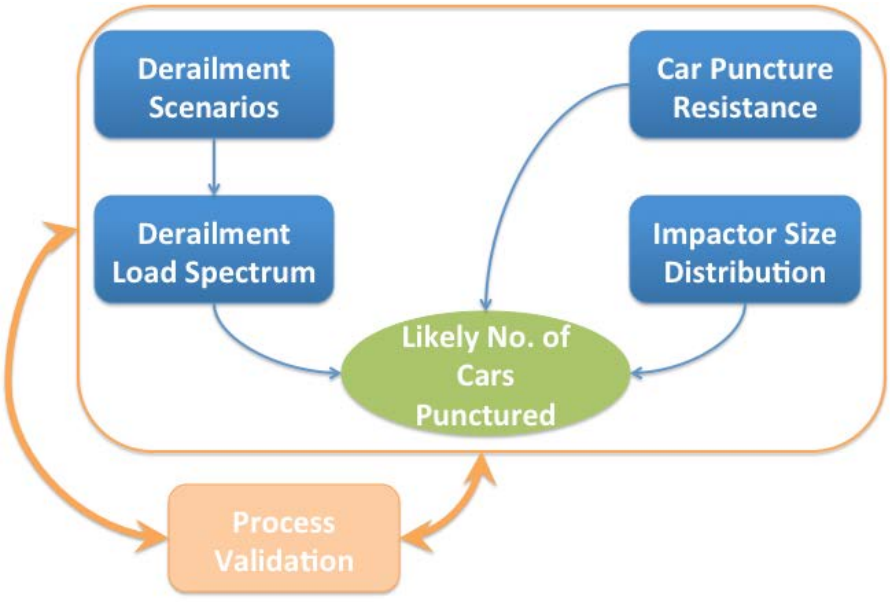

Figure 1. Overall Concept of Approach

3. Detailed Methodology

The overall methodology outlined below was used to estimate the likely number of punctures for the base case and propose mitigating strategies, such as a thicker tank shell or reduced operating speeds. It does the following:

- Develop a consistent measure of the load environment associated with nominal tank car derailments by using multiple derailment simulations to derive a histogram of 'nominal' impact forces.
- Quantify the puncture resistance of given tank car designs for a nominal range of impactor sizes and impact forces by using past published research.
- Evaluate the safety performance or probability of puncture for a set of designs and operating conditions by combining the load environment histograms, the puncture resistance curves, and nominal impactor size distributions.
- Confirm the validity of the methodology by reviewing engineering expectations and comparisons to historical data.

While all elements of the proposed methodology have not been combined to evaluate risk reduction before, individual elements such as derailment dynamics modeling or tank puncture resistance modeling are established technical approaches [2] [3]. Additionally, the car puncture resistance curves for several conventional designs have been developed and published by the FRA [4], thereby lending higher confidence to the approach undertaken. The following sub-sections outline the methodology in more detail.

3.1 Modeling the Derailment Scenarios

The load environment associated with derailments events is not easily quantified. While one can broadly infer the magnitude of forces involved in a derailment event after the event has occurred, there is little or no data available on the specific impact loads that are generated during a derailment event. Each derailment event generates not one, but a spectrum of forces, as each tank car is impacted by other tank cars in its vicinity, as well as by other objects in the vicinity of the derailment site. Given the lack of empirical (or other) data associated with derailment loads, this approach has estimated the forces generated during a derailment through detailed computer simulations of derailment events. These computer simulations model the derailment dynamics of a tank car train operating at a given speed by initiating the derailment event through a brief, externally applied force on the leading car and then allowing the derailment to unfold, as defined by the physical circumstances of that derailment.

Simulation of derailments requires the use of a finite element modeling program with an explicit integration mechanism, and the capability to incorporate complex contact algorithms, nonlinear material models, and nonlinear dynamics. LS-DYNA3D is an explicit finite element solver that meets these requirements and was used for all the derailment simulations reported here [5]. Detailed derailment simulations are inherently computationally intensive.

To optimize computational efficiency without compromising the fidelity of the simulations, the following assumptions were made:

- The trains simulated were composed of up to 100 loaded (to 263,000 lb.) tank cars.

- The cars were individually modeled in three dimensions (3D), with appropriate representation for the tank shells, tank heads, and stub sills. Shell elements with a Belytscko-Tsay formulation were used with a nominal element length of 12 inch, with finer mesh densities where appropriate.
- Trucks and track were not explicitly modeled for this effort; instead, the car center plates were defined to move along the centerline of track through a lateral spring connection between the car and the ground, with the spring stiffness representing a measure of the lateral track stiffness; when the displacement of this spring exceeded a nominal 1 inch, the truck was considered to have derailed and the center plate was subsequently free to move laterally.
- The cars were modeled with deformable TC128 material, and connected with discrete draft gear and coupler models. The coupler models allowed a 7 degree swing in each direction, with the knuckles modeled to resist rotation and fail when the rotation exceeds 13.5 degree, which is consistent with the coupler rotation limits defined for E-type couplers in the AAR Manual [6]
- The tanks were free to move in any direction, while on the bolsters and were constrained to move in a horizontal plane (i.e., the tanks were allowed to slide, but not roll over).

The derailment scenarios were simulated on level, tangent track, with the leading truck of the first car subjected to a brief lateral force to initiate the derailment. Upon initiation of derailment, a retarding force equivalent to an emergency brake application is imparted to all the cars, propagating from the front (point of derailment) to the rear of the train, for a train with conventional brakes. The retarding force applied was 13,255 lb. per car which represents an emergency associated with a 12 percent Net Braking Ratio (NBR). A pneumatic emergency propagation rate of 950 ft/s was used with a 12 second build up time. In the case of trains equipped with two-way End-Of-Train (2-EOT) devices, the brake signal propagation was initiated at both ends of the train. For trains with ECP, it was assumed that all cars would get the braking signal simultaneously. Figure 2 presents the results of one simulation, showing the post-derailment state of the cars, which is generally consistent with the 'accordion' type pile-ups observed in multiple real-life derailments.

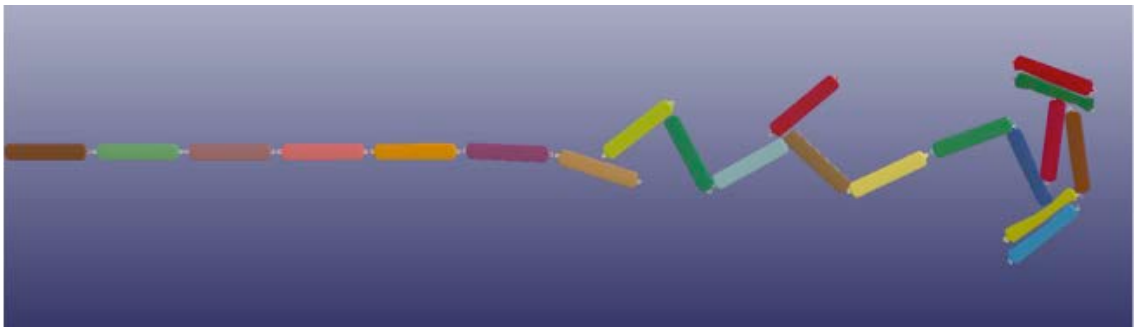

Figure 2. Example of a Pile-up Resulting from a Simulated Derailment at 30 mph

As noted earlier, the intent of this effort was to evaluate the effect of a given mitigating strategy in a 'global' sense, instead of tying the simulation to a specific event or set of circumstances. A key goal was to make sure that the results of this effort could be applied broadly, and this

required the development of a force spectrum that could be associated with a universal 'nominal' derailment, rather than a specific one. However, collision or derailment events are chaotic and can unfold very differently, depending on the specific circumstances of a given derailment. Among others, the specific sequence of events and impact loads associated with a derailment could vary depending on:

- **The underlying terrain where the derailment occurs:** A derailment in the muddy soils of the southeastern US, could unfold quite differently compared to a derailment in the frozen ground (during winter) of the northern states.
- **The speed of derailment initiation:** The higher the speed at the point of derailment initiation, the higher the kinetic energies are, and thus, higher the forces and damage levels
- **The severity of derailment initiation:** This represents an 'initial condition' for the derailment and variations in whether the derailment was initiated by a 'gentle' wheel climb, or, a more abrupt event such as track/equipment failure, would result in different derailment sequences
- **The quality of track:** Flexible track of poor quality could lead to more cars jumping rail once a derailment is initiated, compared to a higher quality, stiffer track, which can provide a higher level of lateral restraint.

In order to derive a "nominal" force spectrum not from the simulation of a single derailment, but from a set of derailments that reasonably represent the variations in conditions outlined earlier, a series of simulations varying the following parameters were run:

- *Three values of coefficient of friction between tank cars and ground to represent multiple terrain conditions: 0.27, 0.30, and 0.33.* This range is consistent with nominal values for friction between steel and soil, which generally range from 0.2 to 0.4. Higher friction values, especially values that are near 1.0 are unrealistic and represent conditions that are closer to 'rubber-on-concrete', rather than 'steel-on-soil.' As an example, a friction level of 1.0 would result in a tank car traveling at 50 mph to decelerate to a stop in 84 ft (less than 1.5 car lengths); there is very little evidence of 50 mph derailments coming to a stop within 1.5 car lengths. Essentially, the range of friction factors used in the analysis is a reasonable blend that allows the relative performance of car designs or mitigating strategies to be evaluated consistently.
- *Three initial train speeds: 30, 40 and 50 mph.* This parameter represented the speed of the train when the derailment was initiated, and not the relative velocity between impacting cars. This range of speeds is consistent with the speeds of several recent derailments, particularly, ones with a notable potential for damage.
- *Three values of lateral force to initiate derailment: 50, 70 and 90 kips.* These values represented a truck side lateral force/vertical force (L/V) ratio of 0.76 to 1.06; a value of 0.6 is considered a safety limit for rail roll over and higher values would be needed to initiate a derailment, as used here.
- *Two values of lateral track stiffness, representing variations in track quality: 30 and 40 kips/in*. The 40 kips/in value represented a truck side L/V ratio of 0.6 at 1 inch of lateral wheel movement, while the 30 kip/in value represented poorer quality track that was 25 percent more flexible

In general, the assumptions made in setting up these and other similar simulations not only reflect physical conditions, but also the preferences of the analyst, as well as requirements for simulation efficiency and speed. This set of simulations is no different, and the authors acknowledge that other analysts and researchers may choose to make different assumptions. Nonetheless, the goal is to effectively evaluate the relative performance of multiple designs and operating conditions, and it is expected that the assumptions made herein will allow for an effective comparison.

3.2 Impact Load Spectrum

The permutations and combinations presented above represent 18 different derailment scenarios for each speed. In other words, rather than having a single derailment represent the dynamics and force distribution, the ‘nominal’ force distribution is an aggregation of forces from a ‘family’ of 18 derailments for each initiating speed.

Figure 3 presents, as an example, the final pile-up images for each of the 18 runs for the derailment initiation speeds of 30 mph. As evident from these images, this set of runs reflects a reasonable breadth of derailment scenarios, which supports the contention that this methodology generates a ‘nominal’ force histogram associated with a ‘nominal’ derailment.

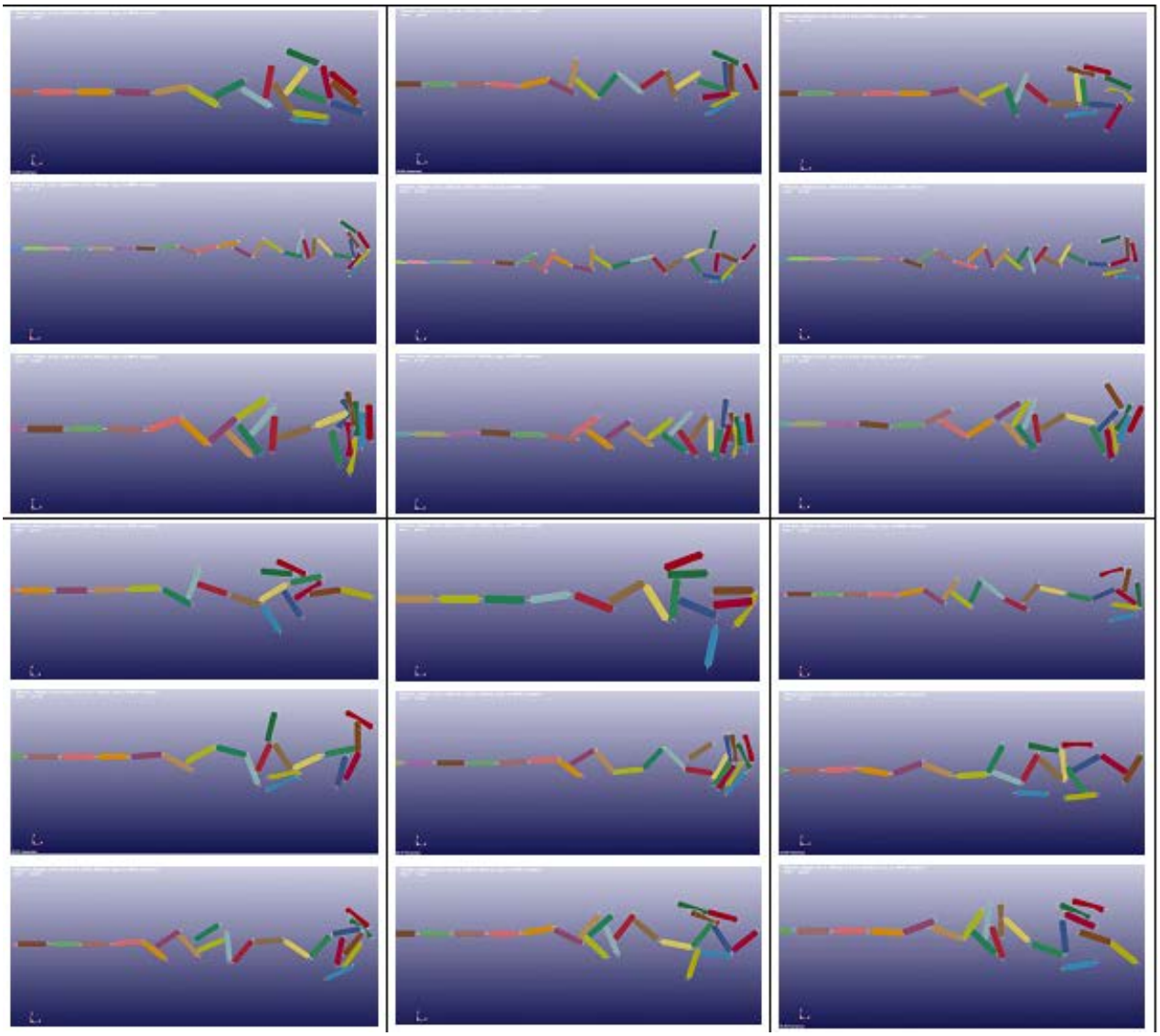

Figure 3. Distribution of Derailments - Final Pile-ups from 18 Scenarios at 30 mph

Each simulation results in several impacts between the involved cars. On average, there were about 28 collisions in a 30 mph derailment, about 44 collisions in a 40 mph derailment, and about 61 collisions in a 50 mph derailment. The forces generated at each impact (between any two cars) then analyzed to generate a histogram of forces associated with that derailment simulation.

The histograms from all simulations were accumulated and then averaged over the 18 simulations at each speed to generate a histogram of impact forces that might be experienced during a 'nominal' 30 mph, 40 mph or 50 mph derailment. Figure 4 presents this 'nominal' force histogram. As observed, the histogram approximates a normal distribution with lower force impacts being more frequent and higher force impacts being less frequent. It can also be observed that the increased speeds result in more numerous impacts at all force levels as well as impacts of higher force (and thus consequence).

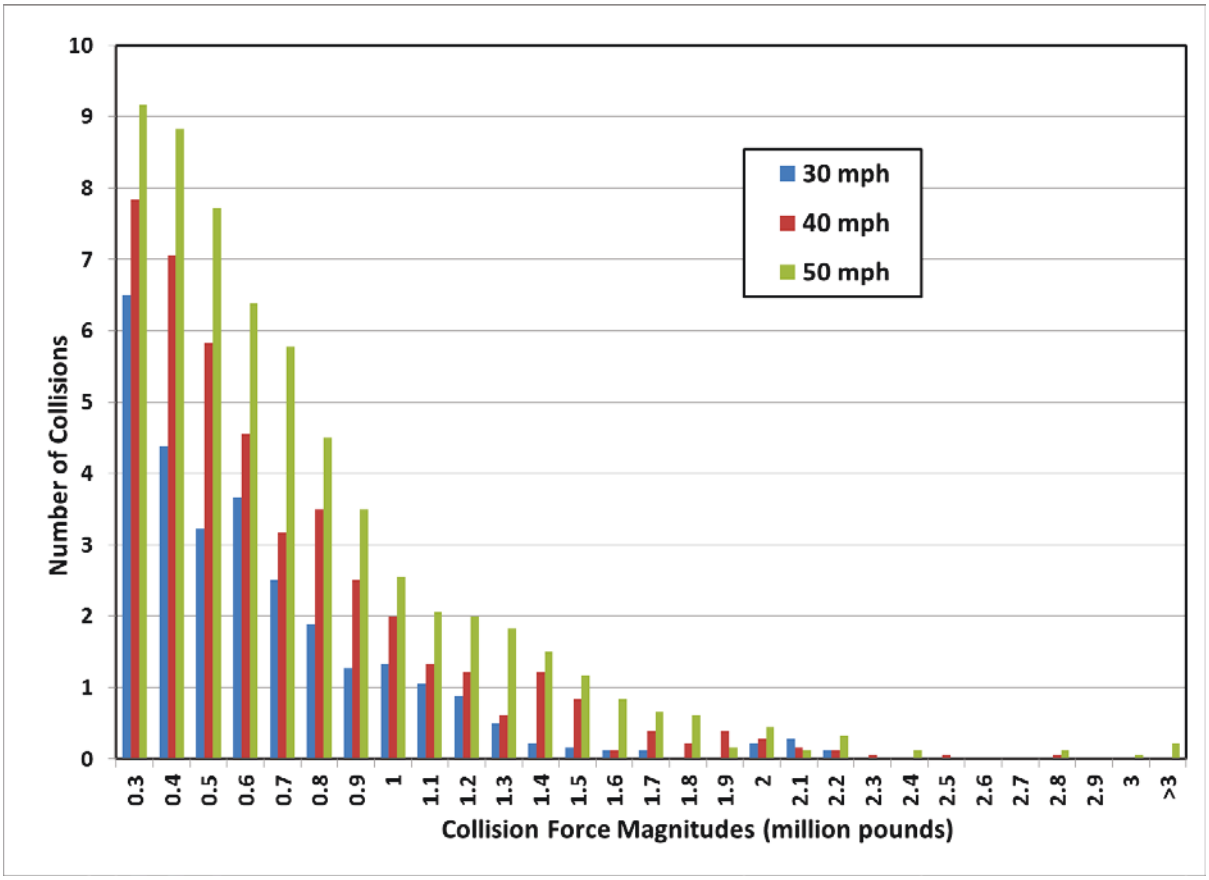

Figure 4. Histogram of Impact Loads Resulting from Derailments Averaged from 18 Scenarios Per Speed

3.3 Tank Car Puncture Resistance

For conventionally designed steel tank cars (which is the focus of the current effort), it is fundamentally based on the thicknesses of the key elements (shell, head, jacket, etc.), and the material properties of the steel used. FRA and the industry have sponsored several studies that have led to the development of detailed and reasonably validated models that can characterize the capacity of a given tank car design to resist an applied impact force (considering the size of the impactor).

Consider the example chart presented in Figure 5 [4]. Such charts were developed to characterize the puncture resistance of different tank car designs, from base-level DOT-111 tanks to modern tank designs. The results are based on detailed finite element analyses of tank shells and tank heads under a variety of puncture conditions, including various impactor sizes. A characteristic length that is the square root of the area of the impactor face defines these impactor sizes. For a baseline DOT-111 tank car (7/16 inch A-516-70 tank shell, no jacket), represented by the green line in Figure 5, a 3-inch impactor will puncture the tank at a little over 200,000 lb, and a 6-inch impactor would not puncture the tank until the force levels approach 400,000 lb. The chart essentially defines the force level at which a given impactor would puncture the tank shell, or in other words, the chart defines the impactor size that would result in tank puncture for a given force level.

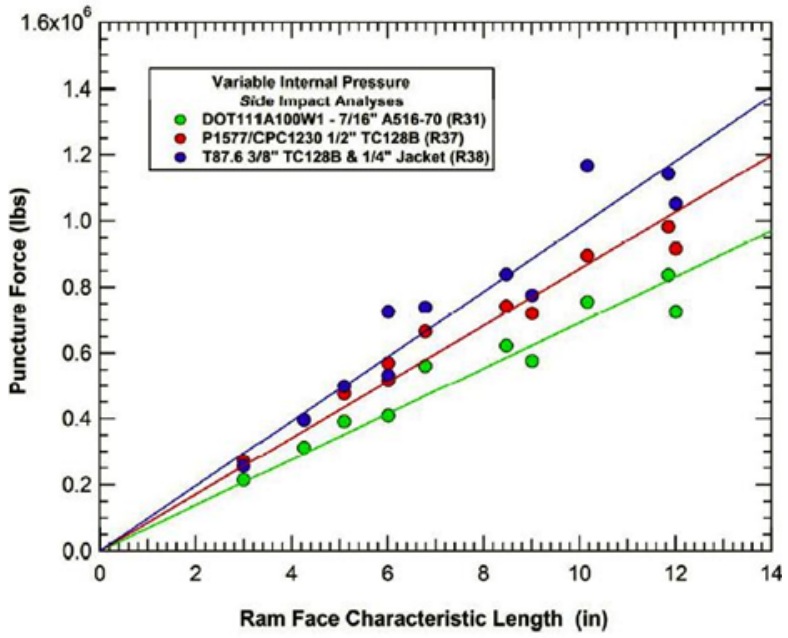

Figure 5. Capacity of Tank Car to Withstand Impact

3.4 Impactor Distributions

Under derailment conditions, a given tank car may be subject to impacts from a variety of impactors, including broken rail, coupler heads and shanks, wheels/truck components, as well as blunt impact from other tanks. These impactors vary in size, ranging from less than 3 inch to more than 12 inch, and it is difficult to gather consensus on what a "nominal" impactor is. Given that smaller impactor sizes increase the chances for a tank shell puncture, assuming too small of an impactor size can lead to very conservative results, and assuming too large an impactor size can lead to risk underestimation. In this approach, the actual impactors are not explicitly modeled; rather, a distribution of impactor sizes is assumed.

For these analyses, the impactor distribution shown in Figure 6 was used. This distribution assumes that a large majority of impactors (about 71 percent) are in the range from 3 inch to 9 inch, with a small fraction of impactors (3 percent) being smaller, and the rest being larger. About 5 percent of the impactors were considered to be blunt (other tanks). While there is no hard basis for the specific sizes assumed herein, these assumptions are consistent with engineering expectations, and appear to be consistent with real life observations.

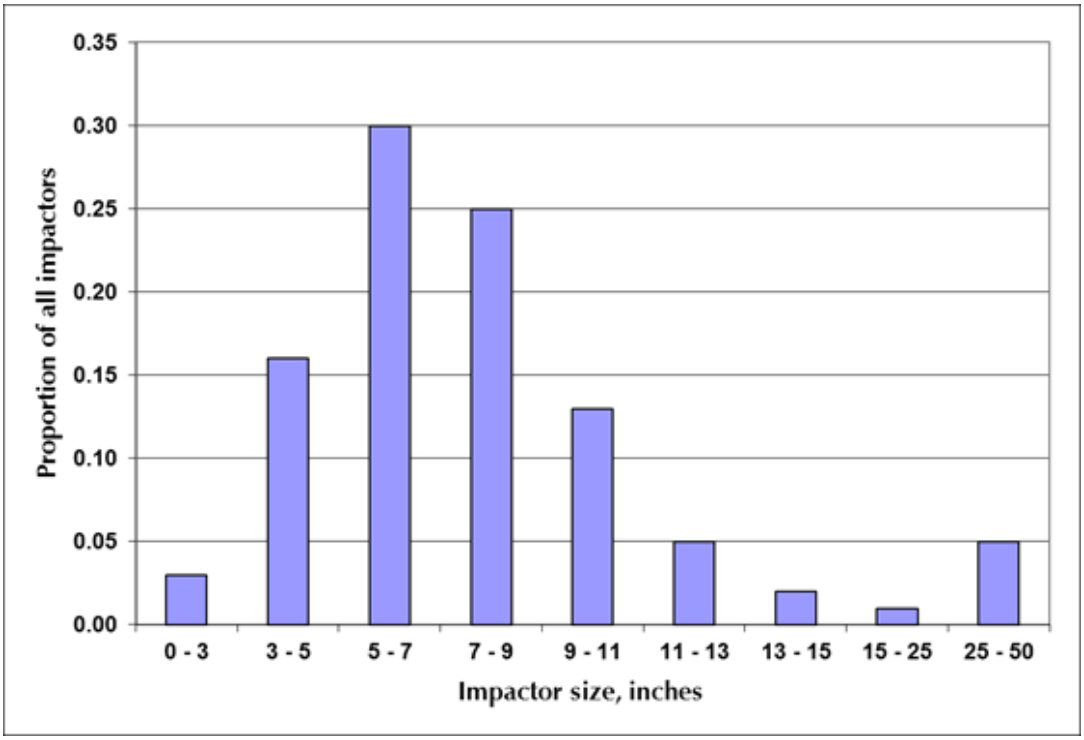

Figure 6. Assumed Impactor Distribution

Prior external review of this work suggested that the distribution above might be skewed towards smaller impactors. However, S. Kirkpatrick stated in page 2 of reference [4] that if the combinations of complex impactor shapes (such as couplers and broken rail) and off-axis impactor orientations are considered, many objects will have the puncture potential of an impactor with a characteristic size that is less than 6 inches.

In addition, to ensure that the assumed impactor distribution does not skew the results (i.e., evaluation of relative merits), a sensitivity analysis of the impactor size distribution was conducted. This effort is described in Appendix A, and identified that the **relative performance** of tank car designs or operating conditions was not very sensitive to the impactor distribution assumed, lending additional confidence to the results developed from this effort.

3.5 Distribution of Head vs. Shell Impacts

The puncture resistance of tank heads is generally quite different from that of the tank shell, due to differing thickness (presence of head shield) and curvature geometry. Typical tank head strengths have been characterized by the prior FRA work and are represented, in a manner similar to the curves illustrated in Figure 5, by varying slopes of puncture force as a function of impactor size. Knowing how the collisions in a derailment are distributed between head and shell impacts allows the methodology to take the different puncture resistances into account. An analysis of the reported head and shell punctures from 16 hazmat release incidents (2006-2014)

indicates that the distribution of impacts between head vs. shell is approximately 50 percent / 50 percent[1].

3.6 Likelihood of Puncture

With the load histograms, car capacities, and impactor distributions in place, the likely number of punctures for a given car design can be calculated. The process is as follows:

1. The appropriate car capacity curves (one each for shell and head design) are selected for the car design that is being analyzed. For example, the shell of a base case DOT-111 car is represented by the green line in Figure 5.
2. For each load magnitude (bin) in the load histogram, the impactor size that will result in car puncture is evaluated for every car capacity curve (head and shell).
3. The proportion of impactors that fall below that size threshold, based on the distribution of impactors (Figure 6), represents the probability that a load of that magnitude will result in a car puncture.
4. Probabilities are then weighted by the corresponding prevalence of the impact type (head or shell) and combined with the number of collisions in the corresponding magnitude bin.
5. By accumulating this probability over all the load bins in the histogram, the probability of any specific number of punctures is calculated.
6. The number of punctures with the highest probability (the most likely number of punctures) is a measure of the damage severity.

As an example, Table 1 (below) presents the results of such an analysis for two different car designs over two different derailment initiation speeds. The resultant comparisons across designs and across speeds, allows one to evaluate the relative merits of each mitigating strategy. As observed, the model is predicting that an alternate tank design with a 9/16 inch TC128 shell, 11 gauge jacket and full-height head shield will perform 52 percent better than a base DOT-111 car in a 40 mph derailment. The model also predicts that the same alternate car will be 42 percent more likely to survive if the derailment happened at 30 mph rather than 40 mph.

Results of the analysis for other designs, other speeds, and other braking configurations are presented in Section 5.

Table 1. Model Estimates for Likely Number of Punctures

		Most Likely Number of Punctures		% Improvement Compared to Base Case		% Improvement Due to Speed Reduction
	Tank Type	**30 mph**	**40 mph**	**30 mph**	**40 mph**	**40 to 30 mph**

[1] FRA derailment data, as received in email from Karl Alexy on 3-Oct-2014.

Base Case	7/16" A516-70 No Jacket No Head Shield	8.5	13.7	~	~	38%
Alternate	9/16" TC128B 11 Gauge Jacket 1/2” Head Shield	3.8	6.6	55%	52%	42%

3.7 Summary

In summary, the methodology presented here is used to estimate the relative merits of multiple strategies proposed to improve tank car safety, whether they are in the form of car design improvements or operational restrictions. The next challenge is to verify that the estimates are consistent with expectations from accident histories.

4. Validation

Validating a methodology ensures that it generates applicable results. Naturally, the validation process might take different forms depending upon the particular issue that is being studied and the availability of accurate real life or test data against which a validation effort can be initiated.

In this case, a two-step validation effort evaluated whether the estimates and predictions made were consistent with historical data. The first step was to ensure that the dynamic derailment simulations were predicting reasonable and consistent results. The second step was to verify whether the estimates of likely numbers of punctures were consistent with observations.

4.1 Dynamic Model Validation

There are no historical records of the force levels associated with tank car punctures under derailment conditions, but data on the number of cars derailed in a given incident are available. Figure 7 compares the number of derailed cars with the train speed for derailment data from the FRA-RAIRS database and the data from the derailment simulations that were generated during this research. According to Figure 7, the simulated predictions of number of cars derailed were consistent with the spread seen in actual derailment data.

Figure 8 presents a similar comparison only using data from recent major tank car derailments (presented in Table 2). Once again, the average of the predictions is in line with the observed data.

These comparisons lend validity to the derailment simulations, confirming that the dynamics predicted by the simulations are consistent with real life observations. Critically, they also demonstrate that the simulations are not just a single point of reference; rather, that they represent a nominal and diverse variety of circumstances, lending credence to the notion that the resulting force histograms are also representative of a 'nominal' derailment.

Table 2. Recent Hazardous Material Derailments

Accident	Speed (mph)	Total cars derailed	Total punctures
LaSalle, CO - May, 2014	9	6	0
Lynchburg, VA - May, 2014	23	17	1
Vandergrift, PA - February, 2014	30	21	1
New Augusta, MS - January, 2014	45	20	5
Plaster Rock, NB - January, 2014	47	19	2
Casselton, ND - December, 2013	42	21	20
Aliceville, AL - November, 2013	38	26	25
Lac-Megantic, QC - July, 2013	65	64	59

Paulsboro, NJ - November, 2012	8	7	
Plevna, MT - August, 2012	25	18	2
Columbus, OH - July, 2012	23	17	1
Tiskilwa, IL - October, 2011	37	26	5
Arcadia, OH - February, 2011	46	33	29
Windham, CT - March, 2010	10	4	0
Cherry Valley, IL - June, 2009	36	19	13
Luther, OK - August, 2008	19	14	3
Painesville, OH - October, 2007	48	31	1
Oneida, NY - March, 2007	47	29	
Shepherdsville, KY - January, 2007	47	26	
Cambria, MN - November, 2006	23.5	7	
New Brighton, PA - October, 2006	37	23	14
Minot, ND - January, 2002	41	31	

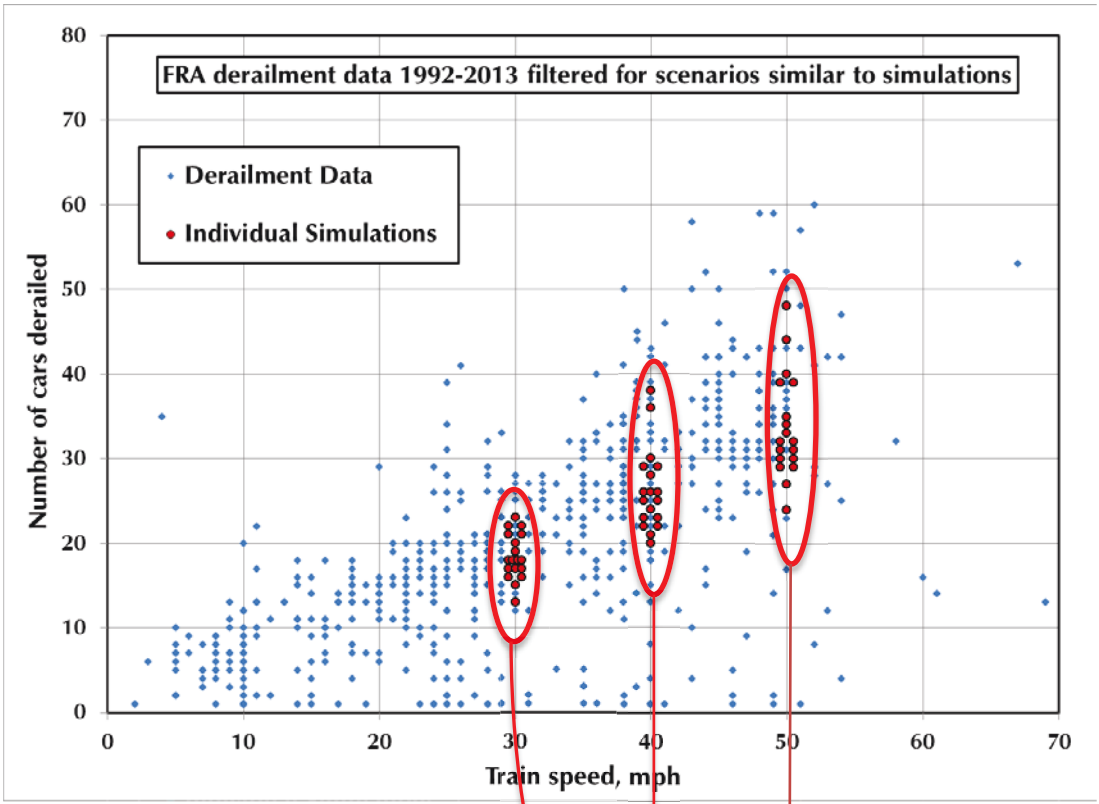

Figure 7. Number of cars derailed vs. Train speed – All derailments

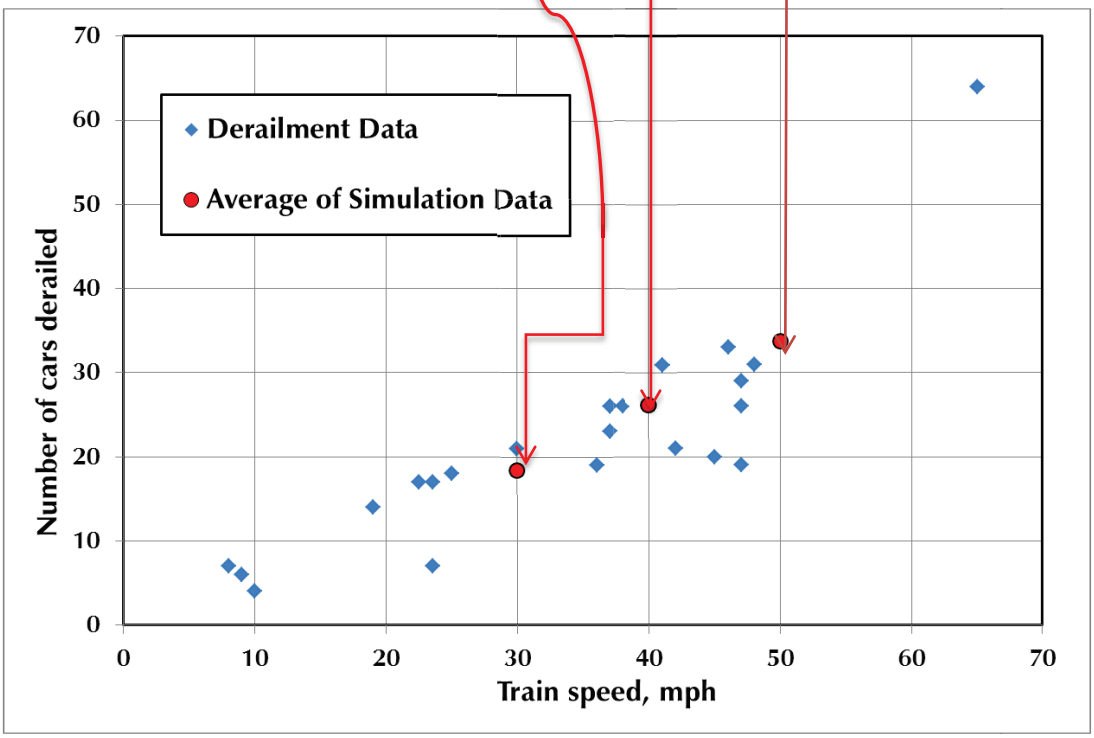

Figure 8. Number of Cars Derailed vs. Train speed – Hazmat Derailments Only (from Table 2)

4.2 Validation of Puncture Estimates

The validation described in Section 4.1 lent confidence to the force histogram data extracted from the derailment simulations. Next, the estimates of likely number of punctures were compared to actual derailment data. Figure 9 compares the model estimates to the number of punctures observed in the various derailments listed in Table 2, including several in which a long string of tank cars, (similar to a unit train) were involved. As expected, the actual derailment data has a wide scatter band (which increases with increasing speed); however, the predictions of the model are well within the cluster of actual values.

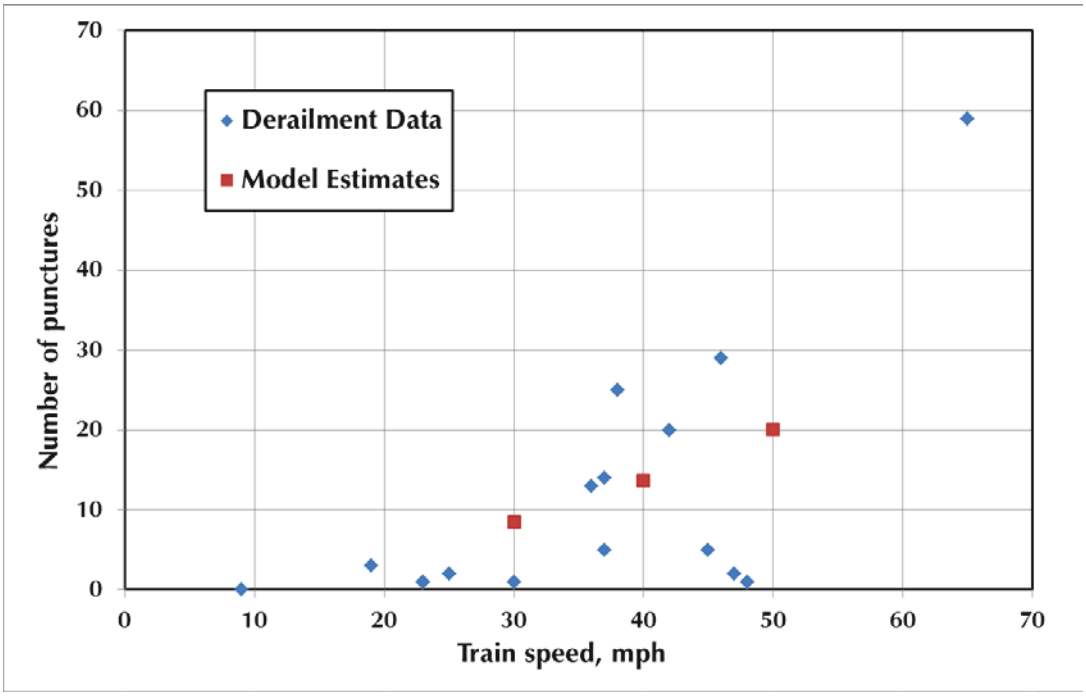

Figure 9. Estimates of Likely Punctures Compared to Derailment Data

5. Relative Performance of Mitigating Strategies

Once this objective methodology was established and validated, work continued on extending the effort to evaluate the relative performance of a larger variety of tank designs and train operating conditions. For the 100-car model, a matrix of simulations was established consisting of three initial speeds (30, 40 and 50 mph), four tank designs (base case and three stronger alternatives), and three braking systems (described below). Table 3 shows the most likely number of punctures calculated for each case of this matrix, as applied to a train of 100 cars in which the derailment occurs near the head end.

For each set of simulations, puncture probability was evaluated for the following tank designs, which are based on FRA proposed tank design standards.

- *Base case*: 7/16" thick A516-70 shell, no jacket, no head shield
- *Alternative #1*: 7/16" thick TC128 shell, 11 gauge jacket, 1/2" full-height head shield
- *Alternative #2*: 1/2" thick TC128 shell, 11 gauge jacket, 1/2" full-height head shield
- *Alternative #3*: 9/16" thick TC128 shell, 11 gauge jacket, 1/2" full-height head shield

Table 3. Most Likely Number of Punctures: 100-Car Train, Derailment at Head End

Tank Type		Speed, mph	Conventional Brakes	2-way EOT (DP: lead + rear)	ECP Brakes
Base Case	7/16" A516-70, no jacket, no head shield	30	8.5	7.2	6.1
		40	13.7	12.1	9.8
		50	20.1	16.3	14.9
Alternate 1	7/16" TC128, 11 gauge jacket, 1/2" full-height head shield	30	4.7	3.9	3.3
		40	8.0	7.1	5.3
		50	12.2	9.8	9.1
Alternate 2	1/2" TC128, 11 gauge jacket, 1/2" full-height head shield	30	4.3	3.6	2.9
		40	7.3	6.5	4.8
		50	11.2	9.0	8.3
Alternate 3	9/16" TC128, 11 gauge jacket, 1/2" full-height head shield	30	3.8	3.2	2.6
		40	6.6	5.9	4.3
		50	10.2	8.2	7.6

In addition to conventional pneumatic braking, derailment simulations were also conducted with alternate braking systems. Electronically Controlled Pneumatic (ECP) braking, where all cars are braked simultaneously, and End-of-Train (EOT) braking, in which the emergency brake signal is

initiated simultaneously at both the front and rear of the train, were simulated. EOT braking can be accomplished with either a two-way EOT device or with a remote distributed power (DP) consist at the rear of the train. For the EOT simulations, since the derailment occurred near the front of the train, it was assumed that the lead locomotive immediately transmitted the emergency brake command to the rear of the train. The EOT simulation, in essence, treated the emergency brake signal as initiating from both ends of the train simultaneously and then propagating pneumatically from each end toward the center of the train.

Only considering those scenarios where the derailment occurs near the front of the train overstates the benefit of the EOT and DP brake systems as compared to the benefit of an ECP brake system. If the derailment occurs anywhere in the rear half of the train, the EOT/DP feature offers no advantage over a conventional brake system in a head-end only train. Most derailments result in a 'break-in-two' scenario, where the intact front segment of the train has clearly separated from the derailing rear segment of the train and the front "un-derailed" train segment does not participate in the braking of the rear "derailed" segment. Thus, the brake response of the rear "derailed" segment (the segment that is the focus of this effort) is identical to that of a conventional head-end only train because the entire portion of the train behind the point of derailment (POD) has already begun braking before the emergency signal reaches the head end. If or when the radio brake signal from the rear of the train does reach the head end, any safety benefit imparted to the front "un-derailed" segment is inconsequential to the rear "derailing" segment, as the train has already separated.

If we assume that the POD within the train is equally distributed along the length of the train (as suggested by other reviewers), EOT/DP systems would offer no benefit over conventional head-end-only systems for fully one-half of the derailments, i.e., ones that are initiated in the second half of the train. For the other half of the derailments, the benefits would vary from the predicted peaks benefits if the derailment was initiated at the front end, down to zero benefit if the derailment was initiated at the mid-point. Thus, if one assumes that the POD within the train is equally distributed along the length of the train, the effective benefit of EOT/DP systems would only be one-fourth of the predicted benefit calculated based on head end derailment initiation. Ideally, instead of assuming that the POD is equally distributed, benefit calculations could incorporate observed historical data about the location of derailment initiation to ensure that the benefits offered by advanced braking systems are effectively quantified. Conversely, ECP brakes always offer an advantage (over conventional brakes) regardless of the derailment location in the train, though the magnitude of the performance benefit may vary.

To investigate the effects of various train lengths on the methodology, and recognizing that derailments can initiate anywhere within a train, several sets of simulations (but not the complete matrix) were performed with trains of 80, 50, and 20 cars. Results of these simulations were submitted to DOT. For a given speed, tank design and brake type, shorter trains had fewer punctures. This is expected due to the lower overall kinetic energy in the train behind the POD. The relative benefit, however, of increased tank thickness and/or reduction of train speed is similar to the corresponding benefit seen for the 100-car train with derailment occurring near the front. The risk reduction benefits for alternate braking systems, in contrast, are most pronounced for long trains with many cars behind the POD. Since emergency brake signal propagation is very quick on short trains, especially if initiated at both ends simultaneously, the relative amount of puncture reduction due to the alternate braking systems EOT and ECP is diminished as the number of cars behind the POD decreases.

The effect of the alternate brake systems on the simulated derailment dynamics is displayed in Figure 10. For each combination of speed and brake type, the range of derailed cars (minimum and maximum) over the set of 18 simulations is shown as a vertical bar, and the average value is also indicated. The number of derailed cars generally increases with increasing speed, as expected. At any given speed, ECP braking shows a clear advantage over the other brake systems—both a lower average number of cars derailed and a narrower range, the later possibly due to the reduced slack action associated with ECP braking.

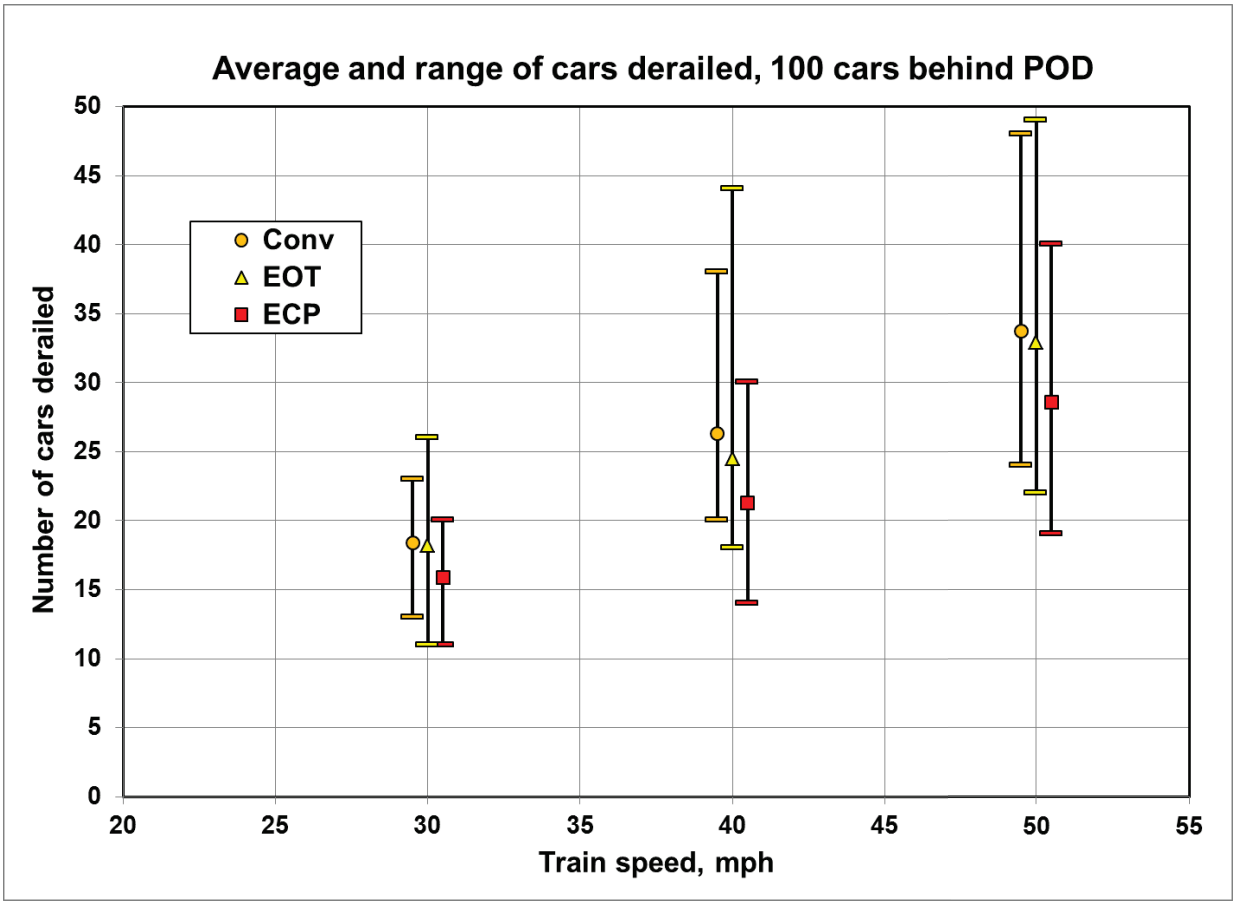

Figure 10. Average and Range of Cars Derailed for Various Brake Systems

Table 4 through Table 6 present the estimated risk reduction (percent improvement) associated with various mitigating measures (brake system employed, tank design, and train speed) for a train of 100 cars in which the derailment occurs near the head of the train. Depending on the train speed and tank design used, ECP brakes can be expected to provide about 30 percent reduction in the number of punctures. EOT brakes, at an average of 16 percent reduction, appear to offer about half the benefit of ECP. A tank designed according to the proposed FRA standard (9/16 inch thick TC128 shell with 11 gauge jacket and 1/2 inch full-height head shield) is estimated to cut the puncture risk in half (over 50 percent improvement) compared to the current base case design. The benefit due to speed reduction varies more, but in general, a 10 mph reduction from 50 to 40 mph results in a 34 percent average reduction in punctures, while a 41 percent improvement is expected from 40 to 30 mph. Comparing the 100-car model performance with ECP to its performance without ECP at speeds from 30 to 50 mph, it appears that using

ECP brakes could offer an 8 mph speed advantage; in other words, the risk exposure from derailing with ECP brakes at 40 mph is about the same as derailing with conventional brakes at 32 mph. Similarly, the risk exposure from derailing with ECP brakes at 50 mph is roughly equivalent to derailing with conventional brakes at 42 mph.

Table 4. Risk Improvement Due to Braking System

100 cars behind POD			Most Likely Number of Punctures			% Improvement due to brakes only		
	Tank Type	Speed, mph	Conventional Brakes	2-way EOT (DP: lead + rear)	ECP Brakes	Conventional Brakes	2-way EOT (DP: lead + rear)	ECP Brakes
Base Case	7/16" A516-70, no jacket, no head shield	30	8.5	7.2	6.1	0%	15%	28%
		40	13.7	12.1	9.8	0%	12%	28%
		50	20.1	16.3	14.9	0%	19%	26%
Alternate 1	7/16" TC128, 11 gauge jacket, 1/2" full-height head shield	30	4.7	3.9	3.3	0%	17%	30%
		40	8.0	7.1	5.3	0%	11%	34%
		50	12.2	9.8	9.1	0%	20%	25%
Alternate 2	1/2" TC128, 11 gauge jacket, 1/2" full-height head shield	30	4.3	3.6	2.9	0%	16%	33%
		40	7.3	6.5	4.8	0%	11%	34%
		50	11.2	9.0	8.3	0%	20%	26%
Alternate 3	9/16" TC128, 11 gauge jacket, 1/2" full-height head shield	30	3.8	3.2	2.6	0%	16%	32%
		40	6.6	5.9	4.3	0%	11%	35%
		50	10.2	8.2	7.6	0%	20%	25%
						Average:	**16%**	**30%**

Table 5. Risk Improvement Due to Tank Construction

100 cars behind POD			Most Likely Number of Punctures			% Improvement due to tank construction only		
	Tank Type	Speed, mph	Conventional Brakes	2-way EOT (DP: lead + rear)	ECP Brakes	Conventional Brakes	2-way EOT (DP: lead + rear)	ECP Brakes
Base Case	7/16" A516-70, no jacket, no head shield	30	8.5	7.2	6.1	0%	0%	0%
		40	13.7	12.1	9.8	0%	0%	0%
		50	20.1	16.3	14.9	0%	0%	0%
Alternate 1	7/16" TC128, 11 gauge jacket, 1/2" full-height head shield	30	4.7	3.9	3.3	45%	46%	46%
		40	8.0	7.1	5.3	42%	41%	46%
		50	12.2	9.8	9.1	39%	40%	39%
Alternate 2	1/2" TC128, 11 gauge jacket, 1/2" full-height head shield	30	4.3	3.6	2.9	49%	50%	52%
		40	7.3	6.5	4.8	47%	46%	51%
		50	11.2	9.0	8.3	44%	45%	44%
Alternate 3	9/16" TC128, 11 gauge jacket, 1/2" full-height head shield	30	3.8	3.2	2.6	55%	56%	57%
		40	6.6	5.9	4.3	52%	51%	56%
		50	10.2	8.2	7.6	49%	50%	49%
						Average:	**53%**	

Table 6. Risk Improvement Due to Speed Reduction

100 cars behind POD			Most Likely Number of Punctures			% Improvement due to 10 mph speed reduction only (50 to 40 mph, and 40 to 30 mph)			Speed (mph) advantage: amount that conventionally braked train must reduce speed to obtain equivalent risk		
	Tank Type	Speed, mph	Conventional Brakes	2-way EOT (DP: lead + rear)	ECP Brakes	Conventional Brakes	2-way EOT (DP: lead + rear)	ECP Brakes	Conventional Brakes	2-way EOT (DP: lead + rear)	ECP Brakes
Base Case	7/16" A516-70, no jacket, no head shield	30	8.5	7.2	6.1	38%	40%	38%	---	---	---
		40	13.7	12.1	9.8	32%	26%	34%	0.0	3.1	7.5
		50	20.1	16.3	14.9	---	---	---	0.0	5.9	8.1
Alternate 1	7/16" TC128, 11 gauge jacket, 1/2" full-height head shield	30	4.7	3.9	3.3	41%	45%	38%	---	---	---
		40	8.0	7.1	5.3	34%	28%	42%	0.0	2.7	8.2
		50	12.2	9.8	9.1	---	---	---	0.0	5.7	7.4
Alternate 2	1/2" TC128, 11 gauge jacket, 1/2" full-height head shield	30	4.3	3.6	2.9	41%	45%	40%	---	---	---
		40	7.3	6.5	4.8	35%	28%	42%	0.0	2.7	8.3
		50	11.2	9.0	8.3	---	---	---	0.0	5.6	7.4
Alternate 3	9/16" TC128, 11 gauge jacket, 1/2" full-height head shield	30	3.8	3.2	2.6	42%	46%	40%	---	---	---
		40	6.6	5.9	4.3	35%	28%	43%	0.0	2.5	8.2
		50	10.2	8.2	7.6	---	---	---	0.0	5.6	7.2
						Average, 40 to 30 mph	**41%**		**Average:**	**4.2**	**7.8**
						Average, 50 to 40 mph	**34%**				

6. Conclusion

The methodology developed in this report allows railroad and tank car industry to estimate the relative performance benefits of changes in tank car designs, braking systems, or operating conditions under derailment conditions, with a focus on the likelihood of a tank to puncture (and thus release hazardous materials). The results presented in this report included the expected relative performance of several proposed tank car designs (compared to a legacy DOT-111 car), the benefits of advanced braking systems (such as ECP brakes) over conventional systems, and the safety performance of lower operating speeds.

The methodology captured several elements/parameters relevant to derailment and puncture performance, as well as its distributions, and combined them into a consistent probabilistic framework for estimating the relative merit of proposed mitigation strategies that aim to tank car puncture performance. When the estimates generated by this methodology were compared to actual derailment data, the methodology properly captured the gross dynamics of a tank car train derailment and the resulting puncture performance of the tank cars. In addition, model estimates regarding the number of cars derailed and number of punctures, as a function of train speed, compared favorably with observed derailment data. Also, puncture risk reduction correlated well with engineering estimates corresponding to increased tank shell thickness and material strength. The validation effort provided confidence that the approach not only captured relative merits, but also that the overall puncture probability predictions resulting from this approach were consistent with observed derailment performance.

Overall, this methodology offered an objective approach to quantify and characterize the reductions in risk as measured by reductions in puncture probabilities that resulted from changes to tank car designs or tank car operating practices.

7. References

[1] Sharma & Associates, Inc., *Objective Evaluation of Risk Reduction from Tank Car Design and Operations Inprovements,* Docket No. PHMSA-2012-0082 (HM-251), Sharma Associates, Inc., 2014. Available at: https://www.federalregister.gov/documents/2015/05/08/2015-10670/hazardous-materials-enhanced-tank-car-standards-and-operational-controls-for-high-hazard-flammable.

[2] Yu, H., Tang, Y. H., Gordon, J. E., Jeong, D. Y., "Modeling the Effect of Fluid-Structure Interaction on the Impact Dynamics of Pressurized Tank Cars," in *Proceedings of the 2009 ASME International Mechanical Engineering Congress and Exposition, IMECE2009-11*, Lake Buena Vista, 2009.

[3] Kirkpatrick, S. W., Peterson, B. D., MacNeill, R. A., "Finite Element Analysis of Train Derailments," in *2006 Proceedings of the Inernational Crashworthiness Concernece*, Athens, Greece, 2006.

[4] Kirkpatrick, S.W., "Detailed Puncture Analyses Tank Cars: Analysis of Different Impactor Threats and Impact Conditions," Federal Railroad Administration, Washington, DC, March 2013.

[5] *LS-DYNA Keyword User's Manual,* Version 971 ed., Livermore Software Technology Corporation, 2007.

[6] "AAR Manual of Standards and Recommended Practices, Section C-II," in *Design, Fabrication & Construction of Freight Cars*, 2011.

Appendix A.
Study of Impactor Distributions

This research effort aimed to develop and validate a methodology that could be used to estimate the relative merit of proposed mitigation strategies to improve tank car puncture performance. One of the key elements and assumptions of this methodology was the distribution of impactor sizes, as this had the potential to significantly influence the results.

To evaluate the sensitivity of the results to variations in impactor size distribution, two additional sets of impactor distributions, one skewed towards smaller impactor sizes and one skewed towards larger impactor sizes (compared to the standard distribution assumed, shown in figure 6) were also analyzed. Figure A1 displays the two distributions compared to the standard one used for the main analyses. The average impactor sizes for the three distributions are about 6.8”, 8.7”, and 11.3”, respectively, with the geometric mean of the averages of smaller and larger distributions being equal to the average of standard distribution. The standard distribution has an average size that is about 29 percent bigger than the smaller one and the larger distribution is about 29 percent bigger than the standard one.

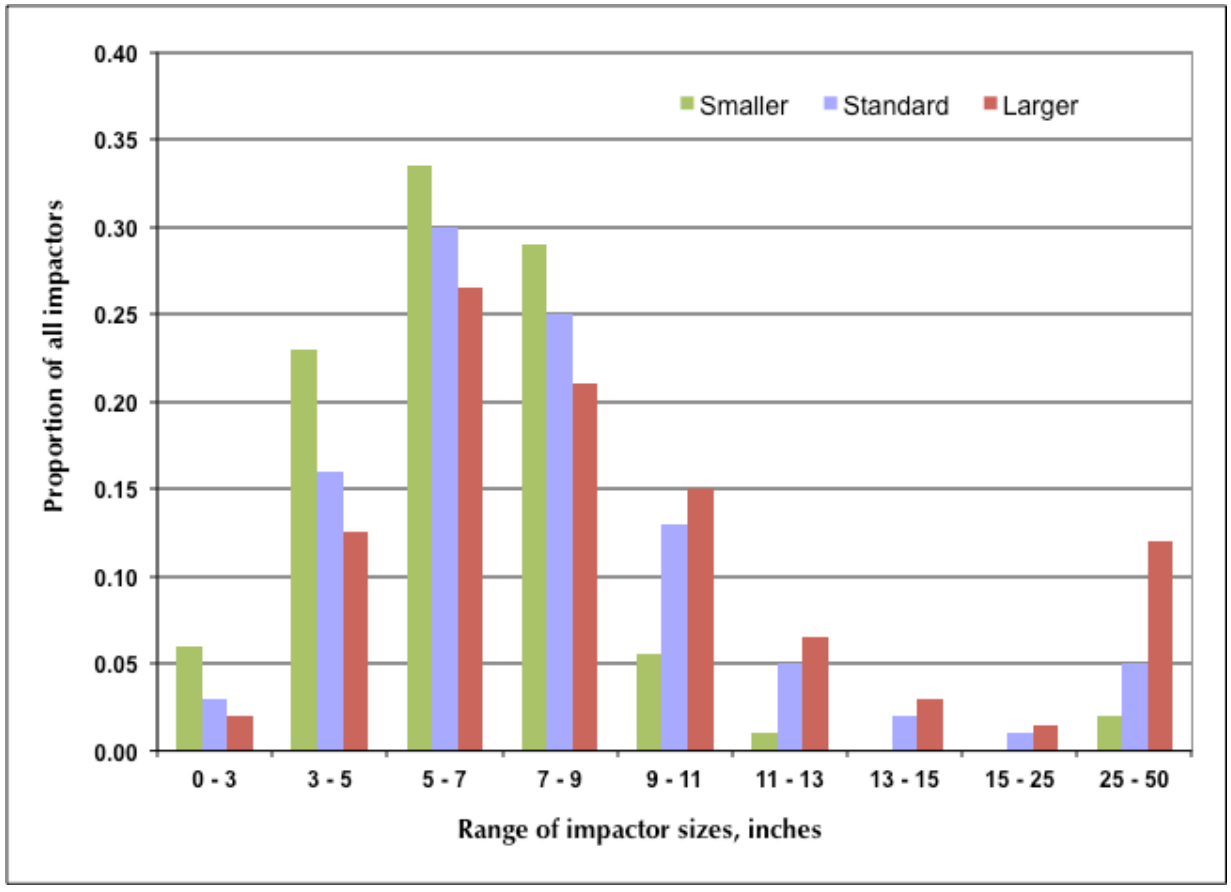

Figure A1. Impactor distributions used for sensitivity analysis

The results of this evaluation are presented in Tables A.1, A.2 and A.3 below. Table A.1 shows the puncture performance of two different designs and two different brake systems for a 100-car train and a derailment initiation speed of 40 mph. As expected, smaller impactors result in more

punctures and larger impactors result in fewer punctures. However, as seen in Tables A.2 and A.3, the variation in relative performance values is far less significant, especially considering that the impactor distributions are significantly different.

Table A.1 Number of Punctures – Variations by Impactor Size Distribution

40 mph, 100 cars > POD			**Most Likely Number of Punctures**		
	Tank Type	**Brakes**	**Smaller size impactors**	**Standard impactor distribution**	**Larger size impactors**
Base Case	7/16" A516-70, No Jacket	Conv	15.1	13.0	11.4
		ECP	11.0	9.3	8.0
Alternate 3	9/16" TC128, 11 gauge Jacket	Conv	10.4	8.5	7.2
		ECP	7.1	5.6	4.7

Table A.2 Relative Performance of ECP Brakes – Variations by Impactor Size Distribution

40 mph, 100 cars behind POD		**% Improvement ECP compared to Conventional Brakes**		
	Tank Type	**Smaller size impactors**	**Standard impactor distribution**	**Larger size impactors**
Base Case	7/16" A516-70, No Jacket	27%	28eirth	30%
Alternate 3	9/16" TC128, 11 gauge Jacket	32%	34%	35%

Table A.3 Relative Performance of Tank Designs – Variations by Impactor Size Distribution

40 mph, 100 cars behind POD	**% Improvement 9/16" shell compared to 7/16" shell**		
Brake System	**Smaller size impactors**	**Standard impactor distribution**	**Larger size impactors**
Conventional	31%	35%	37%
ECP	35%	40%	41%

Again, the tables presented show that the relative performance of changes to tank car designs or operating conditions does not change significantly as a result of changes to the impactor size distribution. While the individual puncture values change notably (as they should), relative performance does not. It is also worth mentioning that the standard impactor size distribution assumed herein results in puncture values that are consistent with real-life observations, lending additional credence to using it for the main work reported here.

Abbreviations and Acronyms

DP	Distributed Power
ECP	Electronically Controlled Pneumatic
EOT	End-of-Train
POD	Point of Derailment
NBR	Net Braking Ratio
2-EOT	Two Way End-of-Train

Updated Derailment and Puncture Estimates

LNG Unit Trains

4/06/2020

Draft

Overview

- Simulations of:
  - 100 LNG Tanks (DOT113s)
    - 7/16” Shell, 0.5” Head, 0.25” Inner Tank
    - Rear DP Configuration
  - Derailments are initiated at the head end of the train.

Updated Results – 40 mph

- At 40 mph, the expected number of punctures is 5 (average).
- Across the simulations conducted, the range of punctures covering 70% of the scenarios ranges from 3 punctures to 7 punctures (2-sigma).
- It is estimated that 20% of the punctures could happen on the same car.
  - In other words, if we consider the number of punctures as 5, the number of cars punctured would be 4.
- About 70% of the punctures happens in the first 8 cars
  - Therefore, there is a reasonable probability that 5 adjacent cars could experience punctures.

Updated Results – 40 mph

- At 40 mph, the expected number of derailed cars is 21 (average).
- Across the simulations conducted, the range of cars derailed covering 70% of the scenarios ranges from 16 to 25 cars (2-sigma).

Draft

Final Updated Results (7/16”)

Speed	30 mph	40 mph	50 mph
No. of derailed cars	15	21	28
No. of Punctures	2.7	5	7.3

Draft

Final results for 9/16th Shell at 40 mph

- Simulations of:
  - 100 LNG Tanks (Proposed Design)
    - 9/16” Shell, 5/8” Head TC 128B , 0.25” Inner Tank SS
    - Rear DP Configuration
  - Derailments are initiated at the head end of the train.
- Results for 40 mph
  - No. of Punctures: 4.2
  - No. of derailed cars: 21 (same as DOT113 7/16”tank)
- It is estimated that 20% of the punctures could happen on the same car.

Draft

Final Updated Results (9/16”)

Speed	30 mph	40 mph	50 mph
No. of derailed cars	15	21	28
No. of Punctures	2.1	4.2	6.0

Draft

Worst-Case Scenarios
LNG releases from tank cars

Source: Gaz de France, Personal Communication

Draft Report — March 2020

Prepared by:

Pipeline and Hazardous Materials Safety Administration

Federal Railroad Administration

Contents

1. Background

Liquefied natural gas (LNG), also known as Methane, Refrigerated Liquid, is created by cooling natural gas at atmospheric pressure to −260°F. The volume of natural gas in its liquid state is about 600 times smaller than its volume in its gaseous state. LNG may be transported by rail in portable tanks with approval from the Federal Railroad Administration (FRA). The Hazardous Materials Regulations (HMR) do not currently authorize the shipment of LNG in rail in tank cars. However, the Pipeline and Hazardous Materials Safety Administration (PHMSA) can authorize shipment of LNG in rail tank cars under a special permit, on a case by case basis. Recently there has been increasing interest in LNG transportation in rail tank cars domestically to supplement supply of natural gas to areas where the pipeline system is limited or inadequate, as well as for international export.

PHMSA, in collaboration with FRA, has been planning and begun carrying out a concerted, multi-task program of research, data gathering, and analysis; testing, modeling, and simulation; and risk assessment and evaluation intended to: (i) increase the agencies' understanding of the types and magnitude of risks posed by LNG when moved by rail; (ii) identify and assess measures that can reduce these risks; and (iii) provide a more complete understanding of what is needed to prepare for and respond to any accidents that may arise. Among the planned tasks are conducting a full-scale impact test on a DOT-113 tank car and analyzing the results; consultations with state and local emergency responders to gauge their levels of awareness, training, and preparation for LNG accidents; simulations of LNG train operations over candidate rail routes; targeted assessments of the effectiveness of more intensive railroad track maintenance, inspection, and repair activity on routes carrying significant hazardous materials traffic; an evaluation of the feasibility of and applicability of technology involving electronically controlled pneumatic brakes on new DOT-113 tank cars in LNG service; and an assessment of the risks associated with transporting LNG by rail compared with risks of LNG transportation in other modes.

2. Objective

One of the concerns of shipping LNG by rail is the potential for a train accident (derailment or collision) involving a large number of (LNG carrying) tank cars in a unit train configuration (70 or more cars). Such an accident scenario may lead to multiple tank car punctures and release of LNG. As part of the multi-task initiative noted above, The Federal Railroad Administration (FRA) and The Pipeline and Hazardous Materials Safety Administration (PHMSA) have identified and developed worst-case scenarios for LNG behavior due to releases from tank cars following a potential accident of a unit train. The main work performed under this task is documented in this report and contains: a) an assessment of the extent of hazards that may be caused by such releases; b) an evaluation of the hazard areas for the worst-case scenarios so that the maximum hazard impact from potential accidents involving unit-trains of LNG tank cars can be assessed; and c) a recommendation for future research areas and analysis for potential catastrophic derailment scenarios resulting in LNG releases.

This is an essential task under PHMSA's overall initiative to evaluate existing safety data and fill knowledge and program gaps regarding the risks of rail transport of LNG.

3. Literature and Data Review

FRA and PHMSA identified available literature, reports, models and data to support details of the various assumptions used to analyze four (4) different worst-case scenarios developed in

Section 4. "Worst-Case Scenarios from LNG releases from Tank Cars" of this report. They consist of hazard area assessment for LNG release from tank car and the physical behavior of the LNG released from tank cars following a unit-train accident.

3.1. Technical literature references

3.1.1. FRA's Train Derailment Model[1]

This report describes a methodology for quantifying and characterizing the changes in risk (or puncture probabilities) that may result from changes to tank car designs or the tank car operating environment. The methodology captures several parameters that are relevant to tank car derailment performance—including multiple derailment scenarios, derailment dynamics, impact load distributions, impactor sizes, operating conditions, tank car designs, etc. The results presented in this report include the expected relative performance of several proposed tank car designs (compared to a legacy DOT-111 car used in transportation of flammable liquids).[2] In addition, the model's predictions regarding the number of cars derailed and number of punctures, as a function of train speed, compare favorably with actual derailment data. Also, puncture risk reduction correlates well with the engineering estimates that correspond to increased tank shell thickness and material strength. These validation efforts improved the credibility of the methodology's efficacy and the results.

In October 2019, PHMSA issued a notice of proposed rulemaking in coordination with FRA that would modify the HMR to allow the bulk transport of LNG in the DOT-113-C120W[3] specification tank car. Based on additional technical review of the puncture resistance analysis results of DOT-113C120W tank cars, PHMSA is amending the current requirement in HMR on DOT-113C120W tank car outer tank shell thickness of 7/16" to requiring a minimum of 9/16" TC 128 outer shell thickness for carrying LNG. PHMSA believes that this change will further enhance the safety of the DOT-113 tank car and the transportation of LNG by rail.

---

[1] Sharma & Associates, Inc., *Objective Evaluation of Risk Reduction from Tank Car Design and* Operations Improvements – Extended Study – March 2015

[2] For example, the methodology estimated that the impact performance of a proposed tank car design with a 9/16" thick shell, 11-gage jacket and ½" full-height head shield would be over 50 percent better than the performance of a base case Department of Transportation (DOT)-111 tank car. Similarly, the analysis also estimated that reducing the operating speed from 40 mph to 30 mph offered a 42 percent reduction in puncture likelihood for the proposed design.

[3] The DOT-113 tank cars are specifically designed for the transportation of refrigerated liquefied gases; these rail tank cars have a 7/16" carbon steel outer shell, a ¼" inner stainless steel and are vacuum-insulated This design provides an increased crashworthiness when compared to a single vessel design rail tank car. The vacuum area and the insulation significantly reduce the rate of heat leak from the atmosphere to the liquid inside the tank car thus minimizing the heating of the cryogenic (i.e., refrigerated) material in the tank car while being transported. The DOT-113 tank car also includes added safety features—such as protection systems for piping between the inner and outer tanks, multiple pressure relief devices (pressure relief valves and vents), thermal integrity tests, and in-transit reporting requirements—designed to address the hazards presented by cryogenic liquids.

As noted earlier, FRA's derailment analysis methodology offers a methodology to quantify the reductions in puncture probabilities that result from changes to tank car designs, or tank car operating practices. The approach can be used to evaluate the reduction in the number of tank cars punctured with an outer tank shell thickness of 9/16" compared to a 7/16" outer shell in train accidents involving a 100-Car unit train derailment.[4] The results can be used to inform the assumptions made in analyzing the worst-case scenarios regarding the number of tank cars releasing LNG following a unit train accident. The worst-case scenarios were performed assuming 1, 2 and 5 tank car breaches and LNG releases. The number of tank car breaches is varied to demonstrate the effects of different potential accident consequences. To specifically inform the assumption made in analyzing the worst-case scenario regarding 5 DOT 113 tank cars with 9/16" shell thickness breached and releasing product following a derailment, the Agencies used the results from a separate effort currently being undertaken by FRA. FRA is currently evaluating the number of LNG tank cars (DOT 113 tank cars) that may be breached in a unit-train derailment accident, at different train speeds[5]. The table below shows the results of FRA's derailment simulations for the number of punctures calculated for a train of 100 LNG Tanks (DOT 113s), with 7/16" Shell, 0.5" Head, 0.25" Inner Tank and Rear DP Configuration in which the derailment occurs near the head end.

Speed	30 mph	40 mph	50 mph
No. of derailed cars	16	21	32
No. of Punctures	3	5	8

The March 2020 results above show that at 40 mph, the number of likely punctures for DOT 113s with tank car shell thickness of 7/16" is 5. The report shows a reduction of 16.9% in the number of punctures due to an increase in the tank car shell thickness from 7/16" to 9/16" at 40 mph.[6] Assuming the same 16.9% reduction in number of punctures occurs due to an increase in the tank car shell thickness from 7/16" to 9/16" for the DOT 113 tank car, then we obtain a reduction in the number of punctures from 5 punctures to 4.2 punctures.[7] This results validates that the assumption made in analyzing the worst-case scenario regarding 5 DOT 113 tank cars with 9/16" shell thickness breached and releasing product following a derailment is a

[4] For the 100-car model, a matrix of simulations was established. Table 3 in the Extended Study – March 2015, noted in footnote 3 above, shows the most likely number of punctures calculated for each case of this matrix, as applied to a train of 100 cars in which the derailment occurs near the head end. Assuming End-Of-Train (EOT) braking, with either a two-way EOT device or with a remote distributed power (DP) consist at the rear of the train, the number of punctures at 30 mph is 3.2. and at 40 mph is 5.9.

[5] The results for the FRA derailment modeling of a DOT 113 tank car with 7/16" shell were released in March 2020.

[6] Sharma & Associates, Inc., *Objective Evaluation of Risk Reduction from Tank Car Design and* Operations Improvements – Extended Study – March 2015: Table 3, page 18 shows a reduction in the number of punctures from 7.1 punctures to 5.9 at 40 mph.

[7] The Agencies assume one tank car puncture per tank car releasing product following a derailment.

conservative assumption. Pending results from additional ongoing work including simulations for DOT 113 tank car with 9/16" thick outer shell, the worst-case scenario analysis will be further reevaluated and if necessary improved accordingly.

3.1.2. Technical Models and Reports references

Appendix B contains a table with references to several models and reports used to support the various assumptions used to analyze the four (4) different worst-case scenarios' hazard area assessments for LNG release from tank cars, and the physical behavior of the LNG released from tank cars following a unit-train accident.

3.2. PHMSA's Consequence Model

PHMSA has a hazmat release consequence model that models several different hazardous materials commodities. PHMSA had this model built to assist in identifying the order of magnitude and likeliness of various levels of event consequences given population distributions along rail routes. The model's impact zones are all based on blast zone assessments using TNT equivalency for the chemicals modeled (these are LPG, LNG, liquid ethylene, liquid hydrogen, crude oil, ethanol and a few others including non-compressed propane).[8] The model uses the heat flux and overpressure blast from the TNT equivalence model to predict human health consequences (deaths and injuries) and other damages.

Three different general types of events can be modeled – a spill with no fire, a spill with a fire, and an explosion. These events are specified by the user rather than based on likelihood that they will occur. The model uses a Monte Carlo simulation to place the event randomly along segments of a route. Based on the impact zone, human casualty and property damage are estimated based on population densities and other characteristics of the site selected in the Monte Carlo simulation. These repeated random simulations are used to generate a probability density function of event consequences for a transportation route, which capture the likelihood of events of a given size based on the population densities and other characteristics at points along the route being simulated.

Although the model has some strengths, it was not seen as the best approach to modelling a specific commodity, such as LNG, due to several limitations. The most important of these limitations is the use of TNT equivalence, which does not take into account all of the relevant aspects and behavior of any specific material and what happens in the event it is released from its container. In the case of LNG, such inherent characteristics include the pressure and

[8] For example, if the user specifies 3 LNG cars releasing with a fire it would calculate an impact zone for a release that size and determine, given the GIS location sampled, what the consequences to human health and property damage would be.

temperature of the material before release from the container, the likelihood that it will ignite and how soon after spillage ignition might occur, the various aspects of terrain and other factors at the release site that determine how much material would vaporize before ignition occurs, how far the material may travel after release, and how much energy the material has the potential to release in a short time frame, among other factors. Basing the impact zones on a somewhat generic TNT equivalence simplification rather than the unique characteristics of the specific commodities which can be modeled makes the model less than ideal for examining incidents of a specific commodity whose inherent characteristics are known.

Another limitation is that the model does not consider the likelihood of release from the package or the likelihood of a derailment, and therefore does not provide a comprehensive risk profile for the material. The model also does not consider the likelihood of a particular type of release given the nature of the material. For LNG, for example, a BLEVE or explosion type event is extremely unlikely given the nature of the material and the design of the tank car used to haul it. Also, multiple types of fire events are possible for LNG – a pool fire, a fireball, or a vapor dispersion cloud that ignites, causing a flash fire. The nuances and characteristics of these different types of events involving LNG release are not fully captured by the model due to the use of a simplified impact zone methodology. The advantage of this approach – that it can be applied to all commodities modelled – is a disadvantage when viewed from the standpoint of detailed modelling of a specific commodity.

Furthermore, the type of event being modeled is specified by the user, so the likelihood of these various types of releases, given the unique characteristics of the commodity involved, is not accounted for in the modelling. All of the most likely types of release scenarios that can result from LNG releases are not entirely encompassed by the three (e.g., spill with no fire, spill with a fire, explosion) that can be specified by the user in this model.

Although the model gives some sense of the potential damages that might ensue from some types of releases of the various types of materials modeled, and enable some level of comparison among them, it is less than ideal for modeling specific scenarios that depend on the unique characteristics of the specific commodity involved and how likely those scenarios are given the inherent nature of the materials. Further model refinements may correct some of the weaknesses of the consequence model discussed in this section, but until then, modelling unique to the specific commodity in question will produce more reliable results. The Agency decided to use modelling that took into consideration the specific characteristics of LNG and its unique behavior when released in building worst case scenarios. This modelling is presented further below in Section 4.

3.3. Historical Derailment Data for Flammable Liquids

This section provides a review of data sources, including hazardous material rail accident reporting data from PHMSA and rail accident data from FRA, to support the development of the different hazard scenarios considered for hazard area assessment.

In addition, the derailment data in Appendix A was collected by representatives of FRA and PHMSA who investigated many of the flammable liquid unit train derailments in the last decade. As part of these investigations, the Agencies collected tank car performance information. The information and lessons learned from the last decade transporting other flammable materials may provide insight to the potential effects of a LNG derailment when transported in similar configurations.

The information documented during these investigations includes:

- Derailment speed
- Number of Tank Cars Derailed
- Number of Tank Car Breaches
- Type and Amount of Product Released
- Tank Car type
- Derailment Impact Area
- Topography of the Derailment Location
- Fire Because of Lading Release

The derailment data for the 19 accidents listed in Appendix A[9] was compared with the PHMSA rail accident data set, which is used as the primary data source for these analyses of rail accidents.[10] After identifying rail accidents based on the PHMSA datasets, we supplemented the database with information from other datasets and incident-specific reports from the Federal Railroad Administration (FRA).[11] For those accidents reported in both the FRA and

[9] This particular set of flammable liquid unit train derailments does not include all the flammable liquids unit train derailments from 2006 to date.

[10] The Hazardous Materials Regulations at 49 CFR Parts 171-180 require that certain types of accidents be reported to PHMSA. Under §171.16, operators are required to report information to PHMSA within 30 days of an accident that meets broadly defined criteria that include: "(1) Any of the circumstances set forth in §171.15(b); (2) An unintentional release of a hazardous material or the discharge of any quantity of hazardous waste; (3) A specification cargo tank with a capacity of 1,000 gallons or greater containing any hazardous material suffers structural damage to the lading retention system or damage that requires repair to a system intended to protect the lading retention system, even if there is no release of hazardous material; or (4) An undeclared hazardous material is discovered." PHMSA compiles the information provided by operators in Form DOT F5800.1 (OMB Approval No. 2137-0039) into publicly available datasets.

[11] FRA receives reports from rail carriers about "all accidents and accidents resulting in injury or death to an individual or damage to equipment or a roadbed arising from the carrier's operation" under the Accident Reports Act (Public Law No. 165). Since the FRA data are not focused on the release of oil (or other substances) resulting from accidents, they typically do not provide detailed information about the release or the associated damages. Further, the FRA has substantially different reporting requirements for accidents, and we expect that the majority of accidents involving stationary trains are not reflected in the FRA data.

PHSMA data sets, FRA data provides additional information (e.g., the number of tank cars carrying hazardous materials derailed) which is not included in the PHMSA rail data.

FRA and PHMSA examined potential analogies between the hazard areas from LNG tank car derailments involving unit train configurations and the hazard areas resulting from crude oil and ethanol unit train derailments.

To estimate the footprint of the derailment area from past rail accidents involving crude oil and ethanol releases, overhead pictures of the major derailments noted above were reviewed by PHMSA and FRA. The average footprint size of derailment (i.e., the area occupied by the jumble of tank cars after derailment) was estimated as 620'L x 280'W (173,600 sq. ft.)[12] The size of the estimated average derailment area decreased from 250 thousand square feet for the accidents involving DOT 111 tank cars to 120 thousand square feet for accidents involving CPC-1232 tank cars and 75 thousand square feet for accidents involving DOT 117R tank cars.[13] However, the historical derailment area data, while informative, was not used to estimate the footprint showing the extent of spread of product released from damaged tank cars in a derailment accident. Ultimately, the product spilled area could not be accurately estimated based on the analysis of the overhead pictures from the derailment sites due to limiting factors such as: visibility of the product spilled, terrain and topography, soil, and effect of weather conditions. The material characteristics, such as ethanol being a colorless material, also resulted in difficulties in estimating the area of spread of the released product from photographs.

The Agencies estimate the footprint of a spill of LNG to be different from the footprint of a spill of crude oil following a unit train accident due to differences in the behavior of LNG soon after its release from its container. LNG both directly flashes to vapor (when released from a pressurized state) as well as evaporates very rapidly upon contact with ground or water, which are generally much "hotter" than the cryogenically cold LNG. Also, the potential fire effect of the derailment with LNG in the consist is different compared to that from other flammable liquid releases.

[12] This represents the average of the derailment impact areas data available for 18 flammable liquid unit train derailments out of the total of 19 flammable liquid unit train derailments shown in Appendix A. The derailment impact area for one of the derailments (Culbertson, MT on 07/16, 2015) of the 19 above mentioned derailments is not available. Therefore, the estimated overall average footprint size of the derailment of 173,600 is based on data points available for 18 derailments.

[13] PHMSA determined the types of tank cars involved in the 18 crude oil and ethanol unit train derailments considered in this section, as follows: DOT-117R tank cars were involved in 2 crude oil and ethanol unit train derailments (e.g., Doon, IA on 06/22/2018; Fort Worth, TX, on 04/24/2019); CPC-1232 tank cars were involved in 6 crude oil and ethanol unit train derailments (e.g., Lynchburg, VA, on 04/30/2014; Mount Carbon, WV, 02/16, 2015; Galena, IL on 03/05/2015; Watertown, WI on 11/08/2015; Mosier, OR, 06/03/2016; Plainfield, IL on 06/30/2017); DOT-111 tank cars were involved in the rest of 9 crude oil and ethanol derailments. The derailment impact area averages were calculated based on the estimated footprint derailment area data points for the 2 derailments involving the DOT-117R tank cars, 6 derailments involving the CPC-1232 tank cars, respectively 9 derailments involving DOT 111 tank cars.

Flammability of a liquid product released into the atmosphere depend on a number of factors including, but not limited to, the vapor pressure of the liquid, and the flammability range of the vapors in air for ignition. Various aspects of terrain and local weather and wind conditions at the release site also determine how much material would vaporize before ignition occurred, how far the vapors of the material may disperse after release without being ignited, and how much energy could be released in a short time (explosion). All of these factors influence the extent of the hazard given a release of a particular material.

The Agencies calculated different types of hazards for various scenarios of LNG release from tank cars in a unit train, including, (i) the radial spread of an unconfined pool of LNG, (ii) radiant heat from an expanding ignited pool of LNG, (iii) dispersion of unignited vapors from the spreading pool, (iii) flash fire, (iv) fireball type of fire. These scenarios and the hazard area results associated with each scenario are discussed in the section below, "Worst Case Scenarios from LNG releases from Tank Cars Analysis." The relevant literature references for the models used to analyze these scenarios are indicated in Appendix B.

4. Worst-Case Scenarios from LNG releases from Tank Cars

4.1. Abstract

This section provides the details of various scenarios considered, assumptions made in the calculation of potential hazard areas, and results of calculations of hazard areas for each scenario of LNG behavior upon release from tank cars following a unit train accident.

Four scenarios are considered, namely, (i) Unconfined and unignited spreading of a LNG pool on land, (ii) Dispersion of flammable vapor cloud emanating from the boiling, spreading LNG pool on the ground, (iii) A pool fire on the spreading pool, and (iv) Fireball type of burning of LNG released catastrophically from the breach of the tank car tank(s).

4.2. Background

As noted above, one of the concerns of shipping a large number of LNG carrying tank cars in a unit train configuration is the potential for a train accident (derailment or collision) which leads to multiple tank car punctures and release of LNG. The extent of the hazards that may be caused by such releases need to be calculated for different scenarios of LNG behavior, post release. Also, it is necessary to evaluate these hazard areas for the worst-case scenarios so that the maximum hazard impact from potential accidents involving unit trains of LNG tank cars can be assessed.

A separate effort is being undertaken to evaluate the number of LNG tank cars that may be breached in a unit-train derailment accident, at different train speeds. Documented in this section are the details of the various assumptions made on the LNG release from tank car, the physical behavior of the LNG released, different scenarios of LNG behavior, and the results of calculation of the hazard areas. Very detailed mathematical models are NOT provided; instead, the relevant literature references for the models used are indicated.

4. 3. Worst-Case Scenarios of LNG Release and Effects

4.3.1. Assumptions made in analyzing the worst-case scenarios

The following assumptions have been made in performing the analyses indicated in this document.

(1) The number of tank car releasing is varied (to see the effects of different number of tank car breaches). The analysis has been performed assuming 1, 2 and 5 tank car breaches and LNG releases.

(2) The release of LNG is assumed to occur from a breach (hole) in the bottom-most part of the inner tank. That is, the hole is at the bottom of the liquid contained, irrespective of the orientation of the tank car.

This assumption was made with the purpose of allowing the worst outcome: the breached tank cars release all their content.

(3) The tank pressure just prior to release is at 411.6 kPa (abs) [45 psig].

In the proposed regulations, the pressure (of LNG vapors) in the tank car at the time it is offered for transportation should not be greater than 15 psig. The start to discharge pressure of the pressure relief valve is 75 psig. Hence, the mean of these pressures (namely, 45 psig) is assumed for worst-case scenario analysis purposes. In addition, based on the compliance with 49 CFR §173.319 (c) the average pressure increase per day will not exceed 3 psig. That is, the 45 psig pressure represents the conditions in the tank car at the end of 10 days after the car is offered for transportation.

(4) The size of the breach is a square hole of size 30.5 cm x 30.5 cm [12” x 12”].

This is because, a majority of punctures of tank cars is caused by the impact of a coupler (from another car) on the shell or head wall of the tank car. The nominal cross-sectional size of a coupler is about 12” x 12”.

(5) The tank pressure does not vary during the release of liquid. That is, the maximum rate of release consistent with the initial tank pressure and liquid depth is calculated and used in estimating hazard areas.

(6) The spills from all tank cars are time synchronized. That is, liquid release from each of the breached tank car is assumed to begin at the same time and is lumped together as if released from a single, central, location.

In this assumption, the physical separations of tank cars releasing liquid are not considered. The release quantities from all tank cars are lumped together, for

calculation purposes, as if the total spill was occurring over a single point. Such an assumption leads to the worst-case release scenario.

(7) The liquid release is on to a flat, unconfined, ground.

This assumption leads the unconfined spread of the liquid to the largest radius of spread; a conservative assumption for a worst-case analysis.

(8) The ground has typical thermal properties. It is also not permeable (i.e., no percolation of LNG into the ground), obstruction free and dry.

All of the above assumptions lead to the consideration of the worst-case outcome for hazards arising due to potential releases from mainline derailment accidents of unit trains carrying LNG.

4.3.2. LNG Hazard Scenarios

Following an LNG release, four (4) different hazard scenarios are considered for hazard area assessment. The initial flashing of a part of the released liquid due to depressurization is also considered. The scenarios for hazard area calculation considered are:

1 Unconfined and unignited spreading and simultaneously evaporation (due to heat transfer from the ground) of a LNG pool on a flat, impervious, ground.

2 Dispersion in the atmosphere of the vapor released by the spreading and evaporating LNG pool on the ground together with the vapor generated by the flashing of LNG due to depressurization.

The hazard of concern is the distance to which the LNG vapors disperse, mixing with the ambient air, before being diluted to below 5% (lower flammability limit[14]) vapor concentration in air.

3 Ignition of the spreading LNG pool resulting in a time-wise expanding pool fire.

The hazard of concern in this case is the distance from the fire center on the ground to a person receiving radiant thermal heat flux of 5 kW/m^2 (1600 $Btu/hr\ ft^2$)[15].

4 Formation of a fireball due to sudden release of a substantial mass of the inventory in a tank car due to a thermal tear or significant damage/destruction of the inner tank of a LNG tank car.

---

14 *"Lower and Upper Explosive Limits for Flammable Gases and Vapors (LEL/UEL),"* ***data extracted*** *from gas data book, 7th edition, copyright 2001 by Matheson gas products, and from bulletin 627, flammability characteristics of combustible gases and vapors, copyright 1965 by U.S. Department of the Interior, Bureau of Mines.*

15 The criterion for hazard calculation from a LNG pool fire is from 49 CFR, Part 193.

The hazard distance is calculated using the modified thermal dosage criterion [300 {kW/m^{2}}$^{(4/3)}$ s] for second degree burn to a person from short-term exposure to high level of radiant heat flux[16].

The references to the published literature used to calculate the hazard distances for each of the LNG behavior scenarios are provided in each of the sections below.

4.3.2.1. LNG Pool Spread on flat ground[17]

The model used to evaluate the radial spread of an unconfined pool of LNG is provided below in the footnote. The release rate continuously decreases with time, with the highest rate being at the time the breach occurs. It is complicated to evaluate the spread when the liquid release rate from the tank car is varying with time. In order to evaluate the worst condition, the maximum spread radius was calculated assuming (i) that the rate remains constant at the initial rate of release and for the duration to completely empty the tank and (ii) the rate is the average of all rates (initial to final) and this average rate persists until all liquid in the tank is emptied. The results from these assumptions are indicated below.

		One Tank Car Spill	Two Tank Car Spill	Five Tank Car Spill		
Parameters	**Symbol**	**Value**	**Value**	**Value**	**Units**	**Remarks**
LNG tank pressure (absolute) before release	P_T	411.6	411.6	411.6	kPa (abs)	45 psig
Equivalent diameter of puncture hole	D_H	0.34	0.34	0.34	m	12" x 12" hole
Mass fraction of released liquid that flashes	f_L	14.7	14.7	14.7	%	
Max. Mass rate of liquid spill on to ground (all tank cars)	$\dot{M}_{L,max}$	883	1,766	4,414	kg/s	
Duration of release at maximum mass rate of release	$t_{S,\,min}$	41	41	41	s	
Maximum radius of spill spread at maximum spill rate	R_{max}	51.2	67.8	95.5	m	
Mean mass rate of liquid spill on to ground (all tank cars)	$\dot{M}_{L,avg}$	441	883	2,207	kg/s	
Duration of spill at mean mass rate of spill	$t_{S,\,mean}$	82	82	82	s	
Maximum radius of spill spread at mean spill rate	R_{max}	47.9	66.6	99.9	m	

16 O'Sullivan & Jagger, "Human Vulnerability to Thermal Radiation Offshore," Health & Safety Laboratory Publication # HSL/2004/0, Harpur Hill, Buxton, Derbyshire, SK17 9JN, England, 2004

17 Raj, P.K. "Models for Cryogenic Liquid Spill Behavior on Land and Water," J. Haz. Mat., V5, p. 111-130, 1981

4.3.2.2. Dispersion of vapor generated by spreading LNG Pool

The unignited pool spreading on the ground results in the simultaneous boiling of LNG due to heat transfer from the ground. The vapor generated by this boiling is cold and has a density higher than that of the atmospheric air; hence, the vapor disperses as a heavy gas. The dispersion of a heavy gas while it is mixing with the ambient air has been studied quite extensively and computer models developed have been reported in the literature[18]. The heavy gas dispersion models provide the area of spread of the gas-air mixture at any instant of time for both continuous releases as well as instantaneous heavy gas releases. In effect the models provide, at any specified time, the vapor concentration contours for specified average gas concentration in air. In general, the contour and area of interest is that enclosed within the 5% methane concentration contour at ground level. This concentration forms the lower flammability of natural gas in air.

Based on the analysis performed in evaluating the LNG pool spread while evaporating on the ground, the following parameters (forming the source characterization for vapor dispersion modeling) have been developed. These will be used to analyze vapor dispersion using heavy gas dispersion models that meet the requirements specified in the NFPA 59A and 49 CFR Part 193 for acceptable models(16).

[18] Irvings, M.J., et.al., "Vapor Dispersion Models for Safety Analysis of LNG Facilities," Report by Health & Safety Laboratory, Buxton, England, Published by NFPA Research Foundation, Quincy, MA, September 2016.

LNG Vapor Dispersion Calculation						
Item #	Parameter for use in the dispersion calculations	Symbol	Value	Value	Value	Units
1	Number of tank cars spilling		1	2	5	
2	Mean duration of spill from tank cars (calculated) at max release rate	t_{Evap}	41	41	41	s
3	Maximum liquid spill rate on to the ground [from the tank car(s)]	$\dot{M}_{L,max}$	883	1,766	4,414	kg/s
4	Maximum rate of release of flashed vapor	$\dot{M}_{Flash,max}$	152	304	761	kg/s
5	Maximum Diameter of Spread of LNG on the ground, while evaporating	D	102	136	191	m
6	VAPOR SOURCE MASS FLUX from the pool: Mass flux of vapor emanating from the evaporating pool and associated flashed vapor (spread over the diameter) - averaged over diameter and spill time.	$\dot{M}''_{Source}$	0.125	0.143	0.181	kg/s m^2
7	Atmospheric conditions					
8	Atmospheric stability class		F	F	F	
9	Wind speed (mean) associated with the above stability	U_{wind}	2.5	2.5	2.5	m/s
10	Terrain roughness factor	Z_0	0.05	0.05	0.05	m
11	Assume flat ground					

The use of a computer program, PHAST, for calculating the dispersion of LNG vapors (heavy gas dispersion) with the above conditions of pool size, liquid vaporization rate, wind and weather conditions leads to the following results[19,20].

Tank cars breached	1	2	5
Max. cloud distance to LFL [m]	1,310	1,760	2,380
Max. cloud width to LFL [m]	350	450	530
Max. cloud depth to LFL [m]	20	23	27
Max. ground level cloud area to LFL [m^2]	56,300	103,500	221,300

4.3.2.3 Radiant Heat Hazard Distance from a LNG Pool Fire

The correlations and models for radiant heat emanating from large LNG fires on land are used to calculate the radiant heat safe distance from a pool fire occurring near the point of spill of LNG from

19 Gavelli, F., "Results from LNG Dispersion Modeling for the FRA, using PHAST," Email of 3/2/2020 to Phani Raj, FRA from BLUE, Inc.

20 Appendix C to this report includes Figure 1, Figure 2 and Figure 3 illustrating the PHAST LNG vapor dispersion modeling results for 1 tank car scenario, 2 tank car scenario, and 5 tank car scenario, showing the flammable vapor cloud footprint at the time it reaches its maximum area for each of the three scenarios.

tank car(s)[21,22]. The acceptable criterion for exposure of a person to radiant heat from a fire is indicated in 49 CFR, part 193 (and this value is 5 kW/m^2 for a 30 s exposure to cause 2nd degree burns).

The LNG pool boiling rate in a fire (so-called liquid regression rate) is obtained from the experimentally measured values from the 35 m diameter, on land, LNG pool fire tests conducted by Gaz de France and other coalition members. The view factor calculation results published by Rein, et. al.[23] are used to determine the distance downwind where a person has to be located as to not feel 2nd degree burns for 30 s.

The results for the pool fire arising from spill of LNG from 1, 2 and 5 tank cars are shown in the table below. It is assumed that the spill rate remains at the maximum spill rate (a conservative assumption) and that the wind speed is 30 mph (which also gives the farthest downwind distance to radiant heat hazard to a human exposure to radiant heat).

---

21 Malvos, H. and P.K. Raj, "Thermal Emission and Other Characteristics of Large Liquefied Natural Gas Fires," Process Safety Progress (AIChE), v 6, n 3, p 237 - 247, September 2007.

22 Raj, P.K., "LNG Fires: A Review of Experimental Results, Models and Hazard Prediction Challenges," Journal of Hazardous Materials, v 140, n 3, p 444 - 464, 20th February 2007.

23 Rein, R.G., C.M. Sliepcevich & J.R. Welker, "Radiation View Factors for Tilted Cylinders," J. Fire & Flammability, Vol 1, April 1970.

LNG Pool Fire on Land Evaluation of Safe Distance for Human Tolerance of Radiant Heat					
Property or other Parameter	**Symbol**	**Value**	**Value**	**Value**	**Units**
LNG Pool Fire Properties					
Mean emissive power (a cylindrical fire description)	E	165			kW/m^2
Liquid regression rate in a large LNG pool fire due to heat from fire	$\dot{y}_{L,Fire}$	3.30E-04	3.30E-04	3.30E-04	m/s
Average liquid regression rate due to ground heat transfer -max spill rate	$\dot{y}_{L,Ground}$	2.53E-04	2.53E-04	2.53E-04	m/s
Combined liquid regression rate	$\bar{\dot{y}}_L$	5.83E-04	5.83E-04	5.83E-04	m/s
Assumed height to diameter ratio	H/D	2	2	2	
Spilling tank car numbers	N	1	2	5	
Max Mass rate of liquid spill out of the tank car	$\dot{M}_{L,max}$	1034.96	2069.93	5174.82	kg/s
Max Volume rate of liquid flow on to ground (all tank cars)	$\dot{V}_{L,Max}$	2.44	4.88	12.21	m^3/s
Duration of spill at maximum mass rate of spill	$t_{S,\ min}$	41	41	41	s
LNG Pool Fire Characteristics					
Calculated pool fire diameter	D	73.1	103.3	163.4	m
Calculated mean height of radiating/visible fire	H	146.1	206.6	326.7	m
Tolerable radiant heat criterion for human exposure	q	5	5	5	kW/m^2
Radiant view factor to a vertical element for human exposure	VF	0.030	0.030	0.030	
Effective view factor taking into account atmospheric absorption of heat	VF*	0.051	0.052	0.055	
Characteristic wind speed for tilting the pool fire	U_{ch}	5.3	5.9	6.9	m/s
Assumed wind speed (30 mph)	U_{wind}	8.9	8.9	8.9	m/s
Flame axis tilt angle with respect to vertical	θ	51.1	48.3	44.1	degrees
Ratio of radial distance from fire center/Fire pool radius for the specified VF value to a vertical element	S/R	11	11	11	
Radial distance from fire center to human hazard line with atmospheric absorption of radiant heat being considered	S	300	424	670	m
Distance from fire edge to the human hazard contour line downwind	S'	263	372	588	m

4.3.2.4 Radiant Heat Hazard Distance from Fireball type Fire

When a tank car containing a pressurized, flammable liquid in a state of possible temperature higher than that corresponding to its saturated condition under the tank pressure, suffers a sudden wall puncture, thermal tear, or catastrophic wall failure, the liquid inside the tank car boils and significant mass of flashed vapor and entrained liquid is released. If this release is ignited immediately (due to the presence of a fire nearby or another ignition source), the released two-phase, vapor-liquid aerosol mixture burns in the form of a fireball. This fireball is, generally, large in diameter, rises into the air, is short-lived, and puts out significant amount of radiant heat to the environment.

Lees (1998)[24] has reviewed the various fireball models published in the literature. These models describe the fireball characteristics (size, rise height, time of presence, radiative heat output, etc.) as functions of

[24] Lees F.P., "Lees' Loss Prevention in the Process Industries," 4th Edition, (Sam Mannan, editor), Vol 2, §16.15 "Fireballs," Elsevier Publication, New York, 2012.

release mass, initial velocity and density of release, and the chemical released. In addition, the fraction of the fuel released which participates in the fireball is three times the flash fraction [Lees, 2012, p 16.184]. The flash fraction of vapor produced due to LNG release from a storage pressure of 45 psig is 14.7 % (by mass).

The TNO model correlations described in Lees' handbook for fireball characteristics are used in the analysis performed as part of the LNG Action Plan effort. The correlation for the maximum fireball diameter and the duration of persistence are obtained from Pietersen (1985),[25] referenced in Lees' handbook. The criterion for second degree burn to a person when exposed to a fireball is 390 [$(kW/m^2)^{(4/3)}$ s] indicated in the Dutch "Green Book" [26]. The sample calculations for determining the fireball characteristics are indicated in the "Yellow Book." [27]

The results of the fireball analysis with very fast LNG release from tank cars (1, 2 and 5 tank cars, respectively) are indicated in the table below.

---

25 Pietersen, C.M. (1985). Analysis of the LPG Incident in San Juan Ixhuatepec, Mexico City, November 1984. Report # 85-0222. TNO, Apeldoorn, The Netherlands.

26 Van den Bosch, C.J.M, et al., "Statistical Model for Injury due to Heat Radiation," Chapter 1,§ 3. equation 3.6; in the "Green Book," "Methods for the Determination of Possible Damage to People and Objects Resulting from Releases of Hazardous Materials," Report # . CPR 16E, 1st edition, 1992, Committee for the Prevention of Disasters, Published by the Directorate General of Labor of the Ministry of Social Affairs & Employment, Netherlands.

27 Englehard, F.J.M, "Heat Flux from Fires," Chapter 6, § 6.5.7.1 pp 6.88 and §6.6.5, pp6.116, "Fireballs," "Methods for the Calculation of Physical Effects," CPR 14E, Part 2, ["Yellow Book" 3rd edition, 1997], Published by the Directorate General of Labor of the Ministry of Social Affairs & Employment, Netherlands.

Calculated Results for Fireball Effects

Parameters	Symbol	Value	Value	Value	Units
LNG Properties					
LNG tank pressure before release	P_T	45	45	45	psig
		377	377	377	kPa (abs)
LNG temperature at just before release	T_T	129.9	129.9	129.9	K
LNG density at storage pressure	ρ_L	393.8	393.8	393.8	kg/m^3
Vapor and Entrained Liquid Released Catastrophically due to Tank Car Failure					
Number of tank cars releasing	N	1	2	5	
Mass of LNG contained in each group of tank cars	M_T	42,485	84,969	212,423	kg
Mass fraction of liquid that flashes to vapor, instantaneously	f_V	14.7	14.7	14.7	%
Mass of LNG vapor + entrained liquid aerosols participating in fireball	$M_{fireball}$	18,736	37,471	93,679	kg
Maximum fireball radius	R_{fb}	79	99	134	m
Fireball duration of lift	t_{fb}	11.0	13.2	16.7	s
Height of center of fireball from the ground at maximum size	H_{fb}	159	199	268	m
Assumed surface emissive power of fireball	E	250	250	250	kW/m^2
Criterion for people exposure safe distance calculation (modified heat dose)	$\mathcal{D}_{dose,fb}$	390	390	390	$[kW/m^{2](4/3)}$ s
Distance from center of fireball on the ground to 2nd degree burn hazard on ground taking into account the heat absorption by the atmosphere	S_{max}	112	150	230	m

4.3.3. Discussion on the Results

The LNG release scenarios from potential accidents involving LNG-carrying unit trains discussed above and the results presented for the effects of such releases are based on worst possible conditions. The conditions used in these calculations do not occur except in extremely unlikely congruence of train conditions, local topography, soil properties, weather and other conditions. Therefore, the results represent extremely unlikely outcome of an accident involving a LNG unit train. The results are presented for purposes of bounding the possible areas of hazard.

4.3.3.1. LNG leak rate and total volume of release:

It is assumed that in the event of a derailment accident involving a 100-tank car unit train of LNG a maximum of 5 tank cars will be damaged so severely as to release all of their contents, simultaneously. To calculate both the rate of release of LNG from damaged tank cars and the total volume of release from each tank car it was assumed that the puncture hole (in the inner tank) in each tank car was at the bottom most part of the tank car in the final resting position of the tank car and that each puncture was a 12” x 12” hole (representing a coupler-caused puncture). This condition is never realized in real accidents, in that the hole sizes vary over a significant spectrum of sizes and the punctures are located at various levels on the tank car walls. The effect of such a very conservative assumption is to make the rate of release and the volume of LNG released to be high by factors of 2 or 3.

4.3.3.2. Unignited LNG Pool Spread on the Ground

In calculating the extent of pool spread on the ground with simultaneous evaporation of the liquid due to heat transfer from the ground, it has been assumed that the ground is flat and impervious to liquid percolation. This also makes the calculated pool spread considerably larger than what it may be in normal conditions occurring near railroad tracks – grounds are never really flat nor impervious (for example, ballast is very pervious). Many areas have ditches and culverts next to rail tracks making the released LNG pool in more or less "diked" areas. Unfortunately, it is very difficult to estimate the "average ground conditions," both in topography and thermal properties of soils occurring next to rail tracks of unknown origin-destination-route segments. It is known that when the liquid thickness become of the order of the mean roughness of the ground (generally, taken to be 5 mm), the spreading stops. However, in the conservative assumption made in calculating the spread of liquid, the liquid spread stops only when there is no more liquid to spread.

An additional assumption made in calculating the pool spread extent is that all tank cars (1, 2 and 5) release simultaneously and into the same "central" location, and the pool spreads from this central location. In a rail derailment accident, it is highly improbable that neighboring cars in a cut in the consist end up next to each other after derailment, suffer same type of puncture together, and release together into the same spot. Therefore, the assumption that all leaking cars release simultaneously and into the same spot is an overly conservative assumption.

The results for the maximum radius of liquid spread calculated for the maximum rate of release (at the initial times of release when the liquid depth is a maximum in the tank car), and for the mean rate of release over the duration of release, do not differ very much. This is because the spread (for the thermal properties of the soil assumed) is very much controlled by the ground heat transfer. It is seen that for the assumed 5 tank car spill, the radii of spread, respectively, for the maximum spill rate and mean spill rate are 95.5 m and 99.9 m. These are well within the error in calculating the liquid pool spread. This calculation also indicates that all further pool based calculations can use the mean spill rate as the criterion for hazard calculations.

In addition, if the tank cars are lying next to each other and touching with their principal axes parallel (accordion end state), the total length along the diameter for a 5 car pile would be about 20 m (or 10 m semi length). That is, the maximum radius of spread of the unignited liquid pool can be considered to be about 10 times the tank car pileup radius.

4.3.3.3. Dispersion of Vapors Emanating from Spreading LNG Pool

The evaporation flux (kg/m^2 s) of vapor emanating from the spreading, unignited LNG pool is calculated based on the maximum rate of release of LNG from tank cars (including the flash vaporization) and the maximum spread radius calculated earlier. This provides the largest area for pool evaporation and high vapor flux. It is noted that when the pool size is a maximum, the evaporation ceases!

The results presented indicated a LFL downwind distance of 1310 m and 2380 m, respectively, for spills from one and five tank cars. It is noted that the dispersion calculation is based on a continuous vapor injection at the rate used for the spill time of 41 seconds. At 2.5 m/s wind speed, it will take the cloud to reach the LFL distance about 525 s and 950 s, respectively, for the 1 tank car spill and 5 tank cars spill. Therefore, the LFL distances indicated should be viewed as very conservative. It is emphasized that the LFL distances calculated are based on very conservative values assumed for each of the parameters that go into the dispersion calculations.

The flammable area (that is, the area bounded at ground level by the 5% vapor concentration contour) changes with time when the cloud is dispersing in the atmosphere. This area is small initially (with semi-width equal to heavy gas spread laterally due to its high density and downwind distance essentially that is equal to the product of wind speed and time of evaporation). However, the flammable area increases with time, up to a specific time (determined by a number of physical parameters) and subsequently decreases. The table provided above indicates the maximum flammable area that results from each of the release scenario postulated. It is seen that the maximum flammable areas are, 56300 m^2, 103500 m^2 and 221300 m^2, respectively for 1, 2 and 5 tank car releases. These flammable areas occupy, respectively, circles of radii 134 m, 182 m and 265 m.

A flash fire hazard will result if the vapor cloud is ignited at the leading edge during its dispersion downwind. In the case of such cloud ignition, the resulting fire is a flash fire which travels towards the source of the vapor (liquid pool if the trailing edge of the vapor cloud is still tethered to the pool). Once the vapor cloud is dispersing as a “puff” because the evaporation from the liquid pool has ceased, the distance of travel of the flash vapor fire is the “wind direction length” of the cloud at the instant of ignition. Hence, the maximum area a flashing vapor fire can affect is the maximum area bounded by the 5% (flammable) contour of the cloud at any instant. It is known from field tests conducted with ignitions of dispersed LNG vapor clouds in the open terrain, cloud ignitions do not lead to any overpressure hazard associated with a flash fire. The hazard is limited to the area that the rapidly travelling flash fire sweeps, which is the same as the ground level area of the 5% contour.

4.3.3.4. Radiant heat hazard from a spreading pool fire

The spilled LNG, if ignited immediately, forms an expanding burning pool sustaining a pool fire. The diameter of the fire will continuously increase with time until all of the liquid spilled is consumed in the fire. The calculations (for the distance outside the fire for a 2nd degree burn injury to a person) indicated are based on conservative assumption that the fire size is always at the maximum diameter consistent with the spill rate and the total burning rate due to heat input to the liquid pool from the fire and the ground. The fire is not always at this maximum diameter; only during the final stages of the fire. Also, values for the radiant heat emission from the fire are based on experimental data from 35 m diameter fire. The calculations are based on 163 m diameter fire (for 5 tank car

release), which is about 5 times the size that has been tested on land. It is well known that, as the fire size increases, the fire emits less radiant heat due to obscuration by black smoke produced. Therefore, the use of radiant heat emission values from a 35 m diameter LNG pool fire test is conservative.

In addition, the distance to the skin burn hazard is calculated on the basis of a 9 m/s (30 mph) wind, which bends the flame significantly in the direction of the wind. This will cause the distance downwind for the burn criterion to be larger than if the flame were vertical. Again, such a wind speed assumption is very conservative in that the % of time in any place that the wind is 9 m/s (30 mph) is significantly low.

The radiant heat is absorbed by the intervening atmosphere if the distance is large and the relative humidity is high. The results shown above are based on a 50% relative humidity. For the distances calculated, the absorption of radiant heat by the intervening atmosphere is important (almost 40% is absorbed). Using these assumptions, it is noted that the calculated value for the distances to hazard from pool fires, respectively for 1, 2 and 5 tank car spills, are 300 m, 425 m and 670 m. These distances are smaller than the distances to which a dispersing flammable cloud can extend (until the vapor concentration is below the LFL).

It is also noted that in calculating these hazard distances due to pool fires, it is assumed that the large fires (of diameters considerably larger than have been tested in actual experiments) have the same characteristics as relatively small fires (of say 35 m diameter). It is well known that as the fire size increases combustion of the vapors in the fire become incomplete due to limitations of diffusion of air (oxygen) from the outside to the core resulting in the formation of black, heat absorbing soot. Such a sooty fire radiates considerably less heat to the environment outside the fire envelope. Therefore, the calculation results presented above must be viewed as being extremely conservative.

4.3.3.5. Radiant heat hazard from a lifting Fireball

A fireball type of fire is assumed to occur when a thermal tear occurs in the vapor wetted wall of a tank car containing a flammable liquid and exposed to an external engulfing pool fire. The sudden occurrence of a thermal tear when the flammable liquid in the tank car is at elevated pressure and temperature results in rapid boiling of the liquid releasing significant mass (and volume) of vapor in very short time together with a part of the liquid that gets entrained with the vapor due to the violence of boiling.

In the calculations indicated for evaluating the effects of a fireball it is assumed that the flashed vapor due to sudden depressurization and about 30% of the remainder liquid in the tank burn in the fireball. The fireball will be a burning, rising spherical fire radiating heat to the environment. The radiant heat flux emitted from a fireball is generally higher (250 kW/m2) than that from a pool fire (165 kW/m2). However, the results indicate that the skin burn hazard distance at the ground for a

fireball is smaller than that from a pool fire. For a 5-tank car release the fireball hazard distance is 230 m vs. for a pool fire for the same release it is 670 m. This is because, even though the fireball puts out much more radiant heat flux it is short-lived and is rising up in the air compared to a pool fire that is anchored to the ground and lasts much longer (15 s for fireball compared to about 60 s for the pool fire). Hence, the hazard distances from a fireball are less compared to that from a longer burning pool fire.

The issue of BLEVE from a LNG tank car is not considered because the conditions under which the BLEVE occurs are very unlikely to occur in a double walled DOT 113C120W tank car. There are no documented cases of a BLEVE involving highway LNG trucks even though there are reported accidents in which an external fire did impact the outer tank of a LNG truck.

4.3.4. Summary of Hazard Effects from LNG Releases

The hazard distances, calculated with the most conservative and worst-case assumptions for different types of behavior of LNG when released from tank cars is summarized below.

Hazard Distances due to Worst-Case Release Scenarios from LNG Tank Cars in Train Derailment

LNG Behavior	Property or other Parameter	Value	Value	Value	Units
Number of Tank Cars (assumed to be) releasing LNG		1	2	5	
LNG Pool Spread on Land	Maximum Spread Radius of Circular, unignited LNG Pool	51	68	95	m
Vapor Dispersion	Down wind maximum distance to Lower Flammability Limit (LFL) Concentration	1,310	1,760	2,380	m
	Maximum area of 5% (LFL) contour on the ground	56,300	103,500	221,300	m^2
	Circular radius (or semi-width) of maximum area of the 5% contour	134	182	265	m
Expanding Pool Fire	Radial distance from fire center on the ground to 2nd degree skin burn hazard to a ground level observer, with consideration of atmospheric absorption of radiant heat.	300	424	670	m
Fireball	Radial distance for 2nd degree burn hazard (using modified thermal dose criterion) from center of fireball projected on the ground to a ground level observer, with consideration of atmospheric absorption of radiant heat.	112	150	230	m

4.3.5. Conclusions

1) Very conservative assumptions have been made in calculating the hazard areas resulting from LNG release from tank cars in a train accident.

2) The hazard assessments have been made for LNG release from one, two and five tank cars. When multiple tank car releases are considered, a very conservative assumption that all tank cars release simultaneously and at a central point is made – this is far from reality in a train accident.

3) The local topographic conditions are also assumed to be ideal as to make the effects of release particularly large. Real topographies next to rail lines are anything but flat or impervious. The ground is assumed to be flat, impervious to LNG and therefore promotes its unconfined spread to a maximum extent. Hence, the spread and other associated results, even under worst release conditions from a train accident will be less in scale than indicated in the results presented above.

4) Multiple LNG behaviors have been considered including (i) unconfined spread without ignition, (ii) dispersion of vapor generated by the unconfined, unignited liquid spread, (iii) maximum flash fire size (area) if the dispersing vapor is ignited at the instant the vapor cloud foot print has the maximum flammable area, (iv) effects of a pool fire on the spreading LNG, from immediate ignition during release, and (v) a fireball type fire and its effects.

5) It is seen from the results indicated above, the hazard areas presented by both the vapor cloud ignition and fireball radiant heat effects are relatively small (both in area of hazard and the distance from spill point to which the hazard extends).

6) It is seen that the radiant heat hazard distance is the largest of the four different types of LNG behavior considered. This is because of very conservative assumptions related to both the spread of the liquid, unconfined, and the modeling the larger fire that results with characteristics measured in fires of significantly smaller size in field tests. It is well known that as the fire diameter increases, the radiant heat output to locations outside the fire decreases because of incomplete combustion and the resulting formation of dark soot which obscures the burning areas from being “seen” by outside the fire elements. Therefore, the radiant heat effect distances presented for pool fires are overly conservative and are likely to be comparable to distances calculated for other hazard types.

5. Next Steps

Consideration should be given to the possibility (however low the probability is) of occurrence of a BLEVE in a double hulled LNG tank car. BLEVE results when a tank car fails catastrophically releasing all of tank car contents into a fireball and at the same time producing a blast wave due to sudden depressurization (and in very rare flammable liquids due to the formation of a detonation wave).

BLEVE has been mentioned as a potential large impact hazard that could be an outcome of a train accident involving LNG shipments on rail. However, the circumstances, the physical and thermal conditions necessary before such an event can take place in a double tank, DOT113C120W style tank car are completely unknown. This is an important area of research that should be addressed immediately.

APPENDICES

APPENDIX A

Table: Historical flammable liquid unit train derailment data collected by representatives of FRA and PHMSA during investigations at accident sites from 2006 to 2019.

Incident Date	Incident Location	Cars Carrying Hazmat	Hazmat Cars Damaged Derailed	Cars Released Hazmat	Total Cars	Total Cars Derailed loaded	Train Speed	Car Type	Quantity Released (LGA)	Product UN	Footprint of derailment area	General topo of derailment area	Fire
2006/10/20	NEWBRIGHTON, PA	80	23	20	83	23	37	111	485,278	UN1987	600'L X 600'W	Bridge, over river	Yes, with explosions
2009/06/19	CHERRY VALLEY, IL	75	19	15	114	19	34	111	323,963	UN1987	~650'L X 500'W	Local road, rail crossing	Yes
2011/02/06	ARCADIA, OH	60	32	32	62	33	46	111	863,555	UN1987	~1200'L x 450'W	flat field, raised RR bed	Yes
2011/10/07	TISKILWA, IL	65	10	9	131	26	37	111	190,271	UN1987	~1200'L x 250'W	Sparsely wooded field on one side with farmland on opposite side	Yes
2012/08/05	PLEVNA, MT	44	17	12	106	18	23	111	231,418	UN1987	600'L x 200'W	Flat track	Yes
2013/03/07	MATTAWAMKEAG, ME	95	14	0	96	15	8	111	#N/A	Crude Oil	~600'L x 75'W	Slightly curved track	No
2013/11/07	ALICEVILLE, AL	88	30	26	90	27	39	111	455,520	UN1267	~400'L x 200'W	Slightly curved, elevated track through swamp	Yes, with explosions
2013/12/30	CASSELTON, ND	104	20	18	106	21	42	111	474,936	UN1267	600'L X 600'W	Flat/straight tangent track	Yes
2014/04/30	LYNCHBURG, VA	104	17	2	105	17	23	CPC-1232	29,417	UN1267	600'L x 100'W	Tracks next to river bank	Yes
2015/02/04	SHERRILL, IA	80	14	7	81	15	24	111	53,180	UN1987	550'L x 100'W	Waterway	Yes
2015/02/16	MOUNT CARBON, WV	107	27	20	109	27	33	CPC-1232	362,349	UN1267	~720'L x 250'W	Side of mountain	Yes, with explosions
2015/03/05	GALENA, IL	103	21	10	105	21	23	CPC-1232	110,543	UN1267	~500'L x 300'W	Sparsely wooded field	Yes
2015/07/16	CULBERTSON, MT	106	22	5	108	22	44	CPC-1232	26,449	UN1267	Unknown	Unknown	No
2015/11/08	WATERTOWN, WI	110	15	1	110	15	27	CPC-1232	1,000	UN1267	~300'L x 100'W	Flat tangent track at a diamond track crossover	Yes, interior only and self-extinguished
2016/06/03	MOSIER, OR	94	16	5	96	16	24	CPC-1232	42,448	UN1267	~600'L x 200'W	Forest around raised RR bed	Yes
2017/03/10	GRAETTINGER, IA	98	20	14	100	20	28	111	321,818	UN1170	500'L x 300'W	Open field with a creek	Yes
2017/06/30	PLAINFIELD, IL	113	19	5	115	19	40	CPC-1232	28,245	UN1267	500'L x 500'W	Raised RR bed in open field with light commercial development	No
2018/06/22	DOON, IA	98	37	10	101	35	47	117R	162,018	UN1267	600'L x 200'W	Raised RR bed through flooded field	No
2019/04/24	FORT WORTH, TX	96	26	3	98	27	26	117R; 111	74,430	UN1987	400'L x 100'W	Raised RR bed next to forest on one side, abandoned industrial on other	Yes

Appendix B: Table - Models and Reports References		
WCS Scenarios	**Description of data/models**	**Technical Reference(s)**
1) Unconfined and unignited spreading and simultaneously evaporation (due to heat transfer from the ground) of a LNG pool on a flat, impervious, ground	The model evaluated for the radial spread of an unconfined pool of LNG	Raj, P.K. "Models for Cryogenic Liquid Spill Behavior on Land and Water," J. Haz. Mat., V5, p. 111-130, 1981
2) Dispersion of vapor generated by spreading LNG Pool	Analysis of the vapor dispersion using heavy gas dispersion models that meet the requirements specified in the NFPA 59A and 49 CFR Part 193 for acceptable models	Vapor Dispersion Model Evaluation Protocol, "Evaluating Vapor Dispersion Models for Safety Analysis of LNG Facilities," published by the National Fire Protection Research Foundation report.
	PHAST vapor dispersion model	Gavelli, F., "Results from LNG Dispersion Modeling for the FRA, using PHAST," Email of 3/2/2020 to Phani Raj, FRA from BLUE, Inc.
3) Radiant Heat Hazard Distance from a LNG Pool Fire	The correlations and models for radiant heat emanating from large LNG fires on land are used to calculate the radiant heat safe distance from a pool fire occurring near the point of spill of LNG from tank car(s).	Malvos, H. and P.K. Raj, "Thermal Emission and Other Characteristics of Large Liquefied Natural Gas Fires," Process Safety Progress (AIChE), v 6, n 3, p 237 - 247, September 2007. Raj, P.K., "LNG Fires: A Review of Experimental Results, Models and Hazard Prediction Challenges," Journal of Hazardous Materials, v 140, n 3, p 444 - 464, 20th February 2007.
	The acceptable criterion for exposure of a person to radiant heat from a fire (this value is 5 kW/m2 for a 30 s exposure to cause 2nd degree burns).	49 CFR, part 193

	The LNG pool boiling rate in a fire obtained from the experimentally measured values from the 35 m diameter, on land, LNG pool fire tests conducted by Gaz de France and other coalition members.	Gaz de France: [Nedelka, et al., 1989]. In 1987 a consortium of companies including Gaz de France conducted a series of 35 m diameter LNG pool fire tests on an insulated concrete dike, in the field test facility of Gaz de France (GdF) at the Montoir de Bretagne methane terminal in France.
	The distance downwind where a person has to be located as to not feel 2nd degree burns for 30 s.	Rein, R.G., C.M. Sliepcevich & J.R. Welker, "Radiation View Factors for Tilted Cylinders," J. Fire & Flammability, Vol 1, April 1970
4) Radiant Heat Hazard from Fireball type Fire	These models describe the fireball characteristics (size, rise height, time of presence, radiative heat output, etc.,) as functions of release mass, initial velocity and density of release and the chemical released.	Lees F.P., "Lees' Loss Prevention in the Process Industries," 4th Edition, (Sam Mannan, editor), Vol 2, §16.15 "Fireballs," Elsevier Publication, New York, 2012.
	The correlation for the maximum fireball diameter and the duration of persistence.	Pietersen, C.M. (1985). Analysis of the LPG Accidentin San Juan Ixhuatepec, Mexico City, November 1984. Report # 85-0222. TNO, Apeldoorn, The Netherlands.

	The criterion for second degree burn to a person when exposed to a fireball is 390 $[(kW/m2)^{(4/3)}$ s.	Van den Bosch, C.J.M, et al., "Statistical Model for Injury due to Heat Radiation," Chapter 1,§ 3. equation 3.6; in the "Green Book," "Methods for the Determination of Possible Damage to People and Objects Resulting from Releases of Hazardous Materials," Report # . CPR 16E, 1st edition,1992, Committee for the Prevention of Disasters, Published by the Directorate General of Labor of the Ministry of Social Affairs & Employment, Netherlands.
	Sample calculations for determining the fireball characteristics.	Englehard, F.J.M, "Heat Flux from Fires," Chapter 6, § 6.5.7.1 pp 6.88 and §6.6.5, pp6.116, "Fireballs," "Methods for the Calculation of Physical Effects," CPR 14E, Part 2, ["Yellow Book" 3rd edition, 1997], Published by the Directorate General of Labor of the Ministry of Social Affairs & Employment, Netherlands.

Appendix C

Figure 1, Figure 2 and Figure 3 below represent PHAST LNG vapor dispersion modeling results for 1 tank car scenario, 2 tank car scenario, and 5 tank car scenario, showing the flammable vapor cloud footprint at the time it reaches its maximum area for each of the three scenarios.

Figure 1: 1 tank car scenario

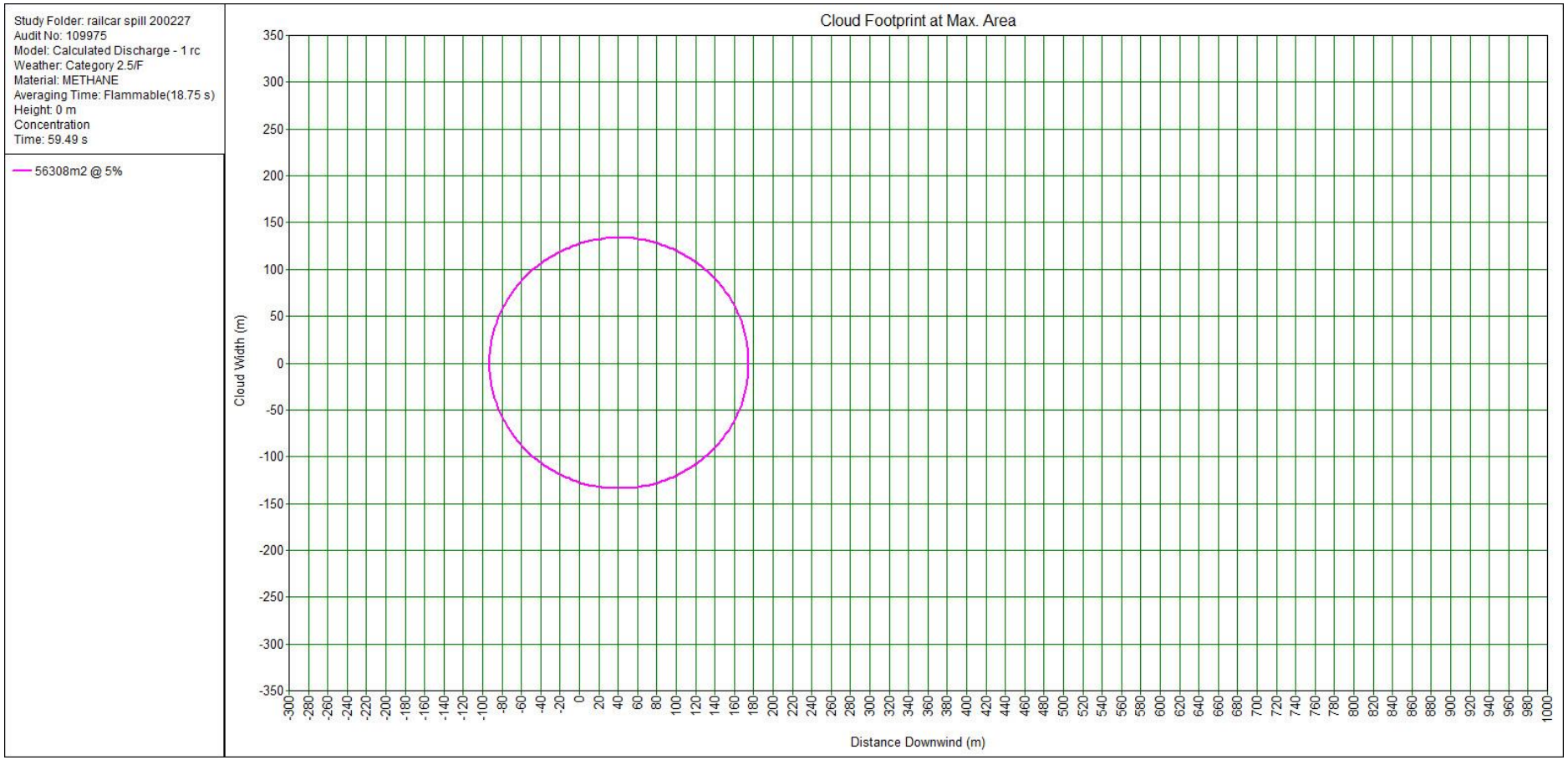

Figure 2: 2 tank car scenario

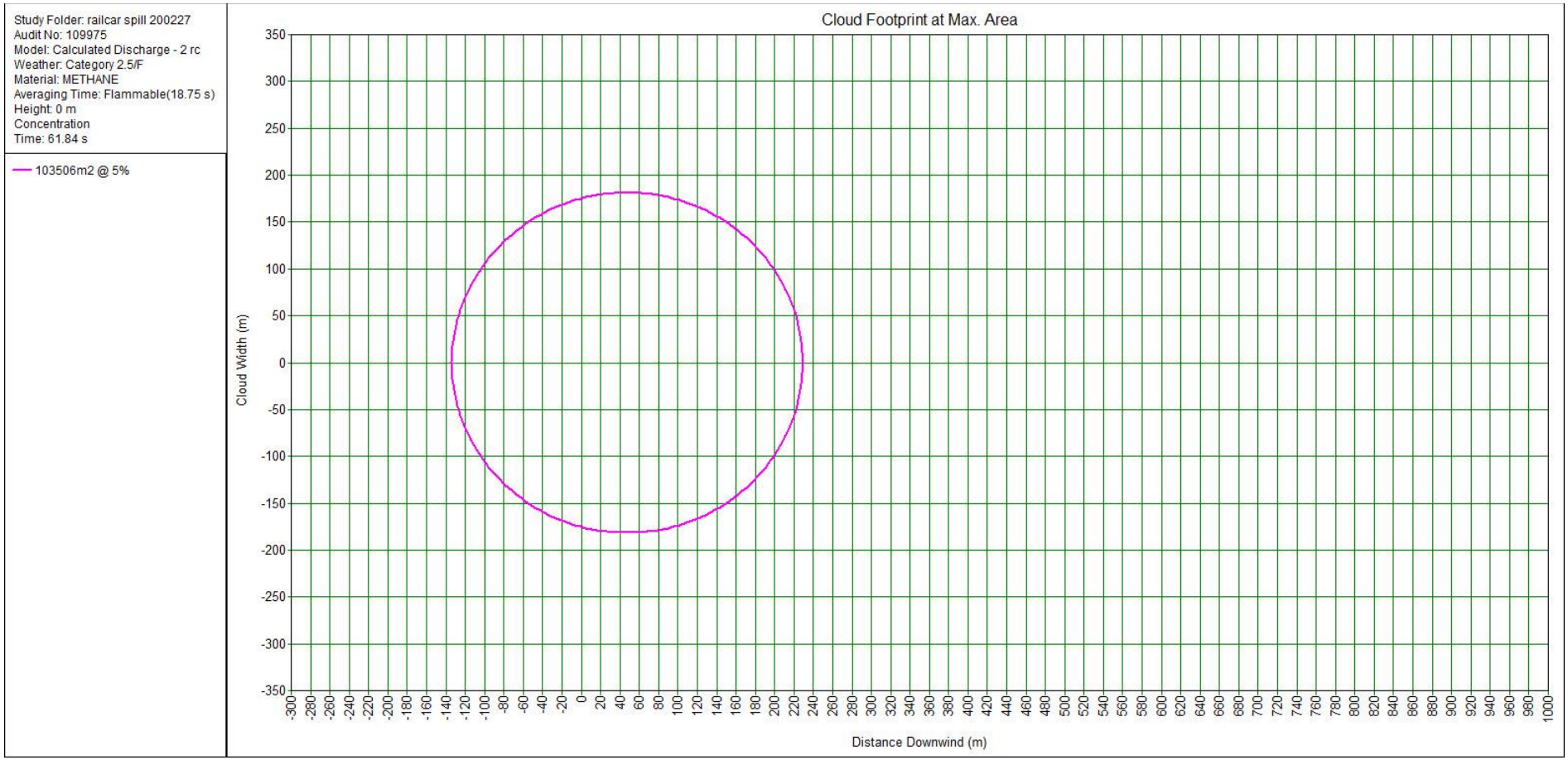

Figure 3: 5 tank car scenario